Gene expression based risk classification in multiple myeloma

Rowan Kuiper

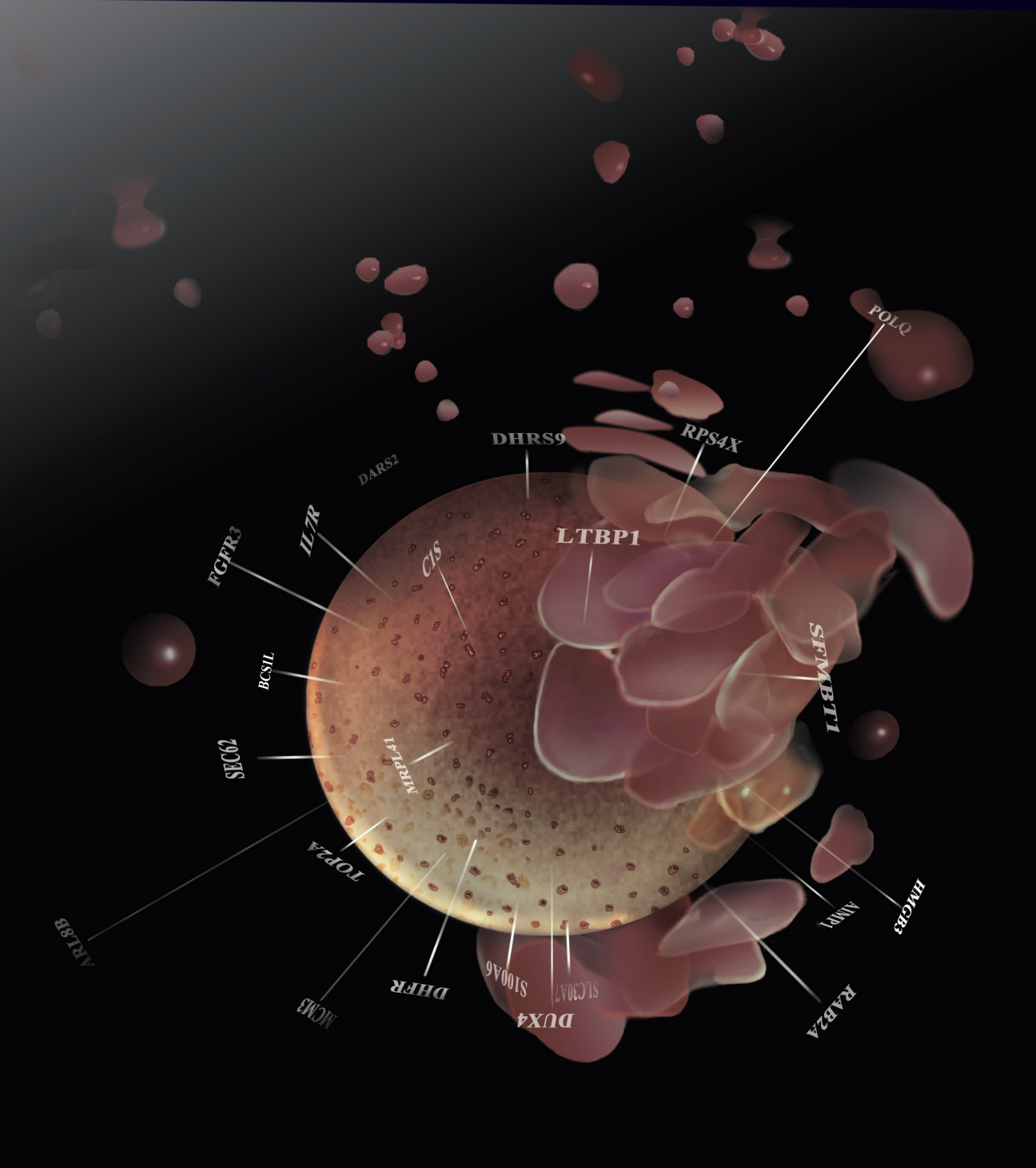

Gene expression based risk classification in multiple myeloma

Rowan Kuiper

Gene expression based risk classification in multiple myeloma

Cover design: Marleen van Es
Layout: Manon Kuiper and Rowan Kuiper
Printing: Ridderprint BV | www.ridderprint.nl

Risicoclassificatie in multipel myeloom gebaseerd op gen expressie

Gene expression based risk classification in multiple myeloma

Proefschrift

ter verkrijging van de graad van doctor aan de
Erasmus Universiteit Rotterdam
op gezag van de
rector magnificus

Prof.dr. R.C.M.E. Engels

en volgens besluit van het College voor Promoties.
De openbare verdediging zal plaatsvinden op

donderdag 20 december 2018 om 11.30 uur

door

Rowan Kuiper
geboren te Vlaardingen

Erasmus University Rotterdam

Promotiecommisie

Promotor:	Prof.dr. P. Sonneveld
Overige leden:	Prof.dr. A.G. Uitterlinden
	Prof.dr. H.R. Delwel
	Prof.dr. S. Zweegman
Co-promotor:	Dr. M. van Duin

Table of contents

CHAPTER 2

A Gene Expression Signature for High-risk Multiple Myeloma

Rowan Kuiper*, Annemiek Broyl*, Yvonne de Knegt,
Martin H. van Vliet, Erik H. van Beers, Bronno van der Holt,
Laila el Jarari, George Mulligan, Walter Gregory, Gareth Morgan, Hartmut
Goldschmidt, Henk M. Lokhorst,
Mark van Duin & Pieter Sonneveld

*These authors contributed equally to this work

Leukemia 2012; **26**(11):2406-13

ABSTRACT

There is a strong need to better predict survival of patients with newly diagnosed multiple myeloma (MM). As gene expression profiles (GEPs) reflect the biology of MM in individual patients, we built a prognostic signature based on GEPs.

GEPs obtained from newly diagnosed MM patients included in the HOVON-65/GMMG-HD4 trial ($n = 290$) were used as training data. Using this set, a prognostic signature of 92 genes (EMC92-gene signature) was generated by supervised principal components analysis combined with simulated annealing.

Performance of the EMC92-gene signature was confirmed in independent validation sets of newly diagnosed (TT2, $n = 351$; TT3, $n = 142$; MRC-IX, $n = 247$) and relapsed patients (APEX, $n = 264$). In all sets, patients defined as high-risk by the EMC92-gene signature show a clearly reduced overall survival with hazard-ratios (HR) of 3.4 ($95\% CI$: $[2.2 - 5.3]$) for the TT2 study, HR: 5.2 $[2.5 - 11]$ for the TT3 study, HR: 2.4 $[1.7 - 3.4]$ for the MRC-IX study and HR: 3.0 $[2.1 - 4.4]$ for the APEX study ($p < 1 \times 10^{-4}$ in all studies). In multivariate analyses this signature was proven independent of currently used prognostic factors.

The EMC92-gene signature is better or comparable to previously published signatures. This signature contributes to risk assessment in clinical trials and could provide a tool for treatment choices in high-risk multiple myeloma patients.

INTRODUCTION

Multiple myeloma (MM) is characterized by accumulation of malignant monoclonal plasma cells in the bone marrow. The median overall survival (OS) for newly diagnosed patients treated with high dose therapy varies from 4 to 10 years.[1,2]

The International Staging System (ISS), based on serum β2-microglobulin and albumin, is widely used as a prognostic system for patients with newly diagnosed MM. ISS has been confirmed as a solid prognostic factor in clinical trials.[1] Additional clinical factors to define high-risk disease have not been consistently reproduced, with the exception of extensive disease represented by renal failure and plasma cell leukemia.[2,3] In addition to ISS, cytogenetic aberrations such as deletion of 17p (del(17p)), translocations t(4;14) and t(14;16) were shown to be associated with an adverse prognosis. The combination of prognostic markers t(4;14), del(17p) and ISS enabled further delineation of patients into prognostic subgroups.[4]

A strategy to include genetic characteristics of MM is the translocation and cyclin D (TC) classification, which distinguishes eight subgroups based on genes which are deregulated by primary immunoglobulin H translocations and transcriptional activation of cyclin D genes.[5] Subsequently, the University of Arkansas for Medical Sciences (UAMS) generated a molecular classification of myeloma based on gene expression profiles of patients included in their local trials. The UAMS molecular classification of myeloma identifies seven distinct gene expression clusters, including the translocation clusters MS, MF, CD-1, CD-2, a hyperdiploid cluster (HY), a cluster with proliferation-associated genes (PR), and a cluster characterized by low percentage of bone disease (LB).[6] More recently, we extended this classification based on the HOVON-65/GMMG-HD4 prospective clinical trial and identified additional molecular clusters, i.e. NFκB, CTA and PRL3.[7] Because these clusters were discriminated based on disease specific gene expression profiles (GEP), we and others hypothesized that they may be relevant for therapy outcome. Indeed, the UAMS defined clusters MF, MS and PR were found to identify high-risk disease in the Total Therapy 2 trial.[6]

Several survival signatures were developed based on samples from clini-

cal trials, such as the UAMS70, the related UAMS17 and the recently published UAMS80 signature which have value in prognostication of MM.[8–10] Other signatures include the Medical Research Council (MRC) gene signature based on the MRC-IX trial, the French Intergroupe Francophone du Myélome (IFM) signature and the Millennium signature based on relapse patients.[11–13] Recently, a GEP based proliferation index was reported.[14] So far, none of these signatures have been introduced in general clinical practice.

The additional and independent prognostic significance of a prognosticator based on gene expression has been acknowledged in mSMART (Mayo Stratification for Myeloma And Risk-adapted Therapy). Hereby, a high-risk MM population can be defined for which alternative treatment is proposed although this has not been validated in prospective clinical trials.[15]

The aim of the present study was to develop a prognostic signature for overall survival in MM patients. This investigation was prospectively included as a secondary analysis of a randomized clinical trial for newly diagnosed, transplant-eligible patients with multiple myeloma (HOVON-65/GMMG-HD4).

MATERIALS AND METHODS

Patients

As training set the HOVON-65/GMMG-HD4 study (ISRCTN64455289) was used. Details of the training set are given in the online supplemental document A.[16] Informed consent to treatment protocols and sample procurement was obtained for all cases included in this study, in accordance with the Declaration of Helsinki. Use of diagnostic tumor material was approved by the institutional review board of the Erasmus Medical Center. Arrays used for analysis passed extensive quality controls, as described previously.[7] Of the 328 gene arrays deposited at the NCBI-GEO repository, clinical outcome data was available for 290 patients (accession number: GSE19784).

Four independent datasets were used as validation of which both survival data were available as well as GEPs of purified plasma cells obtained from bone marrow aspirates of myeloma patients. The datasets Total Therapy 2 (UAMS-TT2, $n = 351$, GSE2658, NCT00573391), Total Therapy 3 (UAMS-TT3, $n = 142$, E-TABM-1138, NCT00081939) and MRC-IX ($n = 247$, GSE15695, ISRCTN6845-4111) were obtained from newly diagnosed patients. The APEX dataset ($n = 264$, GSE9782, registered under M34100-024, M34100-025 and NCT00049478 / NCT00048230) consisted of relapsed myeloma cases (see online supplemental document A).[11,17–23]

Gene expression pre-processing

To allow gene expression analysis in the HOVON-65/GMMG-HD4, plasma cells were purified from bone marrow aspirates obtained at diagnosis, using immune-magnetic beads. Only samples with a plasma cell purity of $\geq 80\%$ were used. Gene expression was determined on an Affymetrix GeneChip® Human Genome U133 Plus2.0 Array (Affymetrix, Santa Clara, CA, USA).

To allow for validation across different studies, only probe sets present on both the U133 Plus2.0 and the U133 A/B platforms were included ($n = 44754$). Probe sets having an expression value below the lowest 1% bioB hybridization control in more than 95% of the samples are excluded. This resulted in 27680

probe sets to be analyzed. All data were MAS5 normalized, $\log_2$ transformed and mean-variance scaled, using default settings in the Affy package in Bioconductor.[24]

The normalized validation gene expression data sets were downloaded from the repositories NCBI-GEO (APEX, MRC-IX and UAMS-TT2) and ArrayExpress (UAMS-TT3). Datasets UAMS-TT2, UAMS-TT3 and MRC-IX were generated using the U133 Plus2.0 (Affymetrix, Santa Clara, CA, USA) platform whereas the Affymetrix HG U133 A/B platform was used in the APEX study. The IFM dataset was not included in our analysis due to an incompatible, custom platform.

The strong batch effect that exists between these GEPs studies was successfully removed by ComBat using the non-parametric correction option.[25] APEX was run on a different array platform with an incomplete overlap in probe sets with the other datasets, and as a result ComBat correction was applied in two separate runs with one run for all analyses involving the APEX data set and an additional run for all other analyses.

Survival signature

The HOVON-65/GMMG-HD4 data were used as a training set. GEP and PFS data were combined for building a GEP based survival classifier. PFS was used for generating a classifier for OS since PFS was the primary endpoint of the HOVON-65/GMMG-HD4 study and PFS demonstrated a higher number of events compared to OS (179 PFS vs. 99 OS events in total in the HOVON-65/GMMG-HD4). All evaluations of the signature are based on OS data in training and validation sets. Analyses were performed using R with the survival package for survival analyses.[26] Out of 27680 probe sets tested, 1093 probe sets were associated to PFS in univariate Cox regression analyses (false discovery rate (FDR) $< 10\%$; for probe sets and survival data see online supplemental document B). Subsequently, this set was used as input into a supervised principal component analysis (SPCA) framework in combination with simulated annealing (online supplemental documents A and B).[27] This analysis yielded a model of 92 probe sets, termed the EMC92 signature. The survival signature is a continuous score, i.e. the sum of standardized expression values multiplied by the probe set specific weighting coefficient (online Table S1, R-script and supplemental document C). High-risk

disease was defined as the proportion of patients with an overall survival of less than two years in the training set.

Validation of the EMC92 signature

A multivariate Cox regression analysis was performed for patients with available covariates. Covariates with $< 10\%$ of the data missing were used as input in a backward stepwise selection procedure ($p < 0.05$).

The EMC92 signature together with seven previously described, external signatures for OS in multiple myeloma have been analyzed in a pair-wise comparison using a multivariate Cox regression analysis. This analysis was performed for all pair-wise comparisons on the pooled datasets excluding the training sets for the signatures being tested. The models were stratified for study.

Pathway analysis was performed using the 92 genes corresponding to the EMC92 signature as well as the 1093 genes generated by univariate PFS analysis (FDR$< 10\%$) with the probe sets used as input for the analysis as a reference set ($n = 27680$, Ingenuity Systems, `www.ingenuity.com`). *p*-values were derived from right-tailed Fisher exact tests and corrected for multiple testing by a Benjamini-Hochberg correction.[28]

RESULTS

The EMC92 signature

GEPs obtained from newly diagnosed MM patients were analyzed in relation to survival data, in order to generate a classifier to distinguish high-risk from standard-risk disease. We used the HOVON-65/GMMG-HD4 data as a training set.[7] After filtering for probe set intensity, using internal Affymetrix control probe sets, 27680 probe sets were analyzed in a univariate Cox regression analysis with progression free survival (PFS) as survival endpoint. This resulted in 1093 probe sets associated with PFS with a false discovery rate of $< 10\%$ (online supplemental document B). Based on these 1093 probe sets, a supervised principal components analysis based model was built in which simulated annealing was applied to generate the optimal model settings in a 20-fold cross-validation. The final predictive model consisted of 92 probe sets with specific weighting coefficients. The sum of normalized intensity values multiplied by this weighting is the output of the signature. This model was termed the EMC92 signature. A positive weighting coefficient indicates that increased expression contributes to a higher value for the EMC92 signature value and thus a higher risk for poor survival. The majority of the probe sets are annotated genes ($n = 85$, with one of the genes represented by two probe sets). The remaining probe sets are open reading frames ($n = 3$), expressed sequence tags ($n = 2$) and one additional probe set without annotation. Several known cancer genes are among these genes, of which *FGFR3* (weighting coefficient$= 0.06$), *STAT1* (weighting coefficient $= 0.05$) and *BIRC5* (weighting coefficient $= 0.02$) were described in detail in relation to myeloma (online Table S1).[29–31] To define a high-risk population, the cut-off threshold for the continuous signature score was set to a value of 0.827 based on the proportion of patients in the training set that had an overall survival of less than two years (63 out of 290 patients (21.7%); online Figure S2).

Four independent validation datasets were available: UAMS-TT2, UAMS-TT3, MRC-IX and APEX. Gene expression datasets UAMS-TT2 and TT3 consisted of 351 and 142 transplant-eligible patients whereas the MRC-IX dataset contained both transplant-eligible and non-transplant-eligible MM patients ($n = 247$). In the

APEX dataset, GEPs of 264 relapse patients were collected. The results of the EMC92 signature in the validation sets are shown in Figure 1 and online Table S2. In the UAMS-TT2 dataset, the EMC92 signature identified a high-risk population of 19.4% with a hazard-ratio of 3.4, 95% confidence interval ($95\%CI$)=$[2.2 - 5.3]$ (p= 5.7×10^{-8}). In the UAMS-TT3, 16.2% of patients were identified as high-risk with a hazard-ratio of 5.2, $95\%CI$ $[2.5 - 11]$, (p= 1.8×10^{-5}). In the MRC-IX dataset, 20.2% of patients were identified as high-risk with a hazard-ratio of 2.4, $95\%CI$ $[1.7 - 3.4]$, (p= 3.6×10^{-6}). The high-risk signature was able to identify patients with significantly shorter survival in both the transplant-eligible and non-transplant-eligible patients included in the MRC-IX study. In non-transplant-eligible patients, 23.9% high-risk patients were identified with a hazard-ratio of 2.4, $95\%CI$ $[1.5 - 3.9]$, (p= 4.3×10^{-4}), whereas 16.8% of transplant-eligible patients were high-risk with a hazard-ratio of 2.5, $95\%CI$ $[1.4 - 4.5]$, (p= 1.5×10^{-3}; Figures 1d and e). The signature was not restricted to newly diagnosed patients as 16.3% of patients included in the APEX relapse dataset were designated high-risk with a hazard-ratio of 3.0, $95\%CI$ $[2.1 - 4.4]$, (p= 1.26×10^{-8}; Figures 1f and 2e).

To assess the relation between EMC92 signature outcome and treatment, we evaluated whether there is evidence for differences in survival between treatment arms in the high-risk group or standard-risk group. Within the high-risk patients of the HOVON-65/GMMG-HD4 trial, the survival of bortezomib treated patients was longer than patients treated with conventional chemotherapy (VAD) (30 months compared to 19 months), albeit not significant (p= 0.06; number of bortezomib treated patients: 26 vs. 37 in the VAD arm). Within the high-risk patients of MRC-IX, no difference was observed between the treatment arms (p= 0.5: MRC-IX non-transplant eligible: CTDA $n = 14$ vs. MP $n = 12$) and p= 1.0 (MRC-IX transplant eligible; CTD $n = 16$ vs. CVAD $n = 7$). For the standard-risk patients no differences in survival between treatment arms were found in either trial.

Multivariate analysis was performed in the training set and in the APEX and MRC-IX validation sets, for which information on a large number of variables were available. This showed that in addition to the EMC92 signature, del(17p) was an independent predictor in HOVON-65/GMMG-HD4. Furthermore, in both

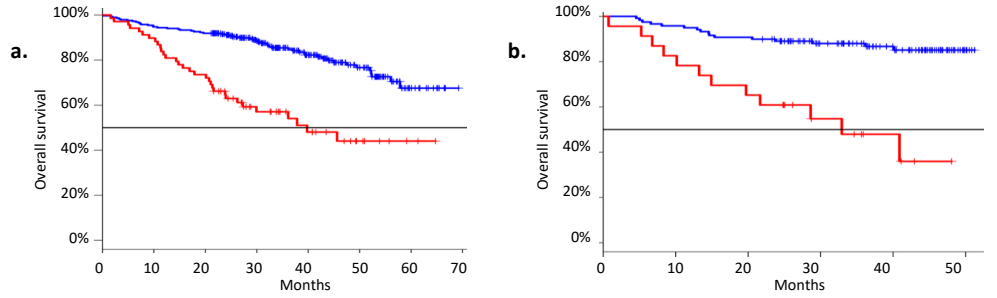

	n (%)	n_{event}	HR [95%CI]	*p*- value	median
Standard	283 (81%)	53	1		n.r
High	68 (19%)	32	3.4 [2.2 - 5.3]	$5.7x10^{-8}$	40

	n (%)	n_{event}	HR [95%CI]	*p*- value	median
Standard	119 (84%)	16	1		n.r
High	23 (16%)	12	5.2 [2.5 - 11]	$1.8x10^{-3}$	33

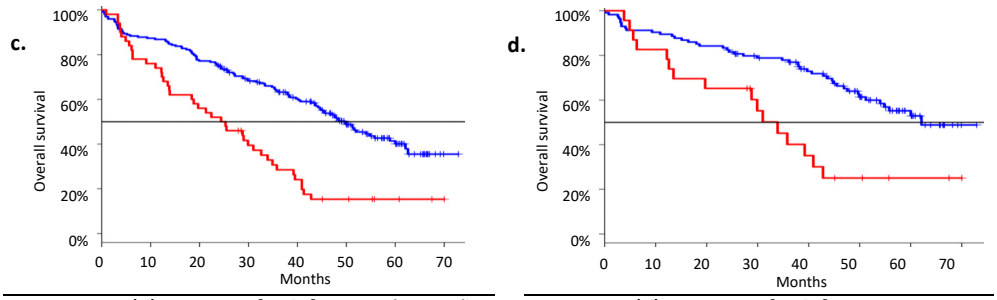

	n (%)	n_{event}	HR [95%CI]	*p*- value	median
Standard	197 (80%)	104	1		50
High	50 (20%)	41	2.4 [1.7 - 3.4]	$3.6x10^{-6}$	24

	n (%)	n_{event}	HR [95%CI]	*p*- value	median
Standard	114 (83%)	46	1		62
High	23 (17%)	16	2.5 [1.4 - 4.5]	$1.5x10^{-3}$	34

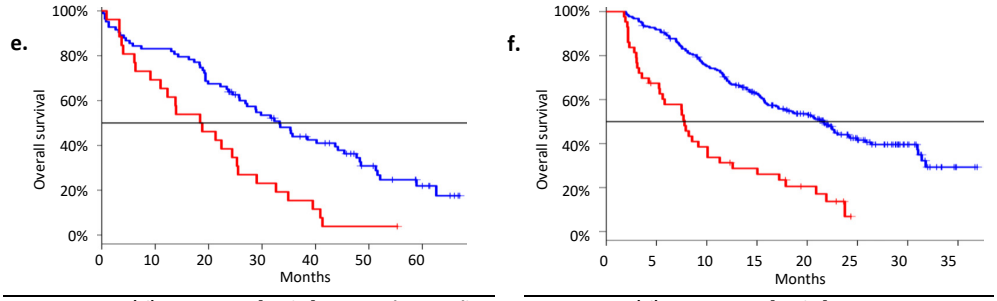

	n (%)	n_{event}	HR [95%CI]	*p*- value	median
Standard	83 (76%)	58	1		33
High	26 (24%)	25	2.4 [1.5 -3.9]	$4.3x10^{-4}$	19

	n (%)	n_{event}	HR [95%CI]	*p*- value	median
Standard	221 (84%)	120	1		22
High	43 (16%)	36	3.0 [2.1 - 4.4]	$1.3x10^{-8}$	8

Figure 1. Kaplan-Meier overall survival curves for EMC92 signature defined high-risk patients versus standard-risk patients in five validation sets. The cut-off value is fixed at 0.827 based on the proportion of patients with OS$<$ 2 years in the HOVON-65/GMMG-HD4 set. In the MRC-IX one patient had an unknown treatment status and was disregarded in Figures d and e. **a**) UAMS Total Therapy 2. **b**) UAMS Total Therapy 3. **c**) MRC-IX. **d**) MRC-IX transplant-eligible patients. **e**) MRC-IX non-transplant-eligible. **f**) APEX. N, number of patients; Events, number of events; HR, hazard ratio; *p*-value for equality to standard-risk group; Median, median survival time; n.r. median not reached.

HOVON-65/GMMG-HD4 and in the APEX multivariate analysis, a component of the ISS was an additional independent prognostic predictor (β2-microglobulin for the HOVON65/GMMG-HD4 set and serum albumin for the APEX data set). Trial specific covariates were seen in each multivariate analysis such as sub-study in the APEX dataset and the MP treatment arm in the MRC-IX set. In conclusion, in all three datasets of newly diagnosed and relapse MM patients the EMC92 signature performed as the strongest predictor for survival after inclusion of available covariates (Table 1). For univariate associations to survival see online Tables S3.1-S3.3.

Using the nearest neighbor classification method, all patients in the validation sets were classified into molecular clusters based on the HOVON-65/GMMG-HD4 classification.[7] A clear enrichment of the MF, MS, PR clusters and decreased proportion of the HY cluster was found in the pooled high-risk populations of all validation sets (online Table S4).

To define the biological relevance of the EMC92 signature and the 1093 probe sets found by initial univariate ranking, pathway analysis of the 92 and the 1093 probe sets was performed. Significant functions for the EMC92 signature included multiple 'cell cycle' pathways ($p= 1.8 \times 10^{-3}$ - 4.9×10^{-2}; online Table S5), including genes such as *BIRC5*, *TOP2A* and *CENPE*. The 1093 probe sets indicated functions such as 'protein synthesis' ($p= 9.5 \times 10^{-31}$ - 1.5×10^{-12}), 'cancer' ($p= 4.8 \times 10^{-12}$ - 4.9×10^{-2}) and 'cell cycle' ($p= 3.7 \times 10^{-9}$ - 4.9×10^{-2}; online Table S6). Next, we compared the chromosomal locations of the probe sets within the EMC92 signature to the expected proportion represented on the Affymetrix chip (online Table S7). None of the chromosomes demonstrated a significant enrichment in the EMC92 signature, while all somatic chromosomes are represented. Within the set of 1093 probe sets, which formed the basis of the EMC92 signature and were identified by univariate survival analyses, chromosomes 1 and 4 were found to be significantly overrepresented. Further analysis of chromosome 1 demonstrated a clear enrichment of the long arm of chromosome 1 in this set of genes (online Table S8).

Table 1. Multivariate analysis. Shown are the EMC92 with a cut-off value of 0.827 in **a**) the HOVON-65/GMMG-HD4, **b**) APEX and **c**) MRC-IX. Covariates that were non-missing in more than 90% of the patients were included. Variants were selected into the model by a backward stepwise approach ($p \leq 0.05$).

a.	**HOVON65/GMMG-HD4 (n=290)**	
	HR [95%CI]	***p***
EMC92 [1/0]	3.4 $[2.2 - 5.4]$	5.1×10^{-8}
B2m [≥3.5mg/L]	2.4 $[1.5 - 3.4]$	4.1×10^{-4}
del(17p) [1/0]	2.2 $[1.4 - 3.7]$	1.6×10^{-3}
WHO [>=1]	2.1 $[1.3 - 3.3]$	2.1×10^{-3}

Likelihood ratio test: 95.8 on 4 df, $p < 2 \times 10^{-16}$, $n = 257$, number of events$= 93$; 33 observations deleted due to missing data.

Available covariates: del(17p)[1/0], del(13p)[1/0], gain(1q)[1/0], age[yr], age[≥60 yr], bortezomib treated[1/0], ISS=2[1/0], ISS=3[1/0], female[1/0], creatinine[mg/dL], creatinine[< 20 mg/dL], B2m[mg/L], B2m[≥3.5mg/L], B2m[≥5.5mg/L], serum albumin[g/L], serum albumin[≤ 3.5 g/L], LDH[>ULN], IgA[1/0], IgG[1/0], light chain disease[1/0], κ light chain[1/0], diffuse osteoporosis[1/0], hemoglobin[mmol/L], hemoglobin[<6.5 mmol/L], hemoglobin[<5.3 mmol/L], calcium[mmol/L], calcium[>2.65mmol/L], WHO[>=1], WHO[>=2], WHO[>=3], WHO[=4]

b.	**APEX (n=264)**	
	HR [95%CI]	***p***
EMC92-gene [1/0]	2.4 $[1.6 - 3.6]$	1.5×10^{-5}
serum albumin [g/L]	0.95 $[0.93 - 0.98]$	1.2×10^{-4}
age [≥60 yr]	1.7 $[1.2 - 2.4]$	1.6×10^{-3}
IgG [1/0]	0.64 $[0.46 - 0.90]$	1.0×10^{-2}
studyAPEX [1/0]	0.58 $[0.41 - 0.82]$	1.8×10^{-3}

Likelihood ratio test: 64.5 on 5 df, $p = 1.43 \times 10^{-12}$,$n = 250$, number of events=150; 14 observations deleted due to missing data

Available covariates: age [yr], age [≥60 yr], age [≥65 yr], bortezomib treated [1/0], female [1/0], black [1/0], white [1/0], IgA [1/0], IgG [1/0], light chain [1/0], studyCREST [1/0], studySUMMIT [1/0], studyAPEX [1/0], studyAPEXprogressive [1/0], serum albumin [g/L], serum albumin [≤3.5 g/L], priorlines

c.	**MRC-IX (n=247)**	
	HR [95%CI]	***p***
EMC92-gene [1/0]	2.5 $[1.7 - 3.6]$	3.4×10^{-6}
age [yr]	1.0 $[1.0 - 1.1]$	3.0×10^{-5}
hemoglobin [mg/L]	0.86 $[0.79 - 0.95]$	1.8×10^{-3}
MP treatment [1/0]	1.6 $[1.1 - 2.4]$	1.8×10^{-2}

Likelihood ratio test: 74.8 on 4 df, $p = 2.1 \times 10^{-15}$,$n = 246$, number of events=145; 1 observation deleted due to missing data.

Available covariates: del(13q)[1/0], IgH split[1/0], hyperdiploid[1/0], t(4;14)[1/0], t(11;14)[1/0], t(14;16)[1/0], t(14;12)[1/0], t(6;14)[1/0], del(17p)[1/0], gain(1q) [1/0], female[1/0], bone disease[1/0], albumin[g/L], albumin[≤3.5g/L], hemoglobin[mg/L], hemoglobin[<8.5 mg/L], hemoglobin[<10.5 mg/L], calcium[mmol/L], calcium[>2.65mmol/L], creatinine[mg/dL], creatinine[< 20 mg/dL], WHO[>=1], WHO[>=2], WHO[>=3], WHO[=4], age[yr], age[≥60 yr], age[≥65yr], intensive treatment[1/0], CVAD treatment[1/0], CTD treatment[1/0], MP treatment[1/0], CTDA treatment[1/0]

Comparison to published gene signatures

We set out to evaluate the performance of the EMC92 signature in relation to available GEP based prognostic signatures for OS in multiple myeloma. To this end, the following signatures were evaluated: UAMS70, UAMS17, UAMS80, IFM15, gene proliferation index (GPI50), MRCIX6 and, MILLENNIUM100.[9–14]

These signatures were evaluated as continuous variables as well as using the cut-off values as published (Figures 2a-e, online Figure S2 and supplemental documents A and B). Overall, the performance of the EMC92 signature is robust, consistent and compares favorably to previously published signatures. Specifically, the EMC92, UAMS, IFM15, MRC-IX and GPI50 signatures demonstrated significance in all validation sets tested both for the dichotomized and the continuous values of the signatures. The MILLENNIUM100 signature had significant performance in the dichotomized model in one out of four independent studies. Thus, performance was less robust for the MILLENNIUM100 signature. Although the proliferation index GPI50 was found to be significant in all validation sets tested, the proportion of high-risk patients was much lower compared to the proportion found using either the EMC92 or the UAMS80 signatures. Ranked, weighted high-risk proportions are GPI: 10.0%, UAMS17: 12.4%, UAMS70: 13.0%, MRCIX6: 13.3%, EMC92: 19.1% and UAMS80: 23.4%. To determine which signature best explained the observed survival, pair-wise comparisons were performed. For every comparison the EMC92 is the strongest predictor for OS tested in an independent environment (Figure 3 and online Table S9).

There is a varying degree of overlapping probe sets between all signatures. Overlapping genes are shown in online Figure S3. Seven out of fifty probe sets present in the GPI50 overlap with the EMC92 signature (*BIRC5, FANCI, ESPL1, MCM6, NCAPG, SPAG5* and *ZWINT*). One of the six MRC-IX genes (*ITM2B*) is also seen in the EMC92. Overlap between EMC92 and the remaining signatures is limited (EMC92 vs. UAMS17/70: *BIRC5* and *LTBP1*; EMC92 vs. MILLENNIUM100: *MAGEA6* and *TMEM97* and EMC92 vs. IFM15: *FAM49A*).

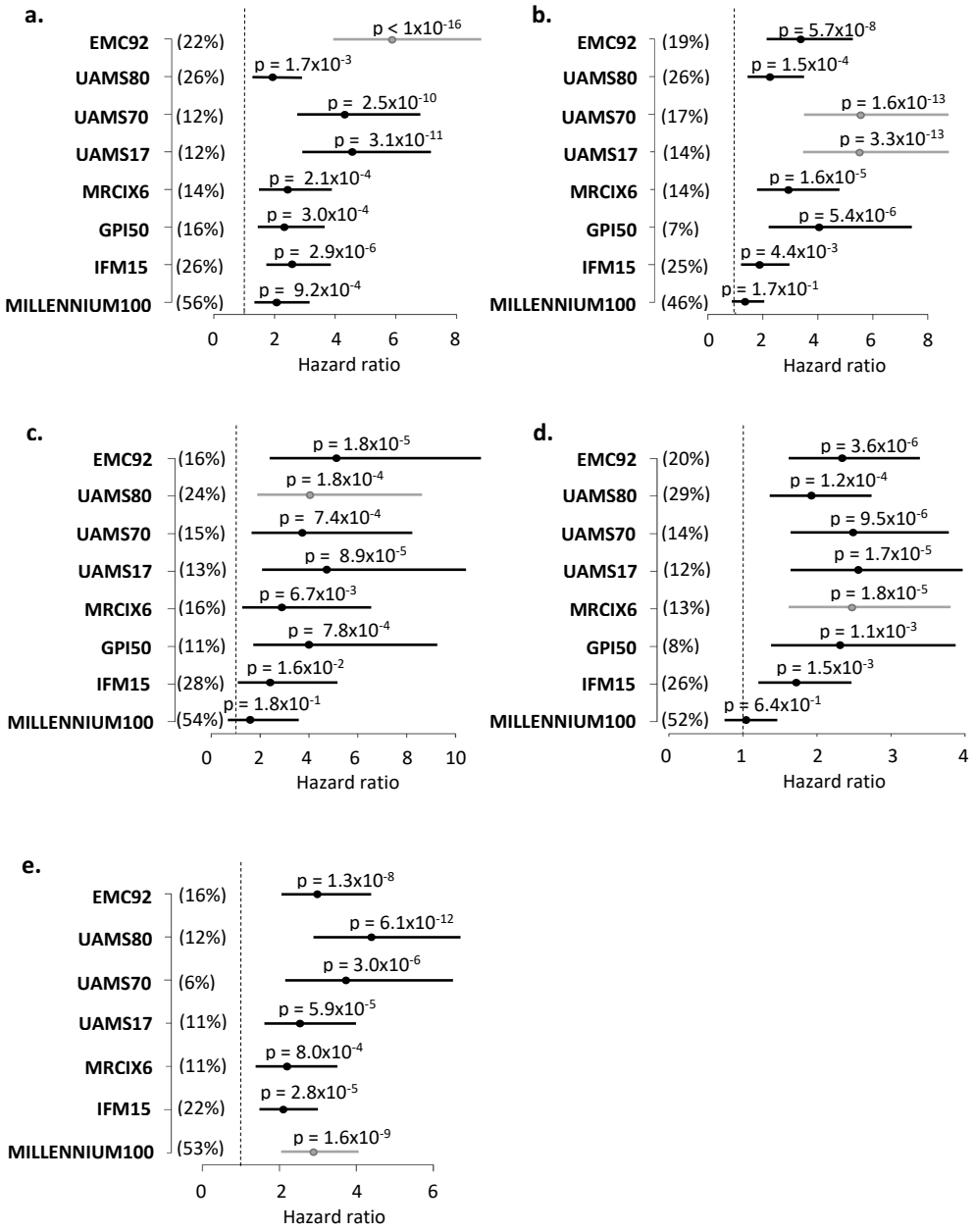

Figure 2. Performance per signature in available datasets. For every signature the hazard ratio (high-risk versus standard-risk) is shown with 95% confidence interval. Grey lines indicate results on training set. **a**) HOVON-65/GMMG-HD4, **b**) UAMS-TT2, **c**) UAMS-TT3, **d**) MRC-IX, **e**) APEX. *p*: *p*-value for equal survival in high and standard-risk groups; percentage: proportion of high-risk defined patients.

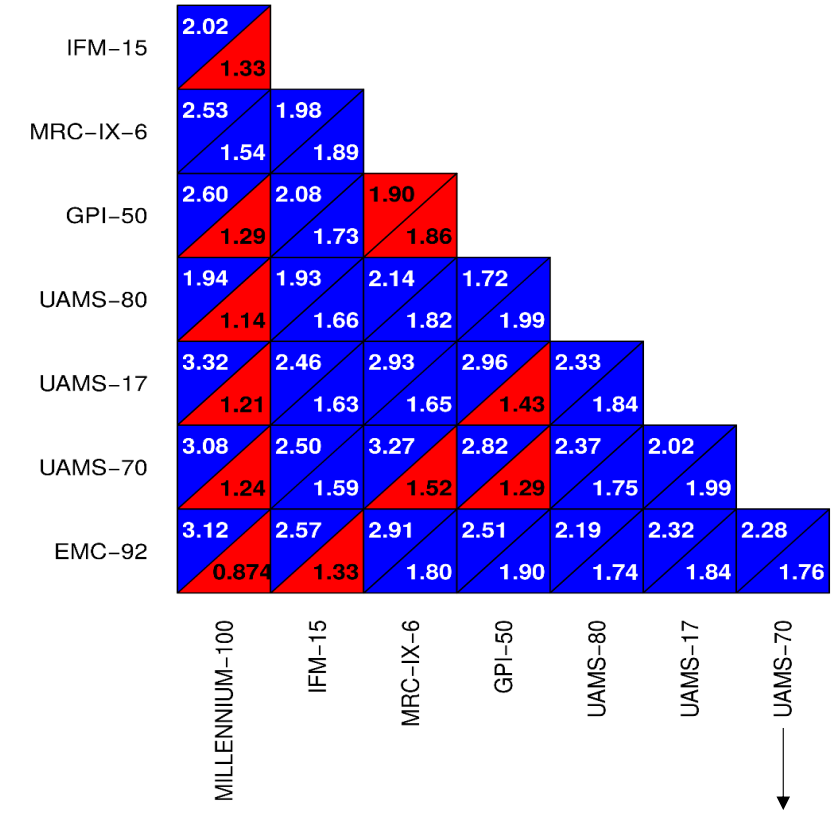

	Hazard ratio [95%CI]	p-value	Bonferroni
EMC92	2.3 [1.7 - 3.1]	4.3×10^{-8}	1.2×10^{-6}
UAMS70	1.8 [1.2 - 2.5]	2.1×10^{-3}	5.8×10^{-2}

Figure 3. Pair-wise comparison for all signatures. To find the signature best fitting the underlying datasets, Cox regression models (high-risk versus standard-risk) were made for all pair-wise signatures. These models are based on pooled independent datasets (i.e. excluding training sets) and stratified for study. The two paired hazard ratios associated with the signatures derived per model are shown in the two cells within the square panels. Only hazard ratios within one panel can be compared because these are based on the same dataset. Blue cells indicate significant hazard ratios (Bonferroni-Holm corrected p-value); red cells denote non-significant findings. For the bottom right panel (i.e. UAMS70 vs. EMC92 signatures) the underlying model is given. All other models can be found in online Table S9.

Combined risk classifiers

The performance of the EMC92 signature was in line with the UAMS signatures, although they were derived from quite different patient populations. The inter-

section of high-risk patients between the EMC92 and UAMS70 signatures was approximately 8% of the total population on the pooled datasets that were independent of both our training set and the UAMS70 training set (i.e. MRC-IX, TT3 and APEX; online Table S11). Approximately 13% of patients were classified as high-risk by either one of these signatures. The intersecting high-risk group had the highest hazard-ratio as compared to the intersecting standard-risk group (HR=3.9, $95\% CI\,[2.8-5.4]$, $p=\,3.6\times10^{-15}$). Patients classified as high-risk by either signature, showed an intermediate risk, i.e. with an HR of 2.4, $95\% CI\,[1.8-3.3]$, for the EMC92 signature ($p=\,5.1\times10^{-8}$) and an HR of 2.2, $95\% CI\,[1.2-4.1]$, for the UAMS70 signature ($p=\,1.1\times10^{-2}$; online Table S12). To test whether there is evidence for better performance if outcomes of two dichotomous predictors are merged, we took the models made in the pair-wise comparison (online Table S9) and tested these in a likelihood-ratio test against a single signature outcome model. Merging the EMC92 with UAMS80 ($p=\,2.2\times10^{-3}$), UAMS17 ($p=\,9.4\times10^{-3}$), GPI50 ($p=\,3.0\times10^{-2}$), MRCIX6 ($p=\,1.6\times10^{-2}$) and UAMS70 ($p=\,4.0\times10^{-2}$) demonstrated a better fit to the data than any of the single models (online Table S10).

EMC92 signature and FISH

To compare the high-risk populations composition as defined by the EMC92 and the UAMS70 signatures, cytogenetic aberration frequencies in both populations were determined using an independent set for which cytogenetic variables were known, i.e. MRC-IX (Figure 4 and online Table S13). As expected, poor prognostic cytogenetic aberrations gain(1q), del(17p), t(4;14), t(14;16), t(14;20) and del(13q) were enriched in the high-risk populations (Figure 5), whereas the standard-risk cytogenetic aberrations such as t(11;14) were diminished in the high-risk populations. In contrast, only 15% (6 out of 39) of MRC-IX cases with high-risk status as determined by the EMC92 signature showed absence of any poor prognostic cytogenetic aberrations, as opposed to 44% (74 out of 168) in standard-risk cases ($p=\,1.8\times10^{-3}$). Similarly, of the UAMS70 defined high-risk patients 4% (1 out of 23) did not have any poor prognostic cytogenetics, whereas of the UAMS70 defined standard-risk patients this proportion was 43% (79 out of 183) ($p=\,5.3\times10^{-3}$).

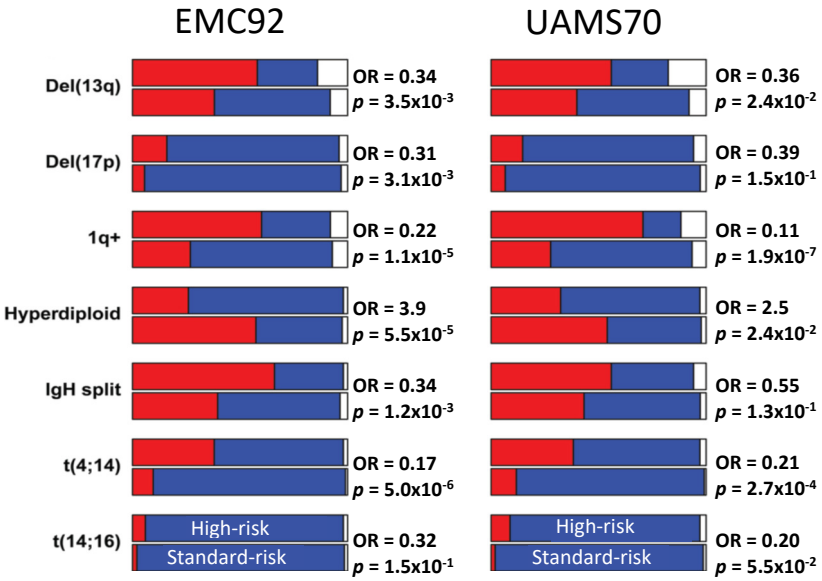

Figure 4. Distributions of high-risk and standard-risk patients per FISH marker in the MRC-IX dataset. Distribution of FISH markers within the high-risk (top panels) and standard-risk (bottom panels) groups for the EMC92 and UAMS70 signatures. The EMC92 and UAMS70 identified 50 and 42 patients out of 247 as high-risk, respectively. OR, Odds ratio; *p*, Fisher exact *p*-value; red, presence of an aberration; blue, absence of an aberration; white, missing data. Details are given in online Table S13.

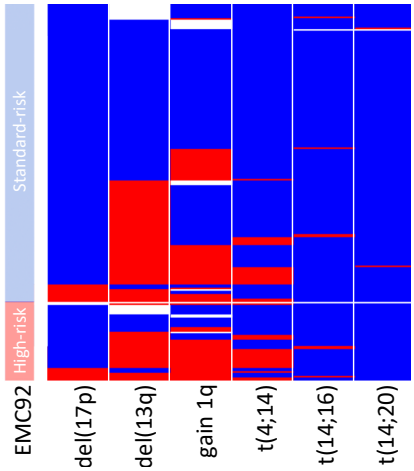

Figure 5. Poor prognostic cytogenetic aberrations in comparison to the EMC92 signature in MRC-IX patients. Each horizontal line represents one patient. The first column denotes the distinction between high-risk (in red, $n = 50$) and standard-risk (in blue, $n = 197$). Columns 2 to 7 represent cytogenetic aberrations as shown. Red, presence of an aberration; blue, absence and white, missing data. More than half of the EMC92 standard-risk patients are affected by one or more poor FISH markers.

DISCUSSION

Here we report on the generation and validation of the EMC92 signature, which was based on the HOVON65/GMMG-HD4 clinical trial. Conventional prognostic markers such as ISS stage and adverse cytogenetics have been augmented by signatures based on gene expression in order to increase accuracy in outcome prediction in MM. More accurate prognosis may lead to the development of treatment schedules which are specifically aimed at improving survival of high-risk MM patients. Prognostic signatures for MM include the UAMS70, the UAMS17, the UAMS80, the IFM15, the gene proliferation index (GPI50), the MRCIX6 and the MILLENNIUM100 signatures.

For clinical relevance, a signature must have both the ability to separate risk groups as clearly as possible and to predict stable groups of relevant size. The EMC92 signature meets both criteria. In all validation sets a high-risk group of patients can be significantly determined and the proportion of high-risk patients is stable across the validation sets. The validation sets represent different drug regimens, including thalidomide (MRC-IX, TT2) and bortezomib (APEX, TT3). Also the signature is relevant to both transplant eligible (e.g. TT3) and non-transplant eligible patients (subset of MRC-IX) as well as newly diagnosed (e.g. TT2) and relapsed patients (APEX).

In contrast, the predictions of the MRCIX6, GPI50, IFM15 and MILLENNIUM-100 were not as convincing as those of the EMC92 and UAMS signatures. Especially the predictions of the MILLENNIUM100 signature in the validation sets fail to reach significance in independent data sets such as MRC-IX, TT2 and TT3. The differences in gene expression platform may have contributed to this in part. Indeed, the IFM signature is based on a custom cDNA-based gene expression platform, rather than the Affymetrix GeneChips, which have become common for MM GEP studies.[32] The cDNA platforms have been reported to be difficult to compare with the Affymetrix oligonucleotide platform.[12] Although the MILLENNIUM100 signature was generated using Affymetrix GeneChips, the use of an earlier version of this platform may have contributed to the limited performance of this signature.[11] The performance of the EMC92 signature is comparable to the UAMS derived signatures, MRCIX6 and the GPI50, as measured by the significance of

prediction in validation sets. For the UAMS70 and GPI50 the proportion high-risk patients appears more variable, which may hinder clinical interpretation, especially when the high-risk proportion is less than 10%. Importantly, pair-wise comparisons of all the signatures evaluated in this paper demonstrated that the EMC92 has the best fit to the observed survival times in independent sets. Strikingly, we found that performance can be improved by simply combining signatures (e.g. EMC92 with UAMS80). However, this analysis is only an indication of the possibilities of combining signatures, and future work involving more complex combined signatures is in progress.

It is important to note that the genes within the signature reflect optimal performance of the signature rather than a biological definition of survival in MM. The initially selected 1093 probe sets which were found to be associated with PFS in univariate testing, are more likely to give a good representation of myeloma biology, as indicated for instance by the protein synthesis related pathways. Although an extended biological discussion is outside the scope of this paper, a number of interesting genes are included in the signature. *BIRC5* was found in 4 signatures evaluated in this paper: EMC92, UAMS17, UAMS70 and the GPI50. This gene is a member of the inhibitor of apoptosis gene family, which encodes negative regulatory proteins that prevent apoptotic cell death, and up-regulation has been described to be associated with lower EFS and OS in newly diagnosed MM patients.[11,12,31] Other important myeloma genes include *FGFR3* and *STAT1*. *FGFR3* is deregulated as a result of translocation t(4;14), which is an adverse prognostic cytogenetic event.[30] *FGFR3* - a transmembrane receptor tyrosine kinase - is involved in the regulation of cell growth and proliferation.[33] *STAT1* - an important component of the JAK/STAT signaling - is involved in multiple pathways including apoptosis induced by interferon signaling.[29]

A clear enrichment of the long arm of chromosome 1 was observed in the 1093 probe sets in this study. Previously the importance of chromosome 1 was reported for the UAMS70 signature. Genes on 1q in the UAMS70 signature include CKS1B and *PSMD4*, both of which were not in the EMC92 signature, although *CKS1B* was found to be associated with PFS in our set and thus in the 1093 set.[9,10] The EMC92 signature did contain 9 genes on 1q of which *S100A6* has been described in relation to 1q21 amplification in MM and other cancer

types.[34] This may also be part of the explanation why, despite the use of the same GEP platform, the overlap between different signatures is limited. Indeed, multiple genes are found within the 1q21 amplicon with downstream factors possibly over-expressed as a result of this. Which gene will be linked most significantly to survival in a specific set is most likely due to factors such as variability in datasets, to which population differences and differences in used techniques may contribute. Other reasons may be found in the difference in treatment strategies used, in which other genes could be responsible for adverse prognosis.

To characterize the high-risk group in depth, we have demonstrated that in the MRC-IX study, high-risk patients are enriched for poor cytogenetic aberrations gain(1q), del(17p), t(4;14), t(14;16), t(14;20) and del(13q). Still more than half of the patients in the standard-risk group showed one or more poor prognostic cytogenetic markers indicating that the occurrence of a single poor-risk marker does not have very strong prognostic value.

Clinical use of a gene signature (UAMS70) has recently been incorporated in the mSMART risk stratification, which additionally includes FISH, metaphase cytogenetics, and plasma cell labeling index. The mSMART risk stratification is the first risk stratification system adjusting treatment regimens according to risk status, although this has not been validated in prospective clinical trials.[15,35] Ultimately, clinical use of any signature must be proven to be of use in prospective clinical trials, which allow treatment choice based on risk assessment. This will result in clinical guidelines to improve treatment of patients with a poor PFS and OS on novel therapies. For practical application of the EMC92 signature it is essential to stress that this signature has not been designed for classification of a single patient. However, collection of a set of more than ~ 25 patients will result in reliable prediction, and each additional patient can be predicted as soon as it is tested.

In conclusion, we developed a risk signature highly discriminative for patients with high-risk versus standard-risk MM, irrespective of treatment regime, age and relapse setting. Use of this signature in the clinical setting may lead to a more informed treatment choice and potentially better outcome for the patient.

REFERENCES

1. Avet-Loiseau H. Ultra high-risk myeloma. *Am. Soc. Hematol. Educ. Program.* . 2010; :489–493.
2. Palumbo A & Anderson K. Multiple myeloma. *N. Engl. J. Med.* . 2011; **17**(364):1046–1060.
3. Munshi NC, Anderson KC, Bergsagel PL, *et al.* Consensus recommendations for risk stratification in multiple myeloma: report of the International Myeloma Workshop Consensus Panel 2. *Blood* . 2011; **117**(18):4696–700.
4. Neben K, Jauch A, Bertsch U, *et al.* Combining information regarding chromosomal aberrations t(4;14) and del(17p13) with the International Staging System classification allows stratification of myeloma patients undergoing autologous stem cell transplantation. *Haematologica* . 2010; **95**(7):1150–7.
5. Bergsagel PL, Kuehl WM, Zhan F, Sawyer J, Barlogie B, & Shaughnessy J J. Cyclin D dysregulation: an early and unifying pathogenic event in multiple myeloma. *Blood* . 2005; **106**(1):296–303.
6. Zhan F, Huang Y, Colla S, *et al.* The molecular classification of multiple myeloma. *Blood* . 2006; **108**(6):2020–2028.
7. Broyl A, Hose D, Lokhorst H, *et al.* Gene expression profiling for molecular classification of multiple myeloma in newly diagnosed patients. *Blood* . 2010; **116**(14):2543–53.
8. Chng WJ, Kuehl WM, Bergsagel PL, & Fonseca R. Translocation t(4;14) retains prognostic significance even in the setting of high-risk molecular signature. *Leukemia* . 2008; **22**(2):459–61.
9. Shaughnessy J J D, Zhan F, Burington BE, *et al.* A validated gene expression model of high-risk multiple myeloma is defined by deregulated expression of genes mapping to chromosome 1. *Blood* . 2007; **109**(6):2276–2284.
10. Shaughnessy J J D, Qu P, Usmani S, *et al.* Pharmacogenomics of bortezomib test-dosing identifies hyperexpression of proteasome genes, especially PSMD4, as novel high-risk feature in myeloma treated with total therapy 3. *Blood* . 2011; **118**:3512–3524.
11. Mulligan G, Mitsiades C, Bryant B, *et al.* Gene expression profiling and correlation with outcome in clinical trials of the proteasome inhibitor bortezomib. *Blood* . 2007; **109**(8):3177–3188.
12. Decaux O, Lode L, Magrangeas F, *et al.* Prediction of survival in multiple myeloma based on gene expression profiles reveals cell cycle and chromosomal instability signatures in high-risk patients and hyperdiploid signatures in low-risk patients: a study of the Intergroupe Francophone du Myelome. *J Clin Oncol* . 2008; **26**(29):4798–4805.
13. Dickens NJ, Walker BA, Leone PE, *et al.* Homozygous deletion mapping in myeloma samples identifies genes and an expression signature relevant to pathogenesis and outcome. *Clin Cancer Res* . 2010; **16**(6):1856–1864.
14. Hose D, Reme T, Hielscher T, *et al.* Proliferation is a central independent prognostic factor and target for personalized and risk-adapted treatment in multiple myeloma. *Haematologica* . 2011; **96**(1):87–95.
15. Dispenzieri A, Rajkumar SV, Gertz MA, *et al.* Treatment of newly diagnosed multiple myeloma

based on Mayo Stratification of Myeloma and Risk-adapted Therapy (mSMART): consensus statement. *Mayo Clin Proc* . 2007; **82**(3):323–41.

16. Sonneveld P, Schmidt-Wolf I, van der Holt B, *et al.* HOVON-65/GMMG-HD4 Randomized Phase III Trial Comparing Bortezomib, Doxorubicin, Dexamethasone (PAD) Vs VAD Followed by High-Dose Melphalan (HDM) and Maintenance with Bortezomib or Thalidomide In Patients with Newly Diagnosed Multiple Myeloma (MM). *Blood* . 2010; **116**(21):40–40.

17. Pineda-Roman M, Zangari M, Haessler J, *et al.* Sustained complete remissions in multiple myeloma linked to bortezomib in total therapy 3: comparison with total therapy 2. *Br J Haematol* . 2008; **140**(6):625–634.

18. Barlogie B, Pineda-Roman M, van Rhee F, *et al.* Thalidomide arm of Total Therapy 2 improves complete remission duration and survival in myeloma patients with metaphase cytogenetic abnormalities. *Blood* . 2008; **112**(8):3115–3121.

19. Morgan GJ, Davies FE, Gregory WM, *et al.* Thalidomide Maintenance Significantly Improves Progression-Free Survival (PFS) and Overall Survival (OS) of Myeloma Patients When Effective Relapse Treatments Are Used: MRC Myeloma IX Results. *Blood* . 2010; **116**(21):623–623.

20. Morgan GJ, Davies FE, Owen RG, *et al.* Thalidomide Combinations Improve Response Rates; Results from the MRC IX Study. *Blood* . 2007; **110**(11):3593–3593.

21. Jagannath S, Barlogie B, Berenson J, *et al.* A phase 2 study of two doses of bortezomib in relapsed or refractory myeloma. *Br Journal Haematol* . 2004; **127**(2):165–172.

22. Richardson PG, Sonneveld P, Schuster MW, *et al.* Bortezomib or high-dose dexamethasone for relapsed multiple myeloma. *N Engl J Med* . 2005; **352**(24):2487–2498.

23. Richardson PG, Barlogie B, Berenson J, *et al.* A phase 2 study of bortezomib in relapsed, refractory myeloma. *N Engl J Med* . 2003; **348**(26):2609–2617.

24. Gentleman RC, Carey VJ, Bates DM, *et al.* Bioconductor: open software development for computational biology and bioinformatics. *Genome Biol* . 2004; **5**(10):R80.

25. Johnson WE, Li C, & Rabinovic A. Adjusting batch effects in microarray expression data using empirical Bayes methods. *Biostatistics* . 2007; **8**(1):118–27.

26. Therneau & Lumley T. survival: Survival analysis, including penalised likelihood. *R package version 2.36-2* . 2010; .

27. Bair E, Hastie T, Paul D, & Tibshirani R. Prediction by Supervised Principal Components. *J Amer Statistical Assoc* . 2006; **101**(473):119–137.

28. Benjamini Y & Hochberg Y. Controlling the False Discovery Rate: A Practical and Powerful Approach to Multiple Testing. *J Roy Stat Soc B Met* . 1995; **57**(1):289–300.

29. Arulampalam V, Kolosenko I, Hjortsberg L, Bjorklund AC, Grander D, & Tamm KP. Activation of STAT1 is required for interferon-alpha-mediated cell death. *Exp Cell Res* . 2011; **317**(1):9–19.

30. Chesi M, Nardini E, Brents LA, *et al.* Frequent translocation t(4;14)(p16.3;q32.3) in multiple myeloma is associated with increased expression and activating mutations of fibroblast growth factor receptor 3. *Nat Genet* . 1997; **16**(3):260–4.

31. Hideshima T, Catley L, Raje N, *et al.* Inhibition of Akt induces significant downregulation of survivin and cytotoxicity in human multiple myeloma cells. *Br J Haematol* . 2007; **138**(6):783–91.

32. Mah N, Thelin A, Lu T, *et al.* A comparison of oligonucleotide and cDNA-based microarray systems. *Physiol Genomics* . 2004; **16**(3):361–70.

33. Trudel S, Ely S, Farooqi Y, *et al.* Inhibition of fibroblast growth factor receptor 3 induces differentiation and apoptosis in t(4;14) myeloma. *Blood* . 2004; **103**(9):3521–8.

34. Inoue J, Otsuki T, Hirasawa A, *et al.* Overexpression of PDZK1 within the 1q12-q22 amplicon is likely to be associated with drug-resistance phenotype in multiple myeloma. *Am J Pathol* . 2004; **165**(1):71–81.

35. Kumar SK, Mikhael JR, Buadi FK, *et al.* Management of newly diagnosed symptomatic multiple myeloma: updated Mayo Stratification of Myeloma and Risk-Adapted Therapy (mSMART) consensus guidelines. *Mayo Clin Proc* . 2009; **84**(12):1095–110.

CHAPTER 3

Prediction of High- and Low-Risk Multiple Myeloma Based on Gene Expression and the International Staging System

Rowan Kuiper, Mark van Duin, Martin H. van Vliet, Annemiek Broijl, Bronno van der Holt, Laila el Jarari, Erik van Beers, George Mulligan, Hervé Avet-Loiseau, Walter M. Gregory, Gareth Morgan, Hartmut Goldschmidt, Henk M. Lokhorst & Pieter Sonneveld

Blood 2015; **126**:1996-2004

ABSTRACT

Patients with multiple myeloma have variable survival, and require reliable prognostic and predictive scoring systems. Currently, clinical and biological risk markers are used independently. Here, ISS, FISH markers and gene expression (GEP) classifiers were combined to identify novel risk classifications in a discovery/validation setting.

We used the datasets of HOVON-65/GMMG-HD4, UAMS-TT2, UAMS-TT3, MRC-IX, APEX and Intergroupe Francophone du Myelome (IFM-G) (total number of patients: 4750). A total of 20 risk markers were evaluated including t(4;14) and deletion of 17p (FISH), EMC92 and UAMS70 (GEP classifiers) and ISS.

The novel risk classifications demonstrated that ISS is a valuable partner to GEP classifiers and FISH. Ranking all novel as well as existing risk classifications showed that the EMC92-ISS combination is the strongest predictor for overall survival, resulting in a four group risk classification. The median survival was 24 months for the highest risk group, 47 and 61 months for the intermediate risk groups and median not reached after 96 months for the lowest risk group.

The EMC92-ISS classification is a novel prognostic tool, based on biological and clinical parameters, which is superior to current markers and offers a robust clinically relevant 4-group model.

INTRODUCTION

In multiple myeloma (MM) patients, malignant plasma cells accumulate in the bone marrow, leading to a wide range of clinical symptoms which include bone disease, hypercalcemia, renal impairment and anemia.[1] The prognosis is variable, with survival for newly diagnosed patients ranging from less than two to more than twenty years.[2] Adequate prognostication of disease outcome is important in order to make treatment choices and to allocate high-risk patients to alternative treatment options. Clinical trials that address specific treatment of high-risk patients include TT4, TT5 and MUK9 (TT4: Total Therapy 4, NCT00734877; TT5: Total Therapy 5, NCT02128230; MUK9, OPTIMUM trial, Myeloma UK Clinical Trial Network).

Heterogeneous treatment outcome can in part be explained by different biological subgroups in MM, which are characterized by primary translocations involving genes such as MMSET (t(4;14)), and c-MAF (t(14;16)).[3,4] These subgroups can be identified using gene expression profiling.[5,6] In addition, gene expression profiling has been utilized to establish classifiers for prognostication. The EMC92 is a robust risk marker for the identification of high-risk MM, and was validated in independent clinical trials showing a solid and independent performance in comparison to other MM GEP classifiers such as UAMS70.[7–13] Clinical prognostic systems for MM, are primarily based on beta2-microglobulin (B2m), albumin, lactate dehydrogenase, C-reactive protein, calcium and creatinine.[14,15] The International Staging System (ISS) is based on B2m and albumin, with stage I representing limited disease, stage II intermediate and stage III the most unfavorable disease.[16] Today it is used as the standard clinical risk classification for MM.

FISH based cytogenetics and gene expression profiling are biology based prognostic markers.[17] ISS was combined with high-risk cytogenetic markers t(4;14) and deletion of 17p (del(17p)) to establish novel prognostic risk classifications as proposed by Neben and Avet-Loiseau.[18,19] Recently, serum lactate dehydrogenase (LDH) was added as a component to this marker combination.[20] Other prognostic systems include combinations of cytogenetic markers, such as the combination of del(17p), translocation t(4;14) and gain of 1q (gain(1q)).[21]

The goal of this study was to evaluate all published risk markers used in MM and to compare combinations of FISH, ISS and GEP based prognostic systems. By applying a study design with independent discovery and validation sets, we demonstrated that ISS can be combined with gene expression signatures into powerful classifiers for MM.

MATERIALS AND METHODS

Clinical data

The clinical data from the the Dutch-Belgium Hemato-Oncology Group (HOVON) and German-speaking Myeloma Multicenter Group (GMMG) (HO65/HD4), Medical Research Council-IX (MRC-IX), University of Arkansas for Medical Sciences Total Therapy (UAMS-TT2 and TT3), Intergroupe Francophone du Myelome (IFM-G; all newly diagnosed patients) and APEX (relapse patients) trials were used.[7–9,19,22,23] The IFM-G cohort is a clinical database of patients not separately published and was included in the ISS development.[16] Treatment regimens of the trials from which these datasets were derived are summarized in Table 1. Overall survival (OS) or progression-free survival (PFS) and at least one prognostic marker were available for all patients (Table 1; Figure S1). All patients signed an informed consent in accordance with the Declaration of Helsinki and all protocols were approved by institutional review boards.

Gene expression profiling (GEP)

All GEP data are Affymetrix HG U133 Plus 2.0 platform based, except for the APEX study (Affymetrix U133 A/B platform). HO65/HD4 GEP was performed in our lab as described previously ($n = 327$; GEO series GSE19784).[6,7,21] Other GEP sets were: TT2 ($n = 345$; GSE24080)[8], TT3 ($n = 238$; E-TABM-1138 and GSE24080)[24], MRC-IX ($n = 247$; GSE15695)[22] and APEX ($n = 264$; GSE9782).[23] Due to unavailable survival data, the Heidelberg-Montpellier (HM) dataset ($n = 206$; E-MTAB-362), was used only to determine the probe set means and variances for the training set of the HM19 classifier.[12]

Standard prognostic markers

Availability of risk markers and patients per dataset is shown in Table 1 and Figure S1. The International staging system (ISS) was determined by combining serum levels of β2M and albumin.[16] Cytogenetics by Fluorescence in situ hybridization (FISH) was used with a 10% cut-off level except for a 20% cut-off used for numerical abnormalities in the MRC-IX trial.[19,25–27] Gain of chromo-

Table 1. Distribution of risk markers and treatments per dataset. The numbers of patients per data set are given with in brackets the number or percentage of positive patients according to the markers' risk classification.

	HO65/HD4	MRC-IX	
		Intensive	**Non-intensive**
N	827	701	491
median age [IQR][yrs]	57 (51 - 61)	58 (54 - 63)	74 (70-77)
Treatment [n]	PAD (413)	CTD(351)	CTDa(257)
Control	VAD(414)	CVAD(350)	MP(234)
High-dose alkylator	YES	YES	NO
EMC92 [n (% high)]	*	138 (17%)	109 (24%)
UAMS17	327 (12%)	138 (9%)	109 (16%)
UAMS70	327 (9%)	138 (7%)	109 (10%)
UAMS80	327 (8%)	138 (8%)	109 (9%)
MRCIX6	327 (5%)	*	*
IFM15	327 (25%)	138 (25%)	109 (28%)
HM19 (low/medium/high%)	327 (34/51/15%)	138 (45/48/7%)	109 (39/53/8)
GPI50	327 (34/51/15%)	138 (52/41/7%)	109 (52/38/10)
ISS [n (1/2/3%)]	756 (38/37/25)	636 (25/39/36)	449 (13/41/45)
t(4;14) [n (% positive)]	429 (12%)	619 (12%)	434 (10%)
t(11;14)	437 (16%)	617 (15%)	434 (12%)
t(14;16)	360 (2%)	612 (3%)	434 (3%)
t(14;20)	255 (0%)	612 (2%)	429 (1%)
IgH split	327 (48%)	609 (44%)	429 (40%)
gain 1q	344 (32%)	531 (37%)	371 (41%)
del(13q)	686 (41%)	612 (46%)	428 (43%)
del(17p)	351 (11%)	591 (8%)	423 (9%)
gain 9	454 (57%)	480 (60%)	351 (66%)
HR.FISH.A [n(%)]	354 (46%)	535 (48%)	368 (48%)
HR.FISH.B/ISS [n(1/2/3%)]	334 (60/22/18)	*	

*, training set for these markers. Only the proportion and number that are not used for building the marker, if any, are shown.

**, intersection of patients with available data between datasets is shown in Figure S1.

***, the HR.FISH.A compound risk classification is based on a patient having either del(17p), t(4;14) or gain of 1q. If only gain of 1q is known (in TT2 patients), these are the only patients classified with certainty as high-risk. The remaining patients cannot be classified, since the status of t(4;14) and del(17p) are unknown. If the missing bias is strong enough (see methods), that marker is excluded from the combination analyses.

	TT2	TT3	APEX	IFM-G	POOLED
	351	238	264	1878	4750**
	57 (49-64)	60 (53-66)	61 (54-67)	57 (51-61)	57 (51-62)
	TD(175)	VTD(238)	BOR(188)	VD(740)	BOR(1579)/THAL(783)
	MD(176)	No controls	DEX(76)	VAD(1138)	BOR(1628)/THAL(760)
	YES	YES	YES	YES	
	345 (19%)	238 (15%)	264 (16%)		1094 (18%)
	*	238 (14%)	264 (12%)		1076 (12%)
	*	238 (12%)	264 (8%)		1076 (9%)
	345 (9%)	*	264 (7%)		1183 (8%)
	345 (7%)	238 (5%)	264 (3%)		1174 (5%)
	345 (24%)	238 (24%)			1157 (25%)
	345 (50/47/8)	238 (47/47/7)	264 (41/50/8)		1420 (44/48/8)
	345 (63/31/7)	238 (58/34/8)			1159 (51/39/10)
		208 (50/28/21)	202 (34/33/33)	1475 (34/39/28)	4074 (34/37/30)
				1635 (14%)	3180 (13%)
					1488 (15%)
				456 (4%)	1862 (3%)
					1296 (1%)
					1410 (44%)
		248 (47%)		891 (37%)	2385 (38%)
				1807 (48%)	3522 (46%)
				1651 (15%)	3016 (12%)
					1285 (60%)
		116 (100%)***		1022 (64%)	2395 (57%)
				516 (55/29/17)	850 (57/26/17)

PAD: bortezomib, doxorubicin, dexamethasone; **VAD**: vincristine, doxorubicin, dexamethasone; **CVAD**: cyclophosphamide, vincristine, doxorubicin, dexamethasone; **MP**: melphalan, prednisone; **CTD(a)**: (attenuated) cyclophosphamide, thalidomide, dexamethasone; **VTD**: bortezomib, thalidomide, dexamethasone; **(V)MD**: (bortezomib,) melphalan, dexamethasone;**VD**: vincristine, dexamethasone; **BOR**: bortezomib; **THAL**: thalidomide.

some 9 (gain(9)) - one of the hyperdiploid chromosomes and most frequently available marker for this purpose - was used as a proxy for hyperdiploidy.[28] FISH probes used in MRC-IX and HO65/HD4 were described before.[25,29] Cytogenetic data obtained by methods other than FISH were excluded. High risk FISH was defined as having either del(17p) or t(4;14) or gain(1q), denoted here as HR.FISH.A.[21] The risk classification described by Avet-Loiseau *et al.* is denoted here as HR.FISH.B/ISS.[19] This risk classification distinguishes grade-I (ISS=1 or 2 with FISH markers t(4;14) and del(17p) both negative), grade-II (not grade-I or III) and grade-III (ISS=2 or 3 with FISH markers t(4;14) or del(17p) positive). In case of an arbitrary situation due to missing data for one of the markers, the observation was excluded.

Gene expression classifiers

The following MM gene expression classifiers were used: EMC92[7], UAMS17[8], UAMS70[8], UAMS80[9], IFM15[10], MRCIX6[13] (all two risk group classifiers) and HM19[12], GPI50[11] (both three risk group classifiers). Normalization and cut-offs were calculated as described previously (see online supplemental methods for a brief description).

Statistical analyses

In Figure 1, a flowchart of the analyses is given. The association of risk markers with survival was assessed using a Cox survival model (R 'survival' package, version 2.38-1).[30–32] To account for heterogeneous survival between studies, models were stratified per trial cohort. The trial cohorts were HO65/HD4, MRC-IX intensive, MRC-IX non-intensive, UAMS-TT2, UAMS-TT3, IFM-G and APEX. Datasets used for generating risk markers were systematically excluded in validation analyses in order to avoid training bias. For instance, HO65/HD4 patients were excluded in analyses involving the EMC92 classifier (Table 1). The method for finding novel combination markers (compound markers) is illustrated in online Figure S2b and extensively described in the online supplemental methods. Briefly, since missing data may confound the analyses, combinations with increased risk for confounding were excluded (Table S1; online supplemental methods). Subsequently, the data were randomly split into a discovery and validation set. The

discovery set was used for finding meaningful combinations of markers as well as the most optimal way to split patients into subgroups, using these combinations. Stringent validation was performed in the designated validation set to confirm their prognostic strength. Finally, all new combinations and existing markers were ranked, with a low rank score indicating a high performing risk marker.

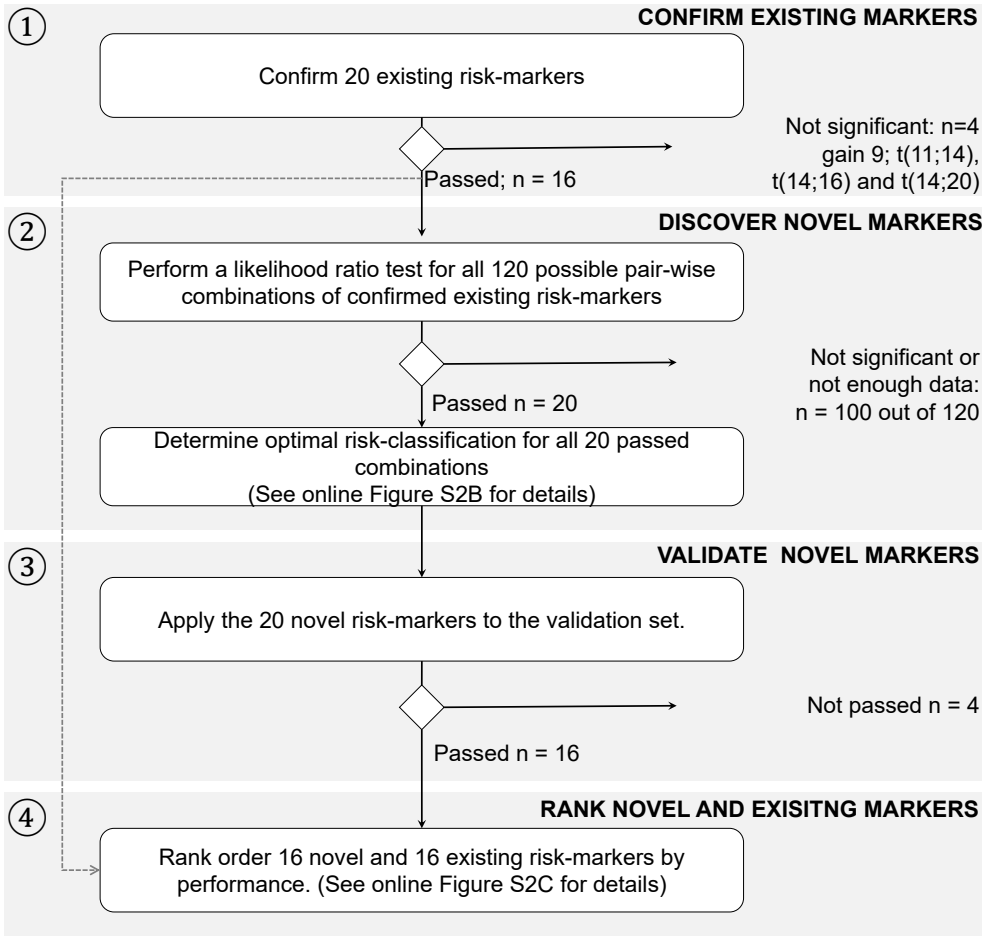

Figure 1. Flowchart of analyses. The analyses are organized as follows: **1**) confirmation of existing risk markers, **2**) systematically finding novel risk markers with improved prognostic strength by combining existing risk markers and **3**) validating them; **4**) ranking of confirmed existing- and validated novel risk markers. See Figure S2a-c for more details.

RESULTS

Confirmation of existing risk markers

The value of 20 existing risk markers was evaluated in a data set of 4750 patients. The markers and used cohorts are given in Table 1. The prognostic value was evaluated correcting for the differences in survival between cohorts (Figure 2, online Figures S3-S5 and Table S2). For all markers at least 2 cohorts were available. All gene expression (GEP) classifiers demonstrated a highly significant performance for OS. Hazard ratios for GEP classifiers ranged from 2.0 ($95\% CI\,[1.6 - 2.4]$; IFM15) up to $3.3\,(2.6 - 4.3]$ (UAMS70). Furthermore, hazard ratios for GEP classifiers were consistently higher than any of the other risk markers, including all FISH markers and ISS. This suggests better risk separation for GEP classifiers compared to FISH markers. GEP classifiers generally performed better for OS than for PFS (Figures S3A-B, S4 and S5; Table S2) with PFS hazard ratios between $1.8\,[1.5 - 2.1]$ (IFM15) up to $2.3\,[1.9 - 2.7]$ (EMC92). The percentage of high-risk patients varied between classifiers: 18% (EMC92), 12% (UAMS17), 10% (GPI50), 9% (UAMS70), 8% (UAMS80 and HM19; Table 1).

FISH markers with prognostic strength can be distinguished from markers with no or disputable value. For OS, markers t(4;14), del(17p), gain(1q) and del(13q) performed well with hazard ratios ranging between 1.7, $95\% CI\,[1.5 - 1.8]$ for del(13q) up to $2.3\,[2.0 - 2.6]$ for del(17p). The markers gain9, t(11;14), t(14;16) and t(14;20) were clearly not significant or had high variance due to lack of predictive value or small number of positive cases. These markers were excluded from further analyses. A similar pattern was found for PFS, but the strength of the markers was generally lower with PFS hazard ratios ranging from $1.4\,[1.3 - 1.5]$ (del(13q)) up to $1.8\,[1.6 - 2.0]$(t(4;14)).

ISS was confirmed as a valuable and highly significant prognostic marker. A hazard ratio of 1.6 $95\% CI\,[1.4 - 1.8]$ (ISS = 2) and $2.3\,[2.1 - 2.6]$ (ISS = 3) was found for OS and $1.4\,[1.3 - 1.6]$ (ISS = 2) and $1.7\,[1.6 - 1.9]$ (ISS = 3) for PFS.Other previously published compound risk markers, denoted here as HR.FISH.A[21] (either t(4;14) or del(17p) or gain(1q)) and a combined FISH/ISS marker (HR.FISH.B-/ISS)[19] showed good performance. The hazard ratio was $2.3\,[2.0 - 2.5]$ (HR.FISH.A).

For the three group HR.FISH.B/ISS risk classification, hazard ratios of $1.8\,[1.4-2.4]$ (intermediate risk) and $3.6\,[2.7-4.7]$ (high-risk) were found.

To correct for heterogeneity between studies, all analyses were corrected for the survival differences between trials as a result of differences in treatment, disease stage and patient populations. To evaluate the effect of this correction, all analyses were repeated per cohort and highly similar results were obtained, suggesting that these risk markers perform similarly across different cohorts (online supplemental results).

Pair-wise combinations of risk markers

The next analysis was performed to explore combinations of risk markers. As indicated above, 16 of 20 evaluated markers had significant associations with OS and/or PFS. Based on these 16, all possible pair-wise combinations were generated. Twenty combinations were significant in the discovery set of which 16 remained significant in the independent validation set (Figure 2, online Figure S8a-b and Table S2-S3). In 10 of 16 combinations, ISS was combined with either GEP classifiers ($n = 5$) or FISH markers ($n = 5$), illustrating the strong additive power of ISS to these markers. Combinations of GEP ($n = 3$) and FISH markers were observed ($n = 3$), but no combinations of FISH with GEP. Two combinations divided patients in 3 groups, ten in 4 groups and four into 5 groups.

Ranking of existing and novel markers

The markers described above, i.e. 16 existing plus 16 validated new risk markers, were ranked on the basis of performance, as described in the Supplemental methods. ISS-GEP combinations consistently ranked at the top with the EMC92-ISS compound risk marker having the best median rank score (RS) (Figure 3; $RS = 0.05$). Other high scoring markers included ISS-UAMS17 ($RS = 0.11$), ISS-HM19 ($RS = 0.13$) and ISS-UAMS70 ($RS = 0.19$). The HR.FISH.B/ISS compound marker ranked in 5^{th} place ($RS = 0.20$) and ISS ranked in 23^{rd} place (out of 32; $RS = 0.61$). In general, compound markers tended to score better than single markers. The best single marker was EMC92 in 7^{th} position ($RS = 0.26$).

EMC92-ISS classifies patients into four groups with proportions of 38%, 24%, 22% and 17% for the lowest to the highest risk group, respectively (Figure 4A-B).

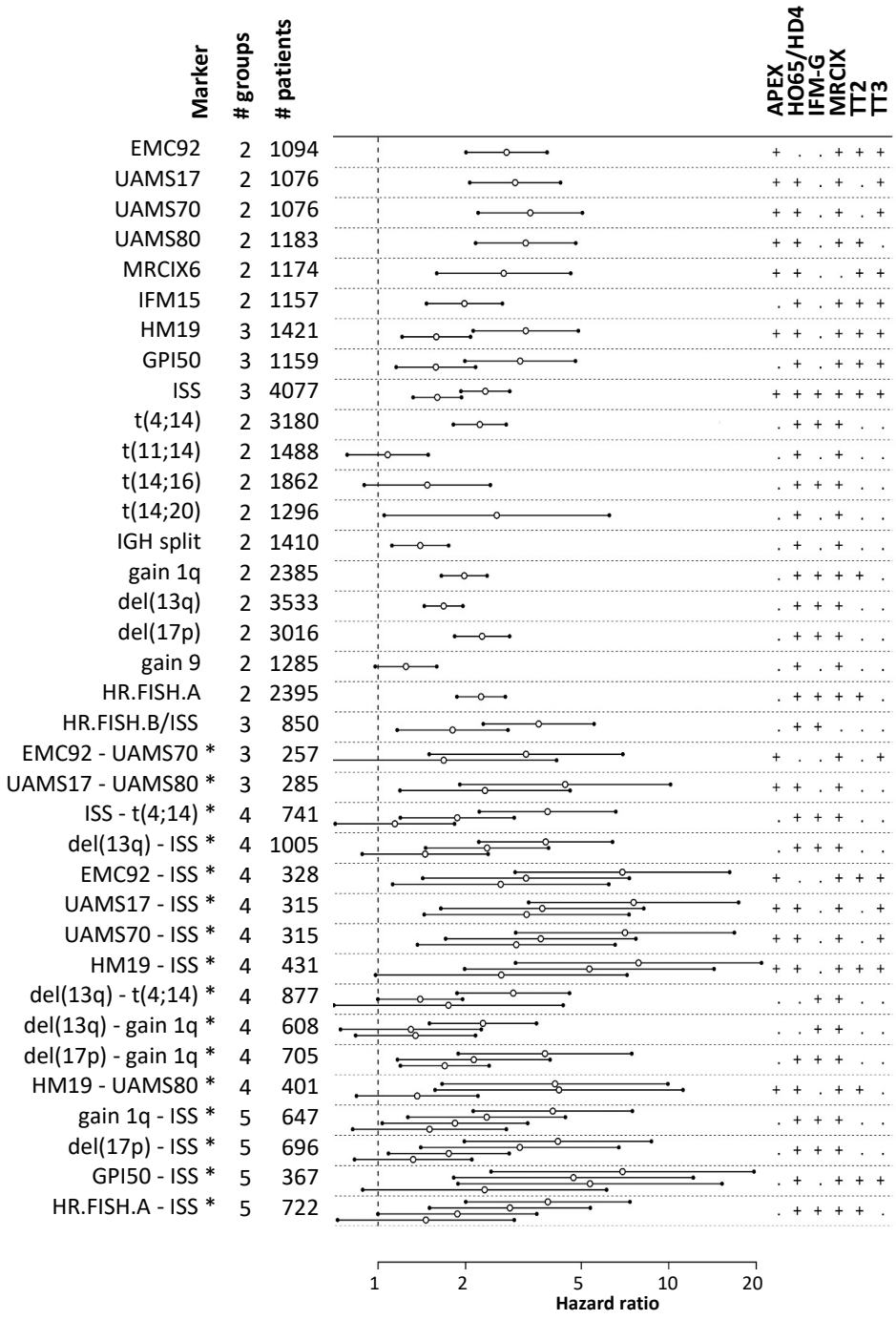
Marker
groups
patients
APEX
HO65/HD4
IFM-G
MRCIX
TT2
TT3
EMC92 2 1094 + . . + + +
UAMS17 2 1076 + + . + . +
UAMS70 2 1076 + + . + . +
UAMS80 2 1183 + + . + + .
MRCIX6 2 1174 + + . . + +
IFM15 2 1157 . + . + + +
HM19 3 1421 + + . + + +
GPI50 3 1159 . + . + + +
ISS 3 4077 + + + + + +
t(4;14) 2 3180 . + + + . .
t(11;14) 2 1488 . + . + . .
t(14;16) 2 1862 . + + + . .
t(14;20) 2 1296 . + . + . .
IGH split 2 1410 . + . + . .
gain 1q 2 2385 . + + + + .
del(13q) 2 3533 . + + + . .
del(17p) 2 3016 . + + + . .
gain 9 2 1285 . + . + . .
HR.FISH.A 2 2395 . + + + + .
HR.FISH.B/ISS 3 850 . + + . . .
EMC92 - UAMS70 * 3 257 + . . + . +
UAMS17 - UAMS80 * 3 285 + + . + . .
ISS - t(4;14) * 4 741 . + + + . .
del(13q) - ISS * 4 1005 . + + + . .
EMC92 - ISS * 4 328 + . . + + +
UAMS17 - ISS * 4 315 + + . + . +
UAMS70 - ISS * 4 315 + + . + . +
HM19 - ISS * 4 431 + + . + + +
del(13q) - t(4;14) * 4 877 . . + + . .
del(13q) - gain 1q * 4 608 . . + + . .
del(17p) - gain 1q * 4 705 . + + + . .
HM19 - UAMS80 * 4 401 + + . + + .
gain 1q - ISS * 5 647 . + + + . .
del(17p) - ISS * 5 696 . + + + . .
GPI50 - ISS * 5 367 . + . + + +
HR.FISH.A - ISS * 5 722 . + + + + .
1
2
5
10
20
Hazard ratio

Figure 2. Risk markers in relation to overall survival. Both existing markers and validated novel combinations are shown. For novel combinations, the results shown represent the validation. For confirmation of existing markers no discovery/validation split is required and results shown are based on all available data. In the left panel, existing markers and novel combinations (denoted by an asterisk) are listed. For each marker, the number of risk groups (#groups) and number of available patients is given (# patients). Markers are sorted by the number of risk groups. In the center panel, the hazard ratios are shown (open circle), with Bonferroni adjusted 95% confidence intervals (indicated by two lines and closed circles). For coherent notation, hazard ratios are expressed relative to the lowest risk group. Every additional risk group results in an extra hazard ratio. For instance, for the novel combination EMC92 – ISS, 4 risk groups result in 3 hazard ratios, as indicated in the text and Table S2A (intermediate low risk relative to low risk: hazard ratio (HR) 2.6, 95%CI [1.6 - 4.5] intermediate high-risk relative to low risk: HR: 3.2, 95%CI [1.9 - 5.4] and high-risk relative to low risk: HR 6.9, 95%CI [4.1 - 12]. In the right panel, a plus sign indicates whether a data set could be used for the analysis of a specific marker or combination (for details of available data, see Table 1 and Figure S1). For the EMC92-ISS combination, the following datasets could be used: APEX, MRC-IX, TT2 and TT3.

The hazard ratios relative to the lowest risk group were $2.6\,[1.6-4.5]$ (intermediate low), $3.2\,[1.9-5.4]$ (intermediate high) and $6.9\,[4.1-11.7]$ (high). Median survival times were 24 months (high), 47 (intermediate high) and 61 months (intermediate low) for the three highest risk groups, with median survival not reached after 96 months for the lowest risk group. To gain insight into the performance of this marker over time, we determined the proportions of surviving patients in each risk group and analyzed the EMC92-ISS at different time points. This marker is clearly applicable to younger as well as older and relapsed patients, and holds its value during follow up (Table 2 and online Figure S10).

The composition of the four groups in terms of ISS, EMC92 and FISH markers is shown in Table 3. Interestingly, within the EMC92-ISS lowest risk group, 75% of patients – with truly favorable prognosis (Table S4) – were positive for either t(4;14), del(17p) or gain(1q). In the other risk categories 32%, 42% and 86% of patients were positive (intermediate low-, intermediate high- and high-risk, respectively) indicating that EMC92-ISS and FISH only partly represent overlapping patient sets.

Table 2. Proportion of surviving patients at multiple time points per EMC92-ISS risk group in a Kaplan Meier analysis on the validation data (from top to bottom: 6, 12, 24 and 72 months respectively). In the left column patient groups are pooled ($n = 328$). Subsequent columns show percentages for newly diagnosed patients younger than 65 years ($n = 174$), newly diagnosed older than 65 years ($n = 90$) and relapsed patients ($n = 64$) respectively. For the relapse category the 72 months' time point is not available.

6 months	Pooled	<65yr.	≥65yr.	Relapse
Low-risk	98%	97%	96%	95%
Intermediate low-risk	96%	95%	91%	85%
Intermediate high-risk	86%	93%	73%	79%
High-risk	84%	88%	56%	57%
Total survival	92%	94%	81%	83%

12 months	Pooled	<65yr.	≥65yr.	Relapse
Low-risk	97%	97%	96%	89%
Intermediate low-risk	87%	93%	91%	54%
Intermediate high-risk	74%	93%	73%	42%
High-risk	67%	72%	56%	57%
Total survival	84%	91%	81%	60%

24 months	Pooled	<65yr.	≥65yr.	Relapse
Low-risk	92%	97%	92%	55%
Intermediate low-risk	76%	88%	73%	23%
Intermediate high-risk	57%	77%	58%	24%
High-risk	46%	56%	31%	0%
Total survival	72%	84%	67%	30%

72 months	Pooled	<65yr.	≥65yr.	Relapse
Low-risk	77%	86%	96%	–
Intermediate low-risk	43%	59%	32%	–
Intermediate high-risk	27%	39%	28%	–
High-risk	22%	33%	0%	–
Total survival	48%	62%	36%	–

Table 3. Distribution of markers in each of the four EMC92-ISS based risk groups. Shown are the numbers in the data for which the EMC92-ISS risk classification could be determined. n, number of patients in the EMC92-ISS based risk group for which the specified marker was available. Positive, the percentage of patients positive for the specified marker; HR, the percentage of patients indicated as high-risk according to the specified marker. For the classifications based on del(13q), 1q gain and HR.FISH.A, a clear correlation was found to the EMC92-ISS classifications. For instance, 93% of EMC92-ISS high-risk patients are positive for HR.FISH.A compared to 44% - 55% of the intermediates and 75% of the low-risk patients.

	EMC92		ISS				del(17p)		del(13q)		gain 1q		HR.FISH.A	
EMC92 - ISS	**HR**	**n**	**1**	**2**	**3**	**n**	**pos.**	**n**	**pos.**	**n**	**pos.**	**n**	**HR**	**n**
Low	0%	365	100%	0%	0%	365	8%	39	44%	39	34%	154	75%	76
Interm. low	0%	231	0%	100%	0%	231	5%	60	37%	60	34%	92	44%	70
Interm. high	0%	211	0%	0%	100%	211	8%	66	44%	66	41%	101	55%	84
High	100%	166	30%	32%	39%	166	16%	38	74%	39	76%	90	93%	76

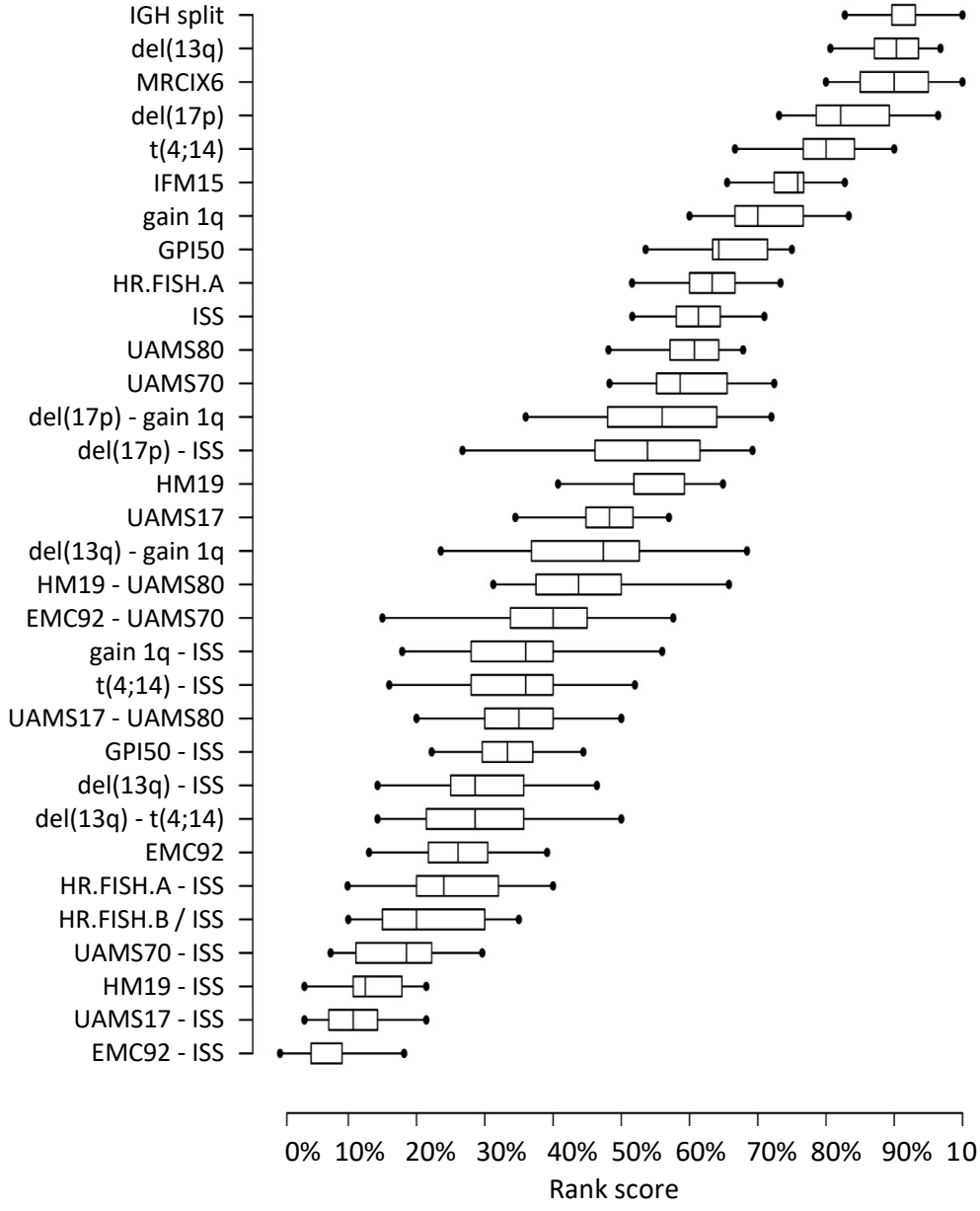

Figure 3. Ranking of confirmed existing risk markers and validated novel risk markers, in relation to overall survival on the validation data. The markers are vertically ordered by rank score, which reflects the observed proportion of risk markers with a better performance. Each box shows the interquartile range of the rank score per marker.

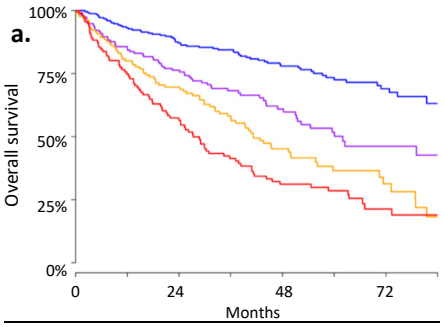

	prop.	HR [95%CI]	*p*- value
EMC92 SR + ISS I	39%	1	
EMC92 SR + ISS II	24%	1.6 [1.1 - 2.2]	0.016
EMC92 SR + ISS III	20%	2.3 [1.6 - 3.2]	3.9×10^{-6}
EMC92 high-risk	17%	4.5 [3.2 - 6.3]	$\leq 1 \times 10^{-15}$

Likelihood ratio test: $p \leq 1 \times 10^{-15}$; n = 645; n.events = 286

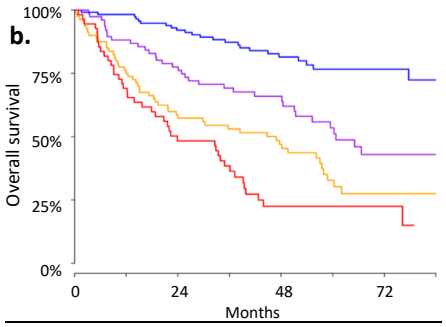

	prop.	HR [95%CI]	*p*- value
EMC92 SR + ISS I	35%	1	
EMC92 SR + ISS II	23%	2.6 [1.6 - 4.5]	3×10^{-4}
EMC92 SR + ISS III	24%	3.2 [1.9 - 5.4]	5.9×10^{-6}
EMC92 high-risk	17%	6.9 [4.1 - 12]	5.9×10^{-13}

Likelihood ratio test: $p = 2.7 \times 10^{-12}$; n = 328; n.events = 149

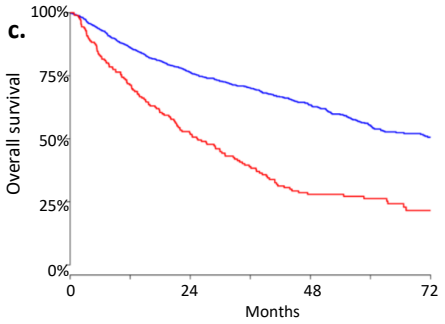

	prop.	HR [95%CI]	*p*- value
EMC92 SR	82%	1	
EMC92 high-risk	18%	2.8 [2.3 - 3.4]	$\leq 1 \times 10^{-15}$

Likelihood ratio test: $p \leq 1 \times 10^{-15}$; n = 1094; n.events = 504

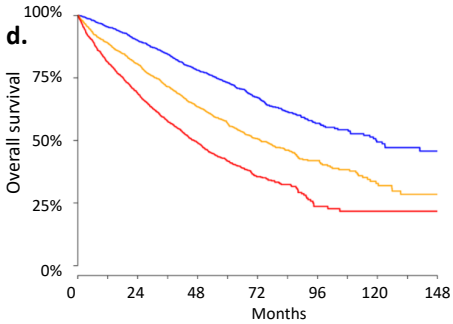

	prop.	HR [95%CI]	*p*- value
ISS I	34%	1	
ISS II	37%	1.6 [1.4 - 1.8]	1×10^{-14}
ISS III	30%	2.3 [2.1 - 2.6]	$\leq 1 \times 10^{-15}$

Likelihood ratio test: $p \leq 1 \times 10^{-15}$; n = 4077 n.events = 1925

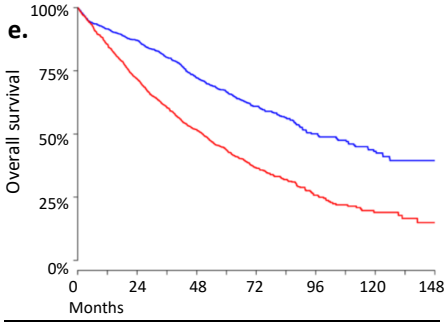

	prop.	HR [95%CI]	*p*- value
HR.FISH.A negative	43%	1	
HR.FISH.A positive	57%	2.3 [2.0 - 2.5]	$\leq 1 \times 10^{-15}$

Likelihood ratio test: $p \leq 1 \times 10^{-15}$; n = 2395; n.events = 1309

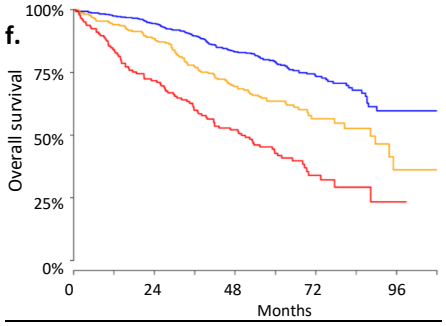

	prop.	HR [95%CI]	*p*- value
HR.FISH.B/ISS Low	57%	1	
HR.FISH.B/ISS Interm	26%	1.8 [1.4 - 2.4]	2.1×10^{-5}
HR.FISH.B/ISS High	17%	3.6 [2.7 - 4.7]	$\leq 1 \times 10^{-15}$

Likelihood ratio test: $p \leq 1 \times 10^{-15}$; n = 850 n.events = 309

Figure 4. Survival analysis of EMC92-ISS, FISH and ISS. Given are Kaplan-Meier curves (not stratified) and Cox models (stratified; i.e. corrected for differences in survival in different cohorts). **a)** EMC92-ISS in the discovery set; **b)** EMC92-ISS in the validation set; **c)** EMC92 in all data; **d)** ISS in all data; **e)** HR.FISH.A in all data; **f)** HR.FISH.B/ISS in all data. In order of increasing risk: low-risk (blue); intermediate low-risk (purple); intermediate high-risk (orange); high-risk (red); SR = standard-risk; HR = high-risk. Below the Kaplan-Meier curves, results of the stratified Cox model are found. prop. = proportion of patients within the specified risk group. HR [95%CI] = hazard ratio relative to the lowest risk group with 95% confidence interval; *p*-value= *p*-value relative to the lowest risk group; The bottom line shows the result of the likelihood ratio goodness of fit test.

Biological relevance of GEP classifiers

Genes within GEP classifiers are selected based on association with survival, rather than a direct link to biology. Still, a gene ontology enrichment analysis[33] can highlight biological processes important for a poor outcome (online Tables S5a-h). All GEP classifiers had enrichment of cell-cycle related genes. When all probe-sets in all classifiers were pooled 191 biological processes were found to be enriched (FDR< 0.05). Top processes included 'nuclear division', 'mitosis' and 'cell division', processes sharing the genes *BIRC5*, *BUB1* and *UBE2C*. Other prominent processes included 'DNA metabolic process', 'DNA packaging' and 'DNA replication' (genes such as *TOP2A* and *MCM2*).

DISCUSSION

Important prognostic markers in MM are based on ISS, FISH markers and GEP classifiers.[7–13,16,17] Previously, we showed that combining various GEP classifiers resulted in a stronger prediction of the high-risk population.[7] Here we systematically evaluated additional, new combinations of prognostic markers. We limited the search for new compound risk markers to pair-wise combinations of existing markers. This choice is mainly driven by the lack of complete data sets which contain all risk markers (online Figure S1), which hinders the analyses of more complex risk models. The number of patients positive for specific markers was remarkably stable between cohorts, irrespective of the type of marker. This adds strength to the belief that these markers, and thus decisions based on them can be reliably replicated.

Three findings are of particular interest: first, ISS has a clear and independent value in combination with either GEP classifiers or FISH markers. GEP classifiers combined with ISS are the strongest risk classifications found here. By combining the EMC92 gene classifier with ISS, patients are effectively stratified into four risk groups including a distinctive low risk group of 38% and a high-risk group of 17%. This strong additive strength of ISS to GEP has been recognized before in a previous smaller study.[34] Also ISS was integrated with GEP and other factors, but this risk score did not take into account correlations between markers, and was generated without using a solid discovery/validation design.[35] In contrast, we have opted for a study design in which part of the data was reserved for validation.

Secondly, our study confirmed that FISH markers can be divided into those consistently associated with shorter OS as opposed to inconsistent markers. Consistent FISH markers included t(4;14), gain(1q), del(17p) and del(13q). Combinations of any of these markers with ISS constituted solid prognostic predictors reported previously, t(4;14) and del(17p) are currently regarded as the most important high-risk FISH markers.[17] Thirdly, by combining these FISH markers into the previously defined risk classifications HR.FISH.A and HR.FISH.B/ISS, a major improvement of prognostic strength is achieved. Interestingly, patients classified as high-risk according to the HR.FISH.A marker but that actually had favorable

survival, were correctly identified as low risk patients by the EMC92-ISS compound marker. In addition to validating EMC92-ISS, we have now also validated the HR.FISH.B/ISS risk classification for the first time in independent data by excluding training data from the analyses. Combining FISH and ISS is thus a valid choice for routine clinical practice, including the existing HR-FISH.B/ISS, as proposed by Avet-Loiseau *et al.*[19] Incorporating LDH and bone imaging was outside the scope of this study because these markers were not consistently available.[20]

Combining GEP with ISS may become an attractive option for prognostication. The EMC92-ISS classification is independent from therapy choice: the EMC92 was shown to function in bortezomib clinical trials as well as in thalidomide and more conventional regimens.[7] In contrast, bortezomib and other novel agents may abrogate the unfavourable impact of some FISH markers on PFS.[29] EMC92-ISS is useful since it can identify both high-risk and low risk MM. This is an advantage over FISH markers which only seem to identify high-risk patients. Moreover, the technical applicability of GEP and its costs are thought to be comparable to FISH.[36] The agreement between GEP classifiers in terms of pathways is of interest. Although the primary force for classifier discovery is association with survival, the genes within classifiers appear to converge on the cell cycle pathways. Indeed, proliferative capacity, assessed as the plasma cell labeling index or by Ki-67 staining, has long been recognized to be an important prognostic factor.[37,38]

The clinical applicability of stratification into four risk groups will be increasingly relevant in the era of novel treatment modalities being available. First, increased accuracy of prognosis can improve patient counseling.[17] Secondly, and more important, risk stratification may lead to adaptation of treatment according to risk status. This composite risk marker opens the way to better risk stratification in clinical trials and explore novel drugs in different risk groups.[39,40] This could effectively be a first step towards a more individual treatment, using patient specific markers as a directional key.

Based on the current study we conclude that the combination of EMC92 with ISS is a strong disease based prognosticator for survival in MM. This risk classification is a good candidate to stratify patients for treatment options in a clinical trial.

REFERENCES

1. Rajkumar SV, Dimopoulos MA, Palumbo A, *et al.* International Myeloma Working Group updated criteria for the diagnosis of multiple myeloma. *Lancet Oncol* . 2014; **15**(12):e538–48.
2. Brenner H, Gondos A, & Pulte D. Recent major improvement in long-term survival of younger patients with multiple myeloma. *Blood* . 2008; **111**(5):2521–6.
3. Bergsagel PL, Chesi M, Nardini E, Brents LA, Kirby SL, & Kuehl WM. Promiscuous translocations into immunoglobulin heavy chain switch regions in multiple myeloma. *Proc Natl Acad Sci U S A* . 1996; **93**(24):13931–6.
4. Fonseca R, Blood E, Rue M, *et al.* Clinical and biologic implications of recurrent genomic aberrations in myeloma. *Blood* . 2003; **101**(11):4569–75.
5. Zhan F, Huang Y, Colla S, *et al.* The molecular classification of multiple myeloma. *Blood* . 2006; **108**(6):2020–2028.
6. Broyl A, Hose D, Lokhorst H, *et al.* Gene expression profiling for molecular classification of multiple myeloma in newly diagnosed patients. *Blood* . 2010; **116**(14):2543–53.
7. Kuiper R, Broyl A, de Knegt Y, *et al.* A gene expression signature for high-risk multiple myeloma. *This thesis and Leukemia* . 2012; **26**(11):2406–13.
8. Shaughnessy J J D, Zhan F, Burington BE, *et al.* A validated gene expression model of high-risk multiple myeloma is defined by deregulated expression of genes mapping to chromosome 1. *Blood* . 2007; **109**(6):2276–2284.
9. Shaughnessy J J D, Qu P, Usmani S, *et al.* Pharmacogenomics of bortezomib test-dosing identifies hyperexpression of proteasome genes, especially PSMD4, as novel high-risk feature in myeloma treated with total therapy 3. *Blood* . 2011; **118**:3512–3524.
10. Decaux O, Lode L, Magrangeas F, *et al.* Prediction of survival in multiple myeloma based on gene expression profiles reveals cell cycle and chromosomal instability signatures in high-risk patients and hyperdiploid signatures in low-risk patients: a study of the Intergroupe Francophone du Myelome. *J Clin Oncol* . 2008; **26**(29):4798–4805.
11. Hose D, Reme T, Hielscher T, *et al.* Proliferation is a central independent prognostic factor and target for personalized and risk-adapted treatment in multiple myeloma. *Haematologica* . 2011; **96**(1):87–95.
12. Reme T, Hose D, Theillet C, & Klein B. Modeling risk stratification in human cancer. *Bioinformatics* . 2013; **29**(9):1149–57.
13. Dickens NJ, Walker BA, Leone PE, *et al.* Homozygous deletion mapping in myeloma samples identifies genes and an expression signature relevant to pathogenesis and outcome. *Clin Cancer Res* . 2010; **16**(6):1856–1864.
14. Greipp PR, Lust JA, O'Fallon WM, Katzmann JA, Witzig TE, & Kyle RA. Plasma cell labeling index and beta 2-microglobulin predict survival independent of thymidine kinase and C-reactive protein in multiple myeloma. *Blood* . 1993; **81**(12):3382–7.
15. Kyle RA, Gertz MA, Witzig TE, *et al.* Review of 1027 patients with newly diagnosed multiple myeloma. *Mayo Clin Proc* . 2003; **78**(1):21–33.

16. Greipp PR, San Miguel J, Durie BG, *et al.* International staging system for multiple myeloma. *J Clin Oncol* . 2005; **23**(15):3412–20.

17. Chng WJ, Dispenzieri A, Chim CS, *et al.* IMWG consensus on risk stratification in multiple myeloma. *Leukemia* . 2014; **28**(2):269–77.

18. Neben K, Jauch A, Bertsch U, *et al.* Combining information regarding chromosomal aberrations t(4;14) and del(17p13) with the International Staging System classification allows stratification of myeloma patients undergoing autologous stem cell transplantation. *Haematologica* . 2010; **95**(7):1150–7.

19. Avet-Loiseau H, Durie BG, Cavo M, *et al.* Combining fluorescent in situ hybridization data with ISS staging improves risk assessment in myeloma: an International Myeloma Working Group collaborative project. *Leukemia* . 2013; **27**(3):711–7.

20. Moreau P, Cavo M, Sonneveld P, *et al.* Combination of International Scoring System 3, High Lactate Dehydrogenase, and t(4;14) and/or del(17p) Identifies Patients With Multiple Myeloma (MM) Treated With Front-Line Autologous Stem-Cell Transplantation at High Risk of Early MM Progression-Related Death. *J Clin Oncol* . 2014; **32**(20):2173–80.

21. Broyl A, Kuiper R, van Duin M, *et al.* High cereblon expression is associated with better survival in patients with newly diagnosed multiple myeloma treated with thalidomide maintenance. *This thesis and Blood* . 2013; **121**(4):624–7.

22. Morgan GJ, Davies FE, Gregory WM, *et al.* Long-term follow-up of MRC Myeloma IX trial: Survival outcomes with bisphosphonate and thalidomide treatment. *Clin Cancer Res* . 2013; **19**(21):6030–8.

23. Mulligan G, Mitsiades C, Bryant B, *et al.* Gene expression profiling and correlation with outcome in clinical trials of the proteasome inhibitor bortezomib. *Blood* . 2007; **109**(8):3177–3188.

24. Nair B, van Rhee F, Shaughnessy J J D, *et al.* Superior results of Total Therapy 3 (2003-33) in gene expression profiling-defined low-risk multiple myeloma confirmed in subsequent trial 2006-66 with VRD maintenance. *Blood* . 2010; **115**(21):4168–73.

25. Ross FM, Ibrahim AH, Vilain-Holmes A, *et al.* Age has a profound effect on the incidence and significance of chromosome abnormalities in myeloma. *Leukemia* . 2005; **19**(9):1634–42.

26. Walker BA, Leone PE, Chiecchio L, *et al.* A compendium of myeloma-associated chromosomal copy number abnormalities and their prognostic value. *Blood* . 2010; **116**(15):e56–65.

27. Ross FM, Avet-Loiseau H, Ameye G, *et al.* Report from the European Myeloma Network on interphase FISH in multiple myeloma and related disorders. *Haematologica* . 2012; **97**(8):1272–7.

28. Wuilleme S, Robillard N, Lode L, *et al.* Ploidy, as detected by fluorescence in situ hybridization, defines different subgroups in multiple myeloma. *Leukemia* . 2005; **19**(2):275–8.

29. Sonneveld P, Schmidt-Wolf IG, van der Holt B, *et al.* Bortezomib induction and maintenance treatment in patients with newly diagnosed multiple myeloma: results of the randomized phase III HOVON-65/ GMMG-HD4 trial. *J Clin Oncol* . 2012; **30**(24):2946–55.

30. Cox DR & Oakes D. Analysis of Survival Data. Taylor & Francis. 1984.

31. Bland JM & Altman DG. Multiple significance tests: the Bonferroni method. *BMJ* . 1995; **310**(6973):170.

32. Therneau TM & Grambsch PM. Modeling survival data : extending the Cox model. Springer, New York. 2000.
33. Ashburner M, Ball CA, Blake JA, *et al.* Gene ontology: tool for the unification of biology. The Gene Ontology Consortium. *Nat Genet* . 2000; **25**(1):25–9.
34. Waheed S, Shaughnessy J J D, van Rhee F, *et al.* International staging system and metaphase cytogenetic abnormalities in the era of gene expression profiling data in multiple myeloma treated with total therapy 2 and 3 protocols. *Cancer* . 2011; **117**(5):1001–9.
35. Meissner T, Seckinger A, Reme T, *et al.* Gene expression profiling in multiple myeloma–reporting of entities, risk, and targets in clinical routine. *Clin Cancer Res* . 2011; **17**(23):7240–7.
36. Hose D, Seckinger A, Jauch A, *et al.* The role of fluorescence in situ hybridization and gene expression profiling in myeloma risk stratification. *Srp Arh Celok Lek* . 2011; **139 Suppl 2**:84–9.
37. Steensma DP, Gertz MA, Greipp PR, *et al.* A high bone marrow plasma cell labeling index in stable plateau-phase multiple myeloma is a marker for early disease progression and death. *Blood* . 2001; **97**(8):2522–3.
38. Gastinne T, Leleu X, Duhamel A, *et al.* Plasma cell growth fraction using Ki-67 antigen expression identifies a subgroup of multiple myeloma patients displaying short survival within the ISS stage I. *Eur J Haematol* . 2007; **79**(4):297–304.
39. Ludwig H, Sonneveld P, Davies F, *et al.* European Perspective on Multiple Myeloma Treatment Strategies in 2014. *Oncologist* . 2014; **19**(9):829–844.
40. Crawley C, Iacobelli S, Bjorkstrand B, Apperley JF, Niederwieser D, & Gahrton G. Reduced-intensity conditioning for myeloma: lower nonrelapse mortality but higher relapse rates compared with myeloablative conditioning. *Blood* . 2007; **109**(8):3588–94.

CHAPTER 6

High Cereblon Expression is Associated with Better Survival in Patients with Newly Diagnosed Multiple Myeloma Treated with Thalidomide Maintenance

Annemiek Broyl, Rowan Kuiper, Mark van Duin, Bronno van der Holt, Laila el Jarari, Uta Bertsch, Sonja Zweegman, Arjan Buijs, Dirk Hose, Henk M. Lokhorst, Hartmut Goldschmidt & Pieter Sonneveld

Blood 2013; **121**(4):624-7

ABSTRACT

Recently, cereblon (*CRBN*) expression was found to be essential for the activity of Thalidomide and lenalidomide. In the present study, we investigated whether the clinical efficacy of Thalidomide in multiple myeloma is associated with *CRBN* expression in myeloma cells. Patients with newly diagnosed multiple myeloma were included in the HOVON-65/GMMG-HD4 trial, in which postintensification treatment in 1 arm consisted of daily Thalidomide ($50mg$) for 2 years. Gene-expression profiling, determined at the start of the trial, was available for 96 patients who started Thalidomide maintenance. In this patient set, increase of *CRBN* gene expression was significantly associated with longer progression-free survival ($p = .005$). In contrast, no association between *CRBN* expression and survival was observed in the arm with Bortezomib maintenance. We conclude that *CRBN* expression may be associated with the clinical efficacy of Thalidomide. This trial has been registered at the Nederlands Trial Register (`www.trialregister.nl`) as NTR213; at the European Union Drug Regulating Authorities Clinical Trials (EudraCT) as 2004-000944-26; and at the International Standard Randomized Controlled Trial Number (ISRCTN) as 64455289.

INTRODUCTION

Introduction of Thalidomide, Bortezomib, and lenalidomide has greatly improved induction treatment for multiple myeloma (MM).[1–4] Attention is now shifting toward improving consolidation and maintenance therapy.[5] Thalidomide and lenalidomide represent immunomodulatory drugs (IMiDs) with variable efficacy during maintenance after high-dose therapy and in the nontransplantation setting.[6–8] So far, there are no biomarkers for prediction of outcome after Thalidomide and/or lenalidomide treatment. *CRBN* was recently identified as the target gene responsible for the teratogenic effects of Thalidomide.[9] CRBN levels were also shown to be critical for the antitumor activity of lenalidomide and Thalidomide in both in vitro model systems and in lenalidomide-resistant patients.[10] In the present study, we report that *CRBN* expression is associated with outcome of Thalidomide maintenance in newly diagnosed MM patients.

MATERIALS AND METHODS

Patients and procedures

In the HOVON-65/GMMG-HD4 trial, patients with newly diagnosed MM were randomly assigned to receive either VAD (Vincristine, Adriamycin, and Dexamethasone) induction, intensification with high-dose Melphalan (HDM), and autologous stem cell transplantation (ASCT) followed by maintenance therapy with Thalidomide or PAD (Bortezomib, Adriamycin, and Dexamethasone), HDM, and ASCT followed by maintenance with Bortezomib. The maximum duration of maintenance therapy in both arms was 2 years.[11] Patients randomized to VAD received maintenance with Thalidomide 50 mg daily for 2 years starting 4 weeks after HDM. This study was approved by the ethics committees of the Erasmus University MC, the University of Heidelberg, and the participating sites. All patients gave written informed consent and the trial was conducted according to the European Clinical Trial Directive 2005 and the Declaration of Helsinki.

Response assessments and end points

Clinical characteristics were registered at diagnosis. Cytogenetic studies were performed as described previously.[12] For this subanalysis, progression-free survival (PFS) and overall survival (OS) were measured from start of the maintenance treatment. For PFS, progression was used as the end point and for OS, death from any cause. Patients alive at the date of last contact were censored. Evaluation of response is described in detail in supplemental Table S4.

GEP and statistical analysis

The gene-expression profiling (GEP) dataset GSE19784 was used, which was derived from patients included in the HOVON-65/GMMG-HD4 trial.[11,13] *CRBN* expression was assessed using the intensity values of the probe sets *218142_s_at* and *222533_at*, combined using the method of Dai *et al.*[14] Presence calls for *CRBN* expression were determined with the PANP algorithm using standard settings (see the PANP reference manual on the Bioconductor web site, `http://bioconductor.org/packages/panp/`).[15] Details of the quantitative RT-PCR

are given in online Figure S3. Multivariate Cox regression analysis was performed to assess the value of *CRBN* as a prognostic factor in relation to the International Staging System (ISS) and high-risk cytogenetics, as described previously.[11]

RESULTS AND DISCUSSION

Patients and response

A total of 833 patients were enrolled in the HOVON65/GMMG-HD4 trial. Of the patients randomized to the VAD arm, 77 of 347 (22%) went off protocol after HDM because of allo-SCT ($n = 21, 6\%$), persisting toxicity ($n = 11, 3\%$), or other reasons ($n = 45, 13\%$), whereas 270 (78%) patients started Thalidomide maintenance treatment. Normal completion of Thalidomide maintenance was achieved in 73 of 270 (27%) patients. Eleven of 270 Thalidomide maintenance patients underwent allo-SCT and were not considered in this subanalysis. Of the remaining 259 patients, GEP and survival data were available for 96. Baseline characteristics between this subgroup ($n = 96$) and the remainder ($n = 163$) were comparable (online Table S1). Present calls were found for both *CRBN* probe sets in 95 of 96 Thalidomide maintenance cases, with one patient demonstrating a borderline present call ("M") for one probe set and a present call for the other. A significant correlation was found between *CRBN* gene expression measured by microarray (National Center for Biotechnology Gene Expression Omnibus [NCBI-GEO] repository: GSE19784) and quantitative RT-PCR (Spearman $\rho = 0.67$, *p* = .002, $n = 18$; online Figure S3). The EMC clustering represents our gene expression based classification of MM.[16] Of the clusters evaluated, the CTA cluster demonstrated a significantly higher *CRBN* expression compared with the other clusters (Bonferroni-Holm corrected *p* = .01, online Figure S2).[16]

In univariate Cox regression analysis, *CRBN* expression was significantly associated with PFS (hazard ratio = 0.68; 95% confidence interval, $[0.52 - 0.89]$; *p* = .005) and with OS (hazard ratio = 0.65; 95% confidence interval, $[0.43 - 0.97]$; *p* = .04; Table 1). Kaplan-Meier analysis was used solely for visualization with *CRBN* expression split in 2 or 4 groups using median or quartile intensities: patients with *CRBN* expression above the median demonstrated longer PFS compared with patients with *CRBN* levels below the median (*p* = .009; Figure 1a-b quartile intensities and online Figure S4). In addition, an optimal *CRBN* cutoff was calculated (online Table S2). For this calculation, the PFS data that prohibit use of this cutoff in this dataset for any analyses related to PFS were used. In contrast,

Table 1. Cox regression analyses. HR indicates hazard ratio; and 95%CI, 95% confidence interval

a. Univariate PFS

Covariate	HR [95%CI]	*p*
CRBN	0.68 $[0.52 - 0.89]$	0.005

b. Univariate OS

Covariate	HR [95%CI]	*p*
CRBN	0.65 $[0.43 - 0.97]$	0.04

c. Multivariate PFS

Covariate	HR [95%CI]	*p*
CRBN	0.66 $[0.45 - 0.96]$	0.03
ISS = 2	2.35 $[1.2 - 4.8]$	0.02
ISS = 3	2.55 $[1.2 - 5.4]$	0.01
High-risk FISH*	2.82 $[1.59 - 5.00]$	0.0004

d. Multivariate OS

Covariate	HR [95%CI]	*p*
CRBN	0.75 $[0.42 - 1.3]$	0.32
ISS = 2	4.66 $[1.4 - 15.8]$	0.01
ISS = 3	5.49 $[1.7 - 18.1]$	0.005
High-risk FISH*	3.65 $[1.5 - 8.7]$	0.003

*High-risk FISH is defined as having del(17p) and/or 1q gain and/or t(4;14).

the median expression value was arbitrarily chosen and used for analysis in relation to response upgrade. Multivariate Cox regression analysis was performed on 81 patients for whom the following covariates were available: ISS, continuous *CRBN* levels, and high-risk FISH [del(17p) and/or 1q gain and/or t(4;14)]. Higher *CRBN* levels remained significantly related to longer PFS, but not OS, with a hazard ratio of 0.66 ($p = .03$) and 0.75 ($p = .3$), respectively (Table 1). No significant correlation was found between any of these covariates and *CRBN*, but lower *CRBN* expression was found in ISS=III compared with either ISS=I or ISS=II (Bonferroni corrected $p = .10$ by Kruskal Wallis test). The *CRBN* gene is positioned on chromosome 3. Chromosome 3 trisomies are frequently found in patients with hyperdiploidy and, indeed, *CRBN* levels were significantly higher in hyperdiploid patients compared with nonhyperdiploid patients ($p = .005$). However, in a multivariate Cox regression analysis, *CRBN* levels, but not hyperdiploidy, were found to be related to PFS ($p = .006$ and $p = .8$, respectively; data not shown).

CRBN expression was not associated with an upgrade of response, considered to be improvement of response during Thalidomide maintenance ($p = .3$, online

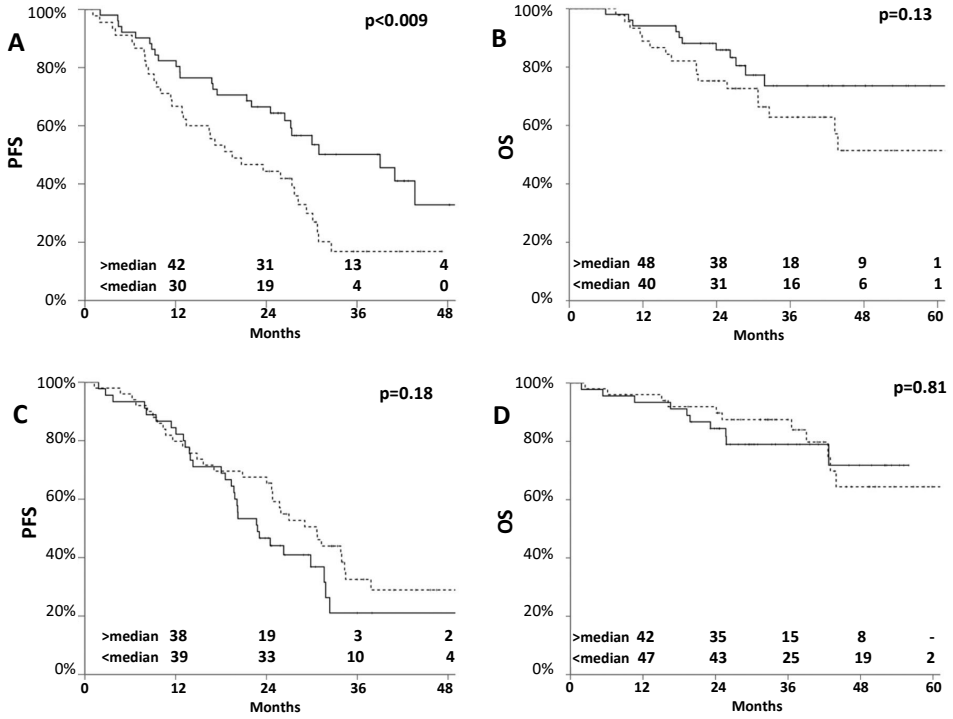

Figure 1. *CRBN* expression in HOVON-65/GMMG-HD4 Shown is *CRBN* expression in relation to PFS and OS Kaplan-Meier curves of *CRBN* expression in relation to survival in Thalidomide treated patients (a-b) and in relation to Bortezomib treated patients (c-d). PFS is shown at left; OS on the right. Log-rank p-values are shown in the right corner of each panel. Broken lines indicate *CRBN* expression levels below the median and solid lines indicate expression levels above the median. Remaining patients at risk are shown above the x-axis (PFS at 1, 2, 3, and 4 years and OS at 1, 2, 3, 4, and 5 years). The median *CRBN* expression was determined on the combined data of both Thalidomide and Bortezomib treated patients: 45 of 96 patients were below the median in the Thalidomide subset, whereas 50 of 95 were below the median in the Bortezomib subset.

Table S4). To determine whether *CRBN* expression was specifically relevant for the outcome of Thalidomide treatment, we also examined the relationship between *CRBN* expression and survival in patients treated with Bortezomib maintenance. No association was observed between *CRBN* expression and PFS/OS after Bortezomib maintenance (Figure 1c-d). For validation of these results, the MRC-IX study was evaluated.[17] Only 30 patients with gene expression were available who received Thalidomide during maintenance but not during induction. This subset was too small to allow solid analysis of the relationship between *CRBN* expression and outcome after Thalidomide maintenance. Finally, CRBN forms an

E3 ubiquitin ligase complex with the proteins DDB1 and CUL4A.[9] This complex has been suggested to be involved in the regulation of β-catenin activity, which in turn affects downstream targets such as CCND1 and C-MYC. CRBN was also found to bind to AMPKα1 (PRKAA1) and to the large conductance Ca^{2+}-activated potassium channel KCNMA1.[18] In a multivariate model with *CRBN* levels, only *CCND1* and *CRBN* were found to be independently related to longer PFS (online Table S3). A relationship with PFS was not found for either *CCND1* or *CRBN* in the patients treated with Bortezomib in the maintenance phase.

In conclusion, in the present study, we observed that higher expression of CRBN was associated with increased PFS during maintenance treatment with Thalidomide, but not in patients with Bortezomib maintenance. This corresponds well to the report of reduced CRBN expression in > 85% of MM patients who were lenalidomide resistant.[10] Our observations warrant analysis of the predictive effect of CRBN expression in newly diagnosed and relapsed/refractory patients treated with IMiDs as part of induction and consolidation treatment.

REFERENCES

1. Richardson PG, Sonneveld P, Schuster MW, *et al.* Bortezomib or high-dose dexamethasone for relapsed multiple myeloma. *N Engl J Med* . 2005; **352**(24):2487–2498.
2. Richardson PG, Barlogie B, Berenson J, *et al.* A phase 2 study of bortezomib in relapsed, refractory myeloma. *N Engl J Med* . 2003; **348**(26):2609–2617.
3. Dimopoulos M, Spencer A, Attal M, *et al.* Lenalidomide plus dexamethasone for relapsed or refractory multiple myeloma. *N Engl J Med* . 2007; **357**(21):2123–32.
4. Weber DM, Chen C, Niesvizky R, *et al.* Lenalidomide plus dexamethasone for relapsed multiple myeloma in North America. *N Engl J Med* . 2007; **357**(21):2133–42.
5. Palumbo A, Attal M, & Roussel M. Shifts in the therapeutic paradigm for patients newly diagnosed with multiple myeloma: maintenance therapy and overall survival. *Clin Cancer Res* . 2011; **17**(6):1253–63.
6. Palumbo A, Hajek R, Delforge M, *et al.* Continuous lenalidomide treatment for newly diagnosed multiple myeloma. *N Engl J Med* . 2012; **366**(19):1759–69.
7. Attal M, Lauwers-Cances V, Marit G, *et al.* Lenalidomide maintenance after stem-cell transplantation for multiple myeloma. *N Engl J Med* . 2012; **366**(19):1782–91.
8. Mahindra A, Laubach J, Raje N, Munshi N, Richardson PG, & Anderson K. Latest advances and current challenges in the treatment of multiple myeloma. *Nat Rev Clin Oncol* . 2012; **9**(3):135–43.
9. Ito T, Ando H, Suzuki T, *et al.* Identification of a primary target of thalidomide teratogenicity. *Science* . 2010; **327**(5971):1345–50.
10. Zhu YX, Braggio E, Shi CX, *et al.* Cereblon expression is required for the antimyeloma activity of lenalidomide and pomalidomide. *Blood* . 2011; **118**(18):4771–9.
11. Sonneveld P, Schmidt-Wolf IG, van der Holt B, *et al.* Bortezomib induction and maintenance treatment in patients with newly diagnosed multiple myeloma: results of the randomized phase III HOVON-65/ GMMG-HD4 trial. *J Clin Oncol* . 2012; **30**(24):2946–55.
12. Neben K, Lokhorst HM, Jauch A, *et al.* Administration of bortezomib before and after autologous stem cell transplantation improves outcome in multiple myeloma patients with deletion 17p. *Blood* . 2012; **119**(4):940–8.
13. Broyl A, Corthals SL, Jongen JL, *et al.* Mechanisms of peripheral neuropathy associated with bortezomib and vincristine in patients with newly diagnosed multiple myeloma: a prospective analysis of data from the HOVON-65/GMMG-HD4 trial. *Lancet Oncol* . 2010; **11**(11):1057–65.
14. Dai M, Wang P, Boyd AD, *et al.* Evolving gene/transcript definitions significantly alter the interpretation of GeneChip data. *Nucleic Acids Res* . 2005; **33**(20):e175.
15. Warren P, Taylor D, Martini P, Jackson J, & Bienkowska J. PANP - a New Method of Gene Detection on Oligonucleotide Expression Arrays. *Bioinformatics and Bioengineering, 2007. BIBE 2007. Proceedings of the 7th IEEE International Conference on* . 2007; :108–115.
16. Broyl A, Hose D, Lokhorst H, *et al.* Gene expression profiling for molecular classification of multiple myeloma in newly diagnosed patients. *Blood* . 2010; **116**(14):2543–53.

17. Morgan GJ, Gregory WM, Davies FE, *et al.* The role of maintenance thalidomide therapy in multiple myeloma: MRC Myeloma IX results and meta-analysis. *Blood* . 2012; **119**(1):7–15.

18. Chang XB & Stewart AK. What is the functional role of the thalidomide binding protein cereblon? *Int J Biochem Mol Biol* . 2011; **2**(3):287–94.

CHAPTER 7

Genetic Factors Underlying the Risk of Bortezomib Induced Peripheral Neuropathy in Multiple Myeloma Patients

Sophie L. Corthals, Rowan Kuiper, David C. Johnson, Pieter Sonneveld, Roman Hajek, Bronno van der Holt, Florence Magrangeas, Hartmut Goldschmidt, Gareth J. Morgan & Hervé Avet-Loiseau

Haematologica 2011, **96**(11): 1728-32

ABSTRACT

Bortezomib induced peripheral neuropathy is a dose-limiting side effect and a major concern in the treatment of multiple myeloma. To identify genetic risk factors associated with the development of this side effect in Bortezomib treated multiple myeloma patients, a pharmacogenetic association study was performed using a discovery set (IFM 2005-01; $n = 238$) and a validation set (HOVON-65/GMMG-HD4 and a Czech dataset; $n = 231$). After multiplicity correction, none of the 2149 single nucleotide polymorphisms tested revealed any significant association with Bortezomib induced peripheral neuropathy. However, 56 single nucleotide polymorphisms demonstrated an association with Bortezomib induced peripheral neuropathy with pointwise, uncorrected significance. Pathway analysis of these polymorphisms demonstrated involvement of neurological disease (FDR$< 20\%$). Also a clear enrichment of major Bortezomib metabolizing genes was found. Univariate evaluation of these 56 polymorphisms in the validation set demonstrated one single nucleotide polymorphism with pointwise significance: *rs619824* in *CYP17A1*.

INTRODUCTION

The introduction of Bortezomib (Millennium Pharmaceuticals, Cambridge, MA, USA), an inhibitor of the 26S proteasome, has greatly improved the management of multiple myeloma (MM).[1] The dose-limiting toxicity of Bortezomib is peripheral neuropathy, which frequently requires a dose reduction or treatment discontinuation.[2–4] Bortezomib induced peripheral neuropathy (BiPN) differs from pre-existing peripheral neuropathy associated with 10% of untreated MM patients. BiPN, described in detail by Delforge *et al.*,[4] is predominantly sensory, reversible in most cases, and characterized by distal paresthesias, numbness and neuropathic pain.

A multifactorial pathogenesis for BiPN seems likely, with suggested mechanisms including blockade of nerve-growth-factor-mediated neuronal survival through inhibition of the activation of nuclear factor κB (NFκB),[5] damage to mitochondria and the endoplasmic reticulum through activation of apoptosis,[6] dysregulation of mitochondrial calcium homoeostasis,[7] autoimmune factors, interference with mRNA processing, and translation[8] and inflammation.[9,10] A number of studies, including a report by our own group, have looked at the pharmacogenetic characterization of BiPN.[11,12] In the study carried out by our group, the comparison between early onset (within one treatment cycle) BiPN and late onset (after two or three treatment cycles) BiPN revealed that genes for apoptosis contribute to early onset BiPN, whereas genes that have a role in inflammatory pathways and DNA repair contribute to the development of late onset BiPN, indicating that distinct genetic factors are involved in the development of early onset and late onset forms of this side effect.[11] Recently, Favis *et al*. reported on the association between SNPs and the time to Bortezomib induced peripheral neuropathy within the VISTA trial with associated SNPs including a SNP in the gene *CTLA4*.[12]

In this study, we further explore the genetic risk factors associated with the development of BiPN in patients with MM who had not been previously treated with Bortezomib. A large dataset from the IFM 2005-01 trial was used as discovery set. In addition, a dataset based on the patients from the HOVON-65/GMMG-HD4 trial were used as a validation set.[11]

MATERIALS AND METHODS

Patients

The study was performed on patients who had been included in two randomized clinical trials, i.e. the Institutional Review Board-approved HOVON-65/GMMG-HD4 (ISRCTN64455289) trial for newly diagnosed patients with MM ($n = 833$), and the IFM 2005-01 trial (NCT00200681; $n = 493$) approved by the ethics committee of the University of Nantes, both of which compared standard induction treatment (VAD) with a Bortezomib combination prior to high-dose therapy (HDT) and stem cell transplantation (online Figure S1a). In addition, as part of the cooperative program of the International Myeloma Foundation (IMF) and International Myeloma Working Group (IMWG), a set of 56 patients (i.e. 56 unique DNA samples), uniformly treated with Bortezomib and Dexamethasone at relapse, were obtained. In addition, a prospectively collected set of samples ($n = 56$) from the Babak Research Institute (Czech Republic) was included as part of the cooperative program of the IMF and IMWG. All patients gave written informed consent for this genetic study. Patients with amyloidosis or monoclonal gammopathy of undetermined significance (MGUS) were excluded. Adverse events (AEs) were prospectively assessed using standard National Cancer Institute Common Toxicity Criteria for Adverse Events, version 3.0 (CTCAE 3.0). To ensure homogeneity of allelic frequencies, 15 patients of non-European descent were excluded from the study. In total, 238 of 246 patients from IFM 2005-01, 183 of 412 patients from HOVON-65/GMMG-HD4 and 48 of 56 from the Czech Republic who were randomized for treatment with Bortezomib were included in the analysis. Samples were divided into a discovery and validation set (online Figure S1B and online Table S1).

Genotyping

DNA was extracted from peripheral blood nucleated cells or CD138 negative bone marrow cells. Genotyping was performed using an Affymetrix targeted genotyping custom built panel, comprising 3404 SNPs. These were selected using a hypothesis-driven strategy, targeting genes and SNPs with previously described

associations or putative functional effects.[13]

Statistical analysis

After imputation and applying SNP exclusion criteria (minor allele frequency (MAF) < 0.05, Hardy Weinberg equilibrium $< 1 \times 10^{-5}$), a panel containing 2149 SNPs was analyzed by univariate association analysis using the software package PLINK.[14] Categorical comparisons with respect to frequencies were performed with the χ^2 or Fisher's exact test, and continuous variables were analyzed using the Mann-Whitney U test (online Table S1).

SNP association analysis comparing grade 1–4 BiPN with no BiPN patients in the discovery set (IFM 2005-01) was performed as previously described.[11]

The associated gene sets were subjected to Ingenuity Pathway Analysis (Ingenuity System Inc., USA) using 2149 SNPs as a reference set. Only the top three associated pathways with a FDR≤20% are reported.

As validation, a Cochran Mantel-Haenszel stratified association test was performed in an independent dataset comprised of patients from the HOVON-65/GMMG-HD4 trial and patients from the Czech Republic to evaluate cross validating SNP associations and odds ratios (ORs). Specifically, ORs from significant SNPs (pointwise $p< 0.05$) in the discovery set were selected for validation. A one-sided test for OR was performed to test whether the observed effects in the validation set were associated with the same effect direction as observed in the discovery set.

Based on the numbers of the discovery and validation set, a conservative power calculation for both sets was performed. According to this calculation, ORs need to be higher than 2.28 or lower than 0.44 to be found at a significance level of $\alpha = 0.05$ for SNPs with a MAF of 0.5. These ORs diverge as the MAF decreases (online Figures S2 and S3, online Tables S1 and S2). Please note this is a conservative analysis in which multiplicity correction is performed by Bonferroni correction and no linkage is taken into account.

RESULTS AND DISCUSSION

The BiPN rates and clinical characteristics of both the discovery set ($n = 238$) and the validation set ($n = 231$) are shown in the online Table S1. In the discovery set, 27 patients developed BiPN grade 1, 57 grade 2, 11 grade 3, and 4 grade 4. Online Figure S4 shows the time to BiPN for each grade separately in patients from the HOVON-65/GMMG-HD4 trial, who are included in the validation set. The median time to BiPN grade 1 was six weeks, and seven weeks to grade 2, 3 or 4. The peripheral neuropathy rates in the VAD treatment arm (i.e. not Bortezomib) of the HOVON-65/GMMG-HD4 trial, will not be discussed further here (online Table S3).

After imputation and applying PLINK exclusion filters, a panel containing 2149 SNPs was analyzed for association by conducting a χ^2 association analysis. None of the SNPs were found to be significantly associated with BiPN using the permutated *p*-value correction for multiple testing in the discovery set (IFM2005-01; Table 1). The highest ranking SNP, with corrected *p*-value of 0.3, is in the locus of the cell cycle gene *CDKN1B*. This SNP, *rs3759217*, has been evaluated in a number of cancer studies, but was not reported to be significantly associated with any cancer type.[15] Using the pointwise, uncorrected *p*-value, 56 SNPs were found to be associated with BiPN in this set (Table 1).

The results of the analysis performed in the discovery set (IFM 2005-01 trial) were validated using an independent dataset from the Czech Republic combined with the dataset from the HOVON-65/GMMG-HD4 trial (online Figure S1). A Cochran Mantel-Haenszel stratified association test was performed. Associated SNPs (pointwise $p < 0.05$) in this validation set are shown in online Table S5. To investigate whether associated SNPs (pointwise $p < 0.05$) in the discovery set and available in the validation set ($n = 51$) had the same direction of effect, a one-sided test for ORs was performed in the validation set. This resulted in one pointwise significantly cross validating SNP; *rs619824* in *CYP17A1* (online Table S6).

CYP17A1, cytochrome P-450c17α, is involved in steroid hormone biosynthesis, and has both steroid 17α-hydroxylase activity and 17,20-lyase activity.[16] Steroids have been shown to affect nerve cells, and have even been suggested for

use as a therapeutic option to prevent the development of neuropathy.[17] Treatment with progesterone has been reported to increase the expression of myelin protein zero in both rat sciatic nerve and Schwann cells.[17] Due to the paucity of cross validated SNPs, we have examined the SNPs with a significant pointwise *p*-value in the discovery set (Table 1). Foremost, we have performed a pathway analysis based on this set of SNPs. This analysis showed enrichment of genes involved in cardiovascular disease (11 genes), genetic disorder (22 genes) and neurological disease (21 genes). The latter include the genes NEFL, PON1, PTGS2 and ABCG2, which have been reported frequently in relation to neurological disease such as Alzheimer's. Previous studies showed that Bortezomib is primarily metabolized by cytochrome P450 isoforms CYP3A4, CYP2C19, CYP1A2, with a minor contribution of CYP2D6 and CYP2C9.[18] The results show an enrichment of the major Bortezomib metabolizing genes within the top 56 SNPs ($p = 0.0013$).

Previously, genes involved in inflammation were found to be associated with late onset BiPN.11 Indeed, one of the most associated SNPs, *rs3136516* (pointwise $p = 0.008$) was an intronic SNP located in prothrombin (coagulation factor II; F2), which has been reported in relation to the neuro-toxic cascade leading to neurodegenerative diseases.[19] Two SNPs that lie within or in close proximity to the TNFα gene (*rs2857605* and *rs2228088*; online Figure S5) were associated with BiPN. TNFα has been implicated in the pathogenesis of several neurodegenerative diseases, including multiple sclerosis, Alzheimer's disease, and human immunodeficiency virus-related encephalopathy.[20] Additionally, the TNFα system is activated in diabetic polyneuropathy, which leads to increased microvascular permeability, hypercoagulability and even direct nerve damage. Improvement of diabetic polyneuropathy following suppression of TNFα has been shown in several animal models.[21] Furthermore, neuropathic pain, one of the determinants of the CTCAE-neuropathy score, and thus of BiPN severity, is mediated through TNF-mediated induction of stress-activated kinasesap like p38 MAPK.[22]

The NFκB pathway is central to the immune response and two associated SNPs are located in the *IKBKAP* gene; *rs10979601* and *rs10759326*. This is a particularly relevant association because hereditary sensory and autonomic neuropathy type III, or familial dysautonomia (FD), can be caused by mutations in the *IKBKAP* gene, leading to poor development, reduced survival, and progressive de-

Table 1. SNPs associated with BiPN. Shown are χ^2 associations with pointwise $p < 0.05$. The genomic inflation factor λ is 1.0201.

SNP	CHR	Alleles	OR [95%CI]		$p(\chi^2)$		Gene	SNP Type	In LD with
					pointwise	permuted			
rs3759217	12	C > T	2.76	$[1.58 - 4.84]$	<0.001	0.3291	CDKN1B	Locus	
rs11466155	17	C > T	1.87	$[1.25 - 2.80]$	0.004	0.9744	NGFR	synonymous	
rs6033	1	A > G	2.53	$[1.30 - 4.94]$	0.006	0.9993	F5	nonsynonymous	rs6018, rs6027
rs2228088	6	G>T	0.56	$[0.36 - 0.87]$	0.006	1	TNF	synonymous, TAGSNP:TNF	
rs2686184	8	G>A	1.72	$[1.19 - 2.49]$	0.006	0.9966	FDFT1	3'UTR	
rs12721516	1	C>T	0.55	$[0.34 - 0.90]$	0.007	1	CSF1	nonsynonymous	
rs6945306	7	G>C	1.71	$[1.17 - 2.52]$	0.007	0.9999	STK31	nonsynonymous	
rs228851	20	G>T	0.59	$[0.41 - 0.86]$	0.008	0.9998	NFATC2	Intron	
rs3136516	11	A>G	0.61	$[0.42 - 0.88]$	0.008	1	F2	Intron	
rs584589	17	A>G	2.01	$[1.16 - 3.47]$	0.009	1	NGFR	Promotor	
rs4148949	10	C>T	0.60	$[0.41 - 0.88]$	0.010	1	CHST3	Untranslated	rs4148946
rs619824	10	G>T	0.64	$[0.44 - 0.93]$	0.010	1	CYP17A1	3'UTR	
rs338599	19	G>C	2.97	$[1.24 - 7.08]$	0.011	1	CYP2S1	synonymous	
rs121	7	A>G	1.61	$[1.11 - 2.32]$	0.011	1	OSBPL2	Intron	
rs7169	1	T>C	1.65	$[1.14 - 2.39]$	0.012	1	SLC16A1	Untranslated	rs1049434
rs2239330	16	C>T	0.59	$[0.39 - 0.90]$	0.012	1	ABCC1	synonymous	rs212090, rs212087
rs2295155	22	C>A	0.43	$[0.23 - 0.81]$	0.012	1	CARD10	Intron	
rs2976437	8	A>G	1.63	$[1.13 - 2.37]$	0.013	1	NEFL	Promotor	rs2976436
rs2033178	12	C>T	2.42	$[1.23 - 4.74]$	0.014	1	IGF1	Intron	
rs878201	1	G>A	1.54	$[1.04 - 2.29]$	0.015	1	Admixture	Admixture	
rs1149901	10	C>T	1.62	$[1.07 - 2.45]$	0.015	1	GATA3	Locus, untranslated	
rs2973015	5	A>G	0.63	$[0.44 - 0.91]$	0.017	1	GHR	Intron	
rs2227956	6	T>C	0.52	$[0.30 - 0.88]$	0.018	1	HSPA1L	nonsynonymous	
rs504122	13	C>T	0.63	$[0.43 - 0.93]$	0.018	1	SPRY2	nonsynonymous	
rs1641536	17	G>A	0.43	$[0.22 - 0.86]$	0.021	1	SHBG	3'UTR	
rs2472299	15	G>A	0.62	$[0.42 - 0.92]$	0.022	1	CYP1A1	Promotor	
rs9885672	6	T>C	1.86	$[1.08 - 3.21]$	0.024	1	KIAA0274	nonsynonymous	
rs163078	2	C>T	0.63	$[0.43 - 0.92]$	0.026	1	CYP1B1	Intron, TagSNP: CYP1B1	rs163077
rs20432	1	T>G	0.59	$[0.35 - 0.97]$	0.027	1	PTGS2	Intron	
rs762551	15	A>C	0.63	$[0.42 - 0.93]$	0.027	1	CYP1A2	Intron, TagSNP: CYP1A cluster	
rs3776432	5	G>A	1.52	$[1.04 - 2.24]$	0.028	1	NSUN2	Intron	
rs3817074	19	C>T	1.95	$[1.06 - 3.60]$	0.029	1	BAX	Intron	
rs1126526	1	C>T	1.41	$[0.96 - 2.08]$	0.029	1	ATF3	5'UTR	
rs1805405	1	C>A	0.56	$[0.33 - 0.95]$	0.030	1	PARP1	Intron	rs1805407, rs2280712
rs1002153	1	T>C	0.56	$[0.33 - 0.95]$	0.030	1	PARP1	Intron	rs1805408
rs4799055	18	G>T	1.61	$[1.10 - 2.35]$	0.030	1	NFATC1	Intron	

Table 1. continued.

SNP	CHR	Alleles	OR [95%CI]	$p(\chi^2)$ pointwise	$p(\chi^2)$ permuted	Gene	SNP Type	In LD with
rs854556	7	C>T	0.64 $[0.44-0.95]$	0.031	1	PON1	Intron, TagSNP: PON1	
rs1052637	2	G>C	0.66 $[0.45-0.97]$	0.031	1	DDX18	nonsynonymous	
rs440454	6	C>T	0.62 $[0.39-0.97]$	0.032	1	RDBP	Locus, intron	
rs854555	7	C>A	1.53 $[1.05-2.24]$	0.032	1	PON1	Intron, TagSNP: PON1	
rs854556	7	C>T	0.64 $[0.44-0.95]$	0.031	1	PON1	Intron, TagSNP: PON1	
rs1052637	2	G>C	0.66 $[0.45-0.97]$	0.031	1	DDX18	nonsynonymous	
rs440454	6	C>T	0.62 $[0.39-0.97]$	0.032	1	RDBP	Locus, intron	
rs854555	7	C>A	1.53 $[1.05-2.24]$	0.032	1	PON1	Intron, TagSNP: PON1	
rs2857605	6	A>G	0.57 $[0.36-0.92]$	0.034	1	TNF	Intron, TagSNP: TNF	
rs6768093	3	T>A	0.66 $[0.45-0.96]$	0.036	1	ATR	Locus	rs2227930, rs2227928
rs1405655	19	T>C	1.56 $[1.05-2.32]$	0.036	1	NR1H2	Intron	
rs3733890	5	G>A	0.66 $[0.45-0.98]$	0.037	1	BHMT	nonsynonymous	
rs1801105	2	C>T	1.95 $[1.06-3.60]$	0.041	1	HNMT	nonsynonymous	
rs2231142	4	C>A	2.12 $[1.04-4.31]$	0.042	1	ABCG2	nonsynonymous	
rs3212254	14	C>A	2.12 $[1.04-4.31]$	0.042	1	RIPK3	nonsynonymous	
rs6940663	7	A>G	0.67 $[0.46-0.98]$	0.042	1	PTPN12	nonsynonymous	
rs1050152	5	C>T	0.68 $[0.47-0.99]$	0.044	1	SLC22A4	nonsynonymous	
rs2007231	1	T>C	0.66 $[0.44-0.97]$	0.044	1	NRAS	Intron	
rs1296028	8	A>G	0.64 $[0.42-0.99]$	0.045	1	FDFT1	3'UTR	
rs3758581	10	G>A	2.35 $[1.12-4.97]$	0.047	1	CYP2C19	nonsynonymous	
rs2124459	21	T>C	0.66 $[0.45-0.96]$	0.047	1	CBS	Intron	
rs2228233	14	C>T	0.65 $[0.43-0.98]$	0.048	1	NFATC4	synonymous	
rs10759326	9	T>G	1.57 $[0.99-2.48]$	0.048	1	IKBKAP	nonsynonymous	rs10979601
rs2074351	7	G>A	1.51 $[1.01-2.26]$	0.050	1	PON1	Intron, TagSNP: PON1	

generation of the sensory and autonomic nervous system.[23]

Mutations in neurofilament light polypeptide (NEFL) cause Charcot-Marie-Tooth Neuropathy Type 2E/1F, the most common inherited peripheral neuropathy.[24] Two promoter SNPs (*rs2976437* and *rs2976436*) in *NEFL* were associated with BiPN. Two SNPs were located in the nerve growth factor receptor (*NGFR*; *rs11466155* and *rs584589*), a gene particularly important with respect to neurological functions. The NFGR signals via NFκB activation and binds neutrophin precursors that stimulate neuronal cell survival and differentiation. These results support the finding in our previous study that late onset BiPN is associated with genes involved in the development and function of the nervous system.[11] In a recent paper, the time to BiPN was found to be associated with the occurrence of the SNP *rs4553808* in the gene *CTLA4*.[12] Comparison with that study is not feasible, due to the fact that the SNP set tested had only minimal overlap with our SNP set (2% overlap).

We evaluated genetic risk factors associated with BiPN in MM patients who had not been previously treated with Bortezomib in the largest study to date using a hypothesis-driven approach. This method is limited by the possibility of population heterogeneity. However, a limited set of patients with different genetic backgrounds were selected out, as described in the Material and Methods section and as reported previously.[11] Further limitations are: i) the inability of assessing SNPs outside the candidate panel; and ii) the possibility of finding false-positive associations as a result of multiple testing. To address both issues, we are currently performing a genome-wide scan that will clarify and possibly confirm the associations reported in this study. The power analysis indicated in this study has sufficient power to detect associations with an OR of less than 0.44 or an OR of more than 2.28 and diverging with MAF. It is unlikely that smaller effects can be found. Using the custom BOAC SNP array in a discovery set of 238 patients, no SNP was found to be significantly associated to BiPN at the corrected $p < 0.05$ significance level. However, based on the highest-ranking SNPs found using the uncorrected *p*-value in the discovery set, pathway analysis did demonstrate clear enrichment of neurological disease SNPs.

REFERENCES

1. Richardson PG, Sonneveld P, Schuster MW, *et al.* Bortezomib or high-dose dexamethasone for relapsed multiple myeloma. *N Engl J Med* . 2005; **352**(24):2487–2498.
2. Richardson PG, Briemberg H, Jagannath S, *et al.* Frequency, characteristics, and reversibility of peripheral neuropathy during treatment of advanced multiple myeloma with bortezomib. *J Clin Oncol* . 2006; **24**(19):3113–20.
3. Richardson PG, Xie W, Mitsiades C, *et al.* Single-agent bortezomib in previously untreated multiple myeloma: efficacy, characterization of peripheral neuropathy, and molecular correlations with response and neuropathy. *J Clin Oncol* . 2009; **27**(21):3518–25.
4. Delforge M, Blade J, Dimopoulos MA, *et al.* Treatment-related peripheral neuropathy in multiple myeloma: the challenge continues. *Lancet Oncol* . 2010; **11**(11):1086–95.
5. Richardson PG, Barlogie B, Berenson J, *et al.* A phase 2 study of bortezomib in relapsed, refractory myeloma. *N Engl J Med* . 2003; **348**(26):2609–2617.
6. Cavaletti G, Gilardini A, Canta A, *et al.* Bortezomib-induced peripheral neurotoxicity: a neurophysiological and pathological study in the rat. *Exp Neurol* . 2007; **204**(1):317–25.
7. Landowski TH, Megli CJ, Nullmeyer KD, Lynch RM, & Dorr RT. Mitochondrial-mediated disregulation of Ca2+ is a critical determinant of Velcade (PS-341/bortezomib) cytotoxicity in myeloma cell lines. *Cancer Res* . 2005; **65**(9):3828–36.
8. Casafont I, Berciano MT, & Lafarga M. Bortezomib induces the formation of nuclear poly(A) RNA granules enriched in Sam68 and PABPN1 in sensory ganglia neurons. *Neurotox Res* . 2010; **17**(2):167–78.
9. Cavaletti G & Marmiroli P. Chemotherapy-induced peripheral neurotoxicity. *Nat Rev Neurol* . 2010; **6**(12):657–66.
10. Ravaglia S, Corso A, Piccolo G, *et al.* Immune-mediated neuropathies in myeloma patients treated with bortezomib. *Clin Neurophysiol* . 2008; **119**(11):2507–12.
11. Broyl A, Corthals SL, Jongen JL, *et al.* Mechanisms of peripheral neuropathy associated with bortezomib and vincristine in patients with newly diagnosed multiple myeloma: a prospective analysis of data from the HOVON-65/GMMG-HD4 trial. *Lancet Oncol* . 2010; **11**(11):1057–65.
12. Favis R, Sun Y, van de Velde H, *et al.* Genetic variation associated with bortezomib-induced peripheral neuropathy. *Pharmacogenet Genomics* . 2011; **21**(3):121–9.
13. Van Ness B, Ramos C, Haznadar M, *et al.* Genomic variation in myeloma: design, content, and initial application of the Bank On A Cure SNP Panel to detect associations with progression-free survival. *BMC Med* . 2008; **6**:26.
14. Purcell S, Neale B, Todd-Brown K, *et al.* PLINK: a tool set for whole-genome association and population-based linkage analyses. *Am J Hum Genet* . 2007; **81**(3):559–75.
15. Gayther SA, Song H, Ramus SJ, *et al.* Tagging single nucleotide polymorphisms in cell cycle control genes and susceptibility to invasive epithelial ovarian cancer. *Cancer Res* . 2007; **67**(7):3027–35.
16. Sharp L, Cardy AH, Cotton SC, & Little J. CYP17 gene polymorphisms: prevalence and as-

sociations with hormone levels and related factors. a HuGE review. *Am J Epidemiol* . 2004; **160**(8):729–40.

17. Roglio I, Giatti S, Pesaresi M, *et al.* Neuroactive steroids and peripheral neuropathy. *Brain Res Rev* . 2008; **57**(2):460–9.

18. Curran MP & McKeage K. Bortezomib: a review of its use in patients with multiple myeloma. *Drugs* . 2009; **69**(7):859–88.

19. Mhatre M, Nguyen A, Kashani S, Pham T, Adesina A, & Grammas P. Thrombin, a mediator of neurotoxicity and memory impairment. *Neurobiol Aging* . 2004; **25**(6):783–93.

20. Sriram K & O'Callaghan JP. Divergent roles for tumor necrosis factor-alpha in the brain. *J Neuroimmune Pharmacol* . 2007; **2**(2):140–53.

21. Gonzalez-Clemente JM, Mauricio D, Richart C, *et al.* Diabetic neuropathy is associated with activation of the TNF-alpha system in subjects with type 1 diabetes mellitus. *Clin Endocrinol (Oxf)* . 2005; **63**(5):525–9.

22. Boyle DL, Jones TL, Hammaker D, *et al.* Regulation of peripheral inflammation by spinal p38 MAP kinase in rats. *PLoS Med* . 2006; **3**(9):e338.

23. Anderson SL, Coli R, Daly IW, *et al.* Familial dysautonomia is caused by mutations of the IKAP gene. *Am J Hum Genet* . 2001; **68**(3):753–8.

24. Jordanova A, de Jonghe P, Boerkoel CF, *et al.* Mutations in the neurofilament light chain gene (NEFL) cause early onset severe Charcot-Marie-Tooth disease. *Brain* . 2003; **126**(Pt 3):590–7.

CHAPTER 8

A Genome-Wide Association Study Identifies a Novel Locus for Bortezomib-Induced Peripheral Neuropathy in European Patients with Multiple Myeloma

Florence Magrangeas, Rowan Kuiper, Hervé Avet-Loiseau,
Wilfried Gouraud,CatherineGuérin-Charbonnel, Ludovic Ferrer,
Alexandre Aussem, Haytham Elghazel,Jérôme Suhard,
Henri Der Sakissian, Michel Attal, Nikhil C. Munshi, Pieter Sonneveld,
Charles Dumontet, Philippe Moreau, Mark van Duin,
Loïc Campion & Stéphane Minvielle

Clinical Cancer Research 2016; **22**(17):4350-55

ABSTRACT

Painful peripheral neuropathy is a frequent toxicity associated with bortezomib therapy. This study aimed to identify loci that affect susceptibility to this toxicity. A genome-wide association study (GWAS) of 370605 SNPs was performed to identify risk variants for developing severe bortezomib-induced peripheral neuropathy (BiPN) in 469 patients with multiple myeloma who received bortezomib–dexamethasone therapy prior to autologous stem cell in randomized clinical trials of the Intergroupe Francophone du Myélome (IFM) and findings were replicated in 114 patients with multiple myeloma of the HOVON-65/GMMG-HD4 clinical trial. An SNP in the PKNOX1 gene was associated with BiPN in the exploratory cohort (*rs2839629*; OR=$1.9, 95\%$ confidence interval: $[1.5–2.4]$; $p= 7.6 \times 10^{-6}$) and in the replication cohort (OR$= 2.0\,[1.1–3.3]$; $p= 8.3 \times 10^{-3}$). In addition, *rs2839629* is in strong linkage disequilibrium($r^2 = 0.87$) with *rs915854*, located in the intergenic region between *PKNOX1* and cystathionine-ß-synthetase (*CBS*). Expression quantitative trait loci mapping showed that both *rs2839629* and *rs915854* genotypes have an impact on *PKNOX1* expression in nerve tissue, whereas *rs2839629* affects *CBS* expression in skin and blood. The use of GWAS in multiple myeloma pharmacogenomics has identified a novel candidate genetic locus mapping to *PKNOX1* and in the immediate vicinity of *CBS* at 21q22.3 associated with the severe bortezomib-induced toxicity. The proximity of these two genes involved in neurologic pain whose tissue-specific expression is modified by the two variants provides new targets for neuroprotective strategies.

INTRODUCTION

Some patients with multiple myeloma have subclinical or even clinical peripheral neuropathy at diagnosis. This peripheral neuropathy can be related to comorbidities, such as diabetes mellitus, or associated with the M-protein itself. In the course of the disease, peripheral neuropathy is mostly induced by therapies, especially thalidomide (thalidomide-induced peripheral neuropathy, TiPN) and bortezomib (bortezomib-induced peripheral neuropathy, BiPN), which may be considered as distinct clinical entities.[1] TiPN may arise after prolonged administration of thalidomide (in 30–55% of patients treated for 12 months, including 15–25% with grade 2 or higher peripheral neuropathy) and appears to be due to a cumulative effect. Initial symptoms include sensory changes, such as paresthesia and hyperesthesia, later followed by motor symptoms and autonomic dysfunction. BiPN is characterized by neuropathic pain and a length dependent distal sensory neuropathy with suppression of reflexes. Motor neuropathy may follow and infrequently results in mild to severe distal weakness in the lower limbs. There may also be a significant autonomic component, which manifests as dizziness, hypotension, diarrhea or constipation, and/or extreme fatigue. BiPN is thought to occur at a certain threshold of treatment (within five cycles but rarely beyond) in $40-60\%$ of the patients, including $15-40\%$ who will develop severe peripheral neuropathy (grade 2 or higher). This drug-induced toxicity is well known by physicians and nurses, and patients are now systematically informed about these potential side effects. The use of subcutaneous bortezomib reduces the incidence of BiPN but does not abrogate this toxicity.[2] As no effective prophylactic treatment is available, prompt action in case of symptoms, including dose reduction and weekly administration of bortezomib, is crucial to manage this severe toxicity, which may dramatically affect the quality of life.[3–5] Therefore, the identification of patients at risk of developing BiPN or TiPN is an important issue. This is especially true because the triplet combination of bortezomib–thalidomide–dexamethasone is considered one of the best induction regimens prior to high-dose therapy and autologous stem cell transplantation for the treatment of younger patients with de novo multiple myeloma.[6] The interindividual differences in the onset of BiPN or TiPN is in agreement with an underlying

genetic susceptibility to this toxicity. Rare variants in bortezomib or thalidomide target proteins could affect the patient's sensitivity to these drugs. Among the pharmacogenomic methods to discover genetic loci associated with drug-induced toxicities, the candidate gene approach has shown a significant genetic contribution to the risk of developing TiPN or BiPN.[7–10] However, a genome-wide association study (GWAS) has the capacity to identify new genetic variants that will have a direct or indirect effect on drug sensitivity. Here we report the results of a GWAS of 583 patients with multiple myeloma treated with bortezomib to discover genetic variants associated with severe BiPN. This is the first GWA pharmacogenomic study of bortezomib treatment toxicity and provides novel insights into bortezomib-related pathways.

MATERIALS AND METHODS

Clinical samples

Peripheral blood DNA samples were collected from 598 patients with newly diagnosed multiple myeloma who received bortezomib–dexamethasone (VD) induction therapy. Patients were treated in randomized clinical trials of the Intergroupe Francophone du Myélome (IFM; IFM 2005-01, IFM2007-02) or routine practice in France ($n = 482$) and in a randomized clinical trial of the Dutch/Belgian Haemato-Oncology Foundation for Adults in du the Netherlands (HOVON) and the German-Speaking Myeloma Multicenter Group (GMMG; HOVON-65/GMMG-HD4; $n = 116$). The IFM VD treatment consisted of four 3-week cycles of bortezomib $1.3\ mg/m^2$ administered intravenously on days 1, 4, 8, and 11 plus dexamethasone $40\ mg$ on days 1 to 4 (all cycles) and days 9 to 12 (cycles 1 and 2). The HOVON-65/GMMG-HD4 VD treatment consisted of three cycles of bortezomib $1.3\ mg/m^2$ administered intravenously on days 1, 4, 8, and 11 plus dexamethasone $40\ mg$ on days 1 to 4, 9 to 12, and 17 to 20 (patients enrolled in the HOVON-65/GMMG-HD4 trial received doxorubicin $9\ mg/m^2/day$ on days 1 to 4, in addition to VD according to the bortezomib, doxorubicin, and dexamethasone (PAD) regimen. Adverse events including peripheral neuropathy were graded by NCI Common Toxicity Criteria Version 3.0. All patients provided written informed consent for both the treatment and companion protocols.

Genotyping

Data quality assessment and control steps carried out during GWAS are summarized in online Figure S1. A total of 482 multiple myeloma samples in the exploratory IFM cohort and 116 multiple myeloma samples in the Dutch and German replication cohort were genotyped using Affymetrix SNP6.0 Human DNA chips. Affymetrix CEL files were analyzed either by using Affymetrix Genotyping Console software v4.0 (GTC 4.0), followed by application of the Affymetrix Birdseed algorithm v2.0 to generate SNP genotype calls for the IFM exploratory cohort (GEO accession GSE65777) or by application CRLMM v2 algorithm to generate SNP genotype calls for the replication cohort (GEO accession GSE66903).

Samples quality control

Stringent quality control (QC) thresholds were applied to filter out poorly genotyped subjects: if contrast QC < 0.4, call rate $< 97\%$ and outlying heterozygosity rate (het_rate $>$ mean het_rate + 3SD), the individual was removed. Principal component analysis (PCA) was performed to visualize the genetic ancestry of the IFM samples that passed the QC and assess whether population adjustment should be made (online Figure S2). Random 60000 genotypes of IFM subjects (IFM, $n = 469$) and unrelated individuals from three HapMap phase III populations representing Northwest European (CEU, $n = 162$), African (YRI, $n = 163$), and Chinese (CHB, $n = 82$) ancestries were combined to calculate the PCA. This method identified samples not clustering with the Northwestern European individuals (IFM outliers, $n = 34$), given that these patients were equally distributed between the case and control groups (Fisher exact test $p= 0.36$), no adjustment was needed, and therefore they were kept for the GWAS. Inspection of the observed and expected distribution of the neuropathy association statistic showed absence of hidden population substructure (Cochran–Armitage test of association; genomic inflation factor $\lambda = 1.05$).

Marker QC

SNP QC was conducted in four steps to remove suboptimal markers of the GWA data (Figure S1). i) unannotated SNPs according to hg19 na32 SNP6.0 Affymetrix annotations ($n = 130$) along with SNPs from mitochondrial and sex chromosomes ($n = 37326$) were not considered in the study, ii) SNPs with missing genotype in more than 5% of the subjects ($n = 16743$), iii) SNPs of low minor allele frequency (MAF) less than 5% ($n = 483984$), iv) SNPs showing extensive deviation from Hardy–Weinberg equilibrium (HWE) with an HWE $p< 1 \times 10^{-5}$ ($n = 834$).

Statistical analysis

Statistical analyses were performed using SNPTEST v2.5.[11] First, we compared 370605 genotypes from 155 grade ≥ 2 BiPN IFM patients to 314 control IFM patients defined as grade 1 BiPN or no BiPN. Second, we performed a validation us-

ing the HOVON-65/GMMG-HD4 cohort for the highest associated SNPs ($p_{\text{trend}} < 1 \times 10^{-5}$) as identified in the exploratory cohort. We compared 41 bortezomib-treated grade ≥ 2 BiPN patients with 75 bortezomib-treated control patients. We applied a one-sided logistic regression with 10000 label-swapping permutations to correct for multiple testing to confirm BiPN association in this independent cohort. The predictive value of the SNP validated in the external series was assessed on the overall population ($n = 583$, i.e. 195 cases and 388 controls) with 1×10^7 label-swapping permutations.

RESULTS

We conducted a pharmacogenomic GWA study to identify genetic variants associated with bortezomib toxicity in newly diagnosed patients with multiple myeloma who received VD induction therapy. Using SNP6.0 Affymetrix arrays, we genotyped 909622 tagging SNPs in 482 multiple myeloma cases. Of the 482 DNA samples genotyped, 469 cases passed strict QC criteria (online Figure S1). We considered only the 370605 autosomal SNPs with homozygosity in at least 5% of patients, a genotype call in at least 95% of patients and with an HWE $p > 1 \times 10^{-5}$. We compared the genetic contribution of patients who developed BiPN of grade ≥ 2 ($n = 155$) with that of patients who did not develop severe BiPN or without BiPN ($n = 314$). We separated grade 0 and 1 versus grade 2 or more based on the clinical impact of such a toxicity. Grade 1 neuropathy requires a careful follow-up, but doses of bortezomib are not modified. Doses of bortezomib in the routine clinical practice must be adapted (from $1.3\, mg/m^2$ to $1.0\, mg/m^2$, or from the bi-weekly to the weekly schedule administration) according to the onset of grade 2 peripheral neuropathy, or stopped in case of grade 3 or more, and resumed in case of recovery. The GWA study showed association for six SNPs with OR> 1.8 and $p_{\text{trend}} < 1 \times 10^{-5}$ (Table 1 and online Table S1; online Figure S3 and S4), although none reached the actual significance in a GWA study ($\frac{0.05}{370065} = 1.35 \times 10^{-7}$). To replicate these findings, a validation was performed using SNP6.0 Affymetrix arrays in 114 newly diagnosed patients with multiple myeloma enrolled in the HOVON-65/GMMG-HD4 clinical trial who received VD induction therapy. A significant association was seen for *rs2839629* (OR $= 2.04$; 95%CI $[1.11–3.33]$ ($p = 8.3 \times 10^{-3}$; Table 2) which maps within the 3'UTR of *PKNOX1* (transcription factor PBX/knotted 1 homeobox 1). The overall estimate for *rs2839629* was an OR of $1.89\,[1.45–2.44]$; $p = 5 \times 10^{-7}$). Moreover, *rs2839629* is in strong linkage disequilibrium (LD) with *rs76516641* ($r^2 = 0.94$) and *rs915854* ($r^2 = 0.86$) which map within the intergenic region of $19.5kb$ between *PKNOX1* and cystathionine-ß-synthetase (*CBS*; Figure 1).

Both *PKNOX1* and *CBS* appear to be strong candidates for BiPN susceptibility genes. PKNOX1 is known to modulate transcriptional activity of chemokine monocyte chemoattractant protein-1 (*MCP-1*) gene.[12–15] Through interaction

Table 1. Six highest associated SNPs. SNPTEST results for exploratory population for the six highest associated SNPs

SNP	CHR			BIPN ≥ 2			BIPN < 2			Odds ratio [95%CI]			p_{trend}
		A	B	#AA	#AB	#BB	#AA	#AB	#BB	AB/AA	BB/AA	global	
rs10862339	12	A	C	40	79	36	147	135	32	$2.2_{[1.4-3.4]}$	$4.1_{[2.3-7.5]}$	$2.1_{[1.6-2.7]}$	5.47×10^{7}
rs1344016	12	A	G	41	79	35	145	135	34	$2.1_{[1.3-3.2]}$	$3.6_{[2.0-6.5]}$	$1.9_{[1.5-2.6]}$	3.81×10^{6}
rs2414277	15	T	C	21	70	64	86	155	73	$1.9_{[1.3-3.0]}$	$3.6_{[2.0-6.3]}$	$1.9_{[1.5-2.6]}$	6.17×10^{6}
rs2839629	21	G	A	33	79	43	128	137	49	$1.5_{[0.93-2.5]}$	$3.5_{[2.0-5.9]}$	$1.9_{[1.5-2.5]}$	7.64×10^{6}
rs4776196	15	T	C	21	70	64	85	155	74	$1.9_{[1.2-2.9]}$	$3.5_{[2.0-6.3]}$	$1.9_{[1.4-2.5]}$	9.31×10^{6}
rs11145770	9	G	A	46	72	37	141	144	29	$2.6_{[1.5-4.6]}$	$3.9_{[2.2-7.1]}$	$1.9_{[1.4-2.5]}$	9.70×10^{6}

with its cognate receptor CCR2, MCP-1 contributes to paclitaxel CIPN through changes in dorsal root ganglion neurons.[16] *MCP-1* is universally increased in different models of neuropathic pain and may be considered as a biomarker of chronic pain.[17] MCP-1 is an important mediator of macrophage-related neural damage in different animal models of inherited neuropathies and acute inflammatory demyelinating neuropathy.[18,19] *CBS* encodes the endogenous H2S-producing enzyme CBS. CBS–H2S signaling pathway is implicated in the pathogenesis of a variety of neurodegenerative and inflammatory disorders, diabetic gastric hypersensitivity and plays a crucial role in inflammatory pain in temporomandibular joint.[20–23] To explore the possibility that this association might be mediated through differential expression of *PKNOX1* or *CBS* or both, we examined the correlations between *rs2839629*, *rs76516641*, and *rs915854* genotypes and tissue-specific gene expression levels by using the expression quantitative trait locus analysis available on the SNiPA portal (`www.snipa.org`) that used GTEx Portal v6 and MuTHER consortium as primary sources.[24–26] *PKNOX1* expression was significantly associated with *rs2839629* and *rs915854* genotypes in tibial nerve tissue ($p = 5.6 \times 10^{-8}$ and $p = 1.9 \times 10^{-7}$, respectively; online Tables S2 and S3) with higher expression associated with *rs2839629* risk alleles (Figure

Table 2. Logistic regression results One-sided logistic regression in the validation cohort to test whether the direction of association found in the exploratory cohort can be confirmed. OR_{global}, odds ratio estimate; p, uncorrected parametric p-value; $p_{pointwise}$, pointwise p-value as determined by permutation; p_{FWER}, permuted p-value (familywise error rate correction).

SNP	OR_{global} [95%CI]	p	$p_{pointwise}$	p_{FWER}
rs10862339	$1.02_{[0.58-1.79]}$	0.53	0.54	0.96
rs1344016	$1.05_{[0.60-1.85]}$	0.43	0.44	0.91
rs2414277	$1.20_{[0.71-2.08]}$	0.24	0.22	0.66
rs2839629	$2.04_{[1.11-3.33]}$	9.6×10^{-3}	8.3×10^{-3}	0.036
rs4776196	$1.19_{[0.71-2.08]}$	40.24	0.27	0.70
rs11145770	$1.43_{[0.75-2.33]}$	0.14	0.13	0.46

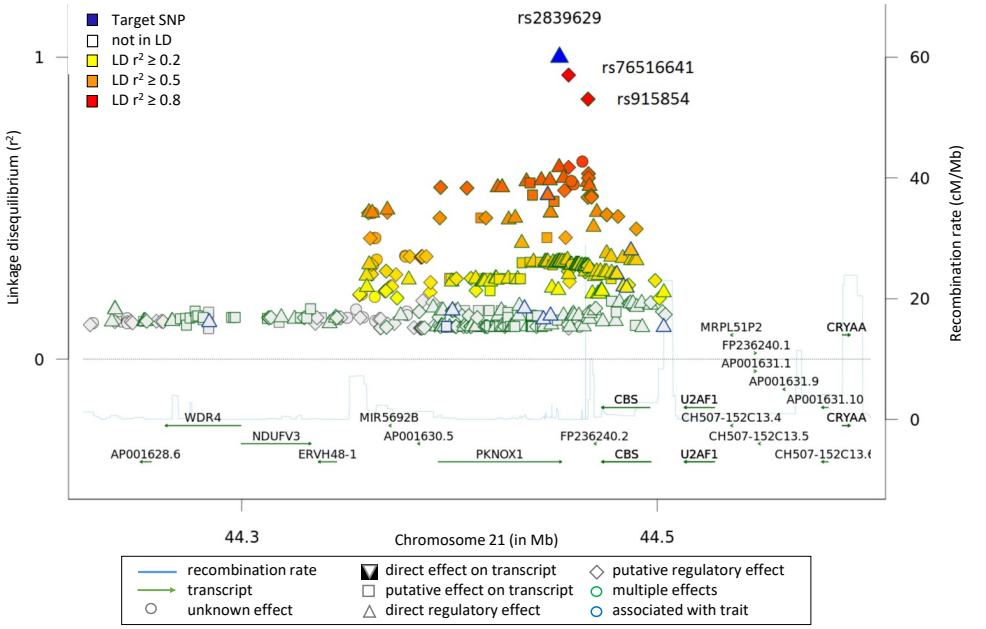

Figure 1. SNP associations with BiPN on the 21q22.3 locus. Showing genome-wide level of evidence of BiPN in multiple myeloma. Illustration of the locus with the local LD and recombination rate over $500kb$ centred on *rs2839629* (blue triangle). Each diamond, triangle, circle, or square represents an SNP found in this locus, *rs76516641* and *rs915854* are indicated (red diamond). The figure was generated using the web-based tool SNiPA (`www.snipa.org`; ref. 24).

2), whereas *CBS* expression was significantly associated only with *rs2839629* in skin ($p= 2.6 \times 10^{-15}$) and in blood ($p= 3.1 \times 10^{-8}$; online Table S2). *rs915854* is annotated with a regulatory feature cluster characterized by histone marks H3K27ac and H3K4me1 enrichment in blood and cervix cells (online Table S3). In addition, a *rs915854* minor allele is predicted to disrupt the binding site for the general pioneer factor FOXA1, this could render the enhancer less active for target gene expression such as *PKNOX1* (Figure 3). Conversely, the *rs76516641* genotype has no significant effect on the gene expression of both *PKNOX1* and *CBS* (data not shown).

As we show that the risk allele A for *rs2839629* is associated with higher levels of *PKNOX1* expression and previous report have demonstrated that PKNOX1 binds preferentially to the -2578G (*rs1024611G*) polymorphism leading to increase *MCP-1* levels,[14] we analyzed the relationship between *rs2839629A* and

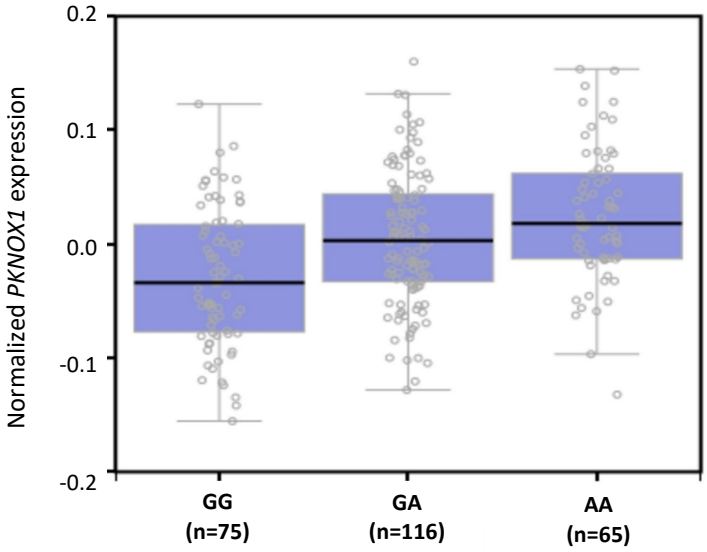

Figure 2. *PKNOX1* expression vs. *rs2839629* genotype. Relationship between tibial nerve *PKNOX1* expression and *rs2839629* genotype from the GTEx Portal v6 (`www.gtexportal.org`; ref. 25).

rs1024611G in the IFM exploratory cohort. We found a significant association between the *rs2839629 A/A* homozygous genotype and the *rs1024611G*-bearing allele (Fisher exact-test $p = 0.01$) suggesting a possible epistatic interaction between *rs2839629* and *rs1024611* to regulate *MCP-1* expression. The current pharmacogenomic GWA study also confirmed the modest association of the rs619824 genotype with BiPN ($p = 0.043$) previously identified by Corthals *et al.*[8] Although there has been no overlap with a previous study on late-onset of BiPN-associated variants reported by Broyl *et al.*[10] as shown in online Table S4. This lack of overlap could reflect the potential complexity of predisposition to BiPN. More importantly, the design of the custom SNP chip used previously only contained 3404 SNPs in 983 hypothesis-driven genes which were thought to be functionally relevant in abnormal cellular functions, inflammation and immunity, as well as drug responses rather than adverse drug reactions which are less obvious candidates.[27]

DISCUSSION

To date there are no established predictors of BiPN, it is impossible to predict which patient will develop neuropathy. Previous studies performed by our group and others using candidate gene approach have revealed significant association between SNP and BiPN; however, the clinical relevance of these findings is not clear.[8–10] To increase our chance to discover variants that might provide new insights in the mechanisms underlying gene phenotype, we used a hypothesis-free approach. GWAS in cancer pharmacogenomics is challenging and few reports have been published to date. This is mainly due to insufficient statistical power in studies.[28] To partially overcome these limitations, we designed our analysis to identify high-effect SNP (OR> 1.8) with MAFs greater than 0.05, in a large cohort of IFM patients with multiple myeloma ($n = 469$) uniformly treated to achieve convincing statistical power[29] and we verified our findings in an independent cohort of Dutch and German patients with multiple myeloma. Furthermore, our GWAS approach eliminates selection case–control bias as both case–control studies included patients in cohort studies, i.e. IFM or HOVON/GMMG clinical trials cohorts. When evaluating toxicity, it is sometimes difficult to distinguish between BiPN and neuropathic pain in general. It is also recognized that the sole use of the NCI CTC for assessment of sensory peripheral neuropathy is suboptimal. It is also recognized that detailed patient-reported symptom data and a quality-of-life assessment more accurately describes this toxicity and that physician-reported NCI-CTC grading underreports peripheral neuropathy. These systematic evaluations are difficult to apply in a multicenter study in the context of pharmacogenomics analyses. Of note, our study has enrolled patients without peripheral neuropathy at baseline, and patients were treated with the doublet combination of bortezomib and dexamethasone, and did not receive other neurotoxic agents.

Our analysis revealed a SNP associated with BiPN (*rs2839629*; OR$= 1.89$; $p= 7.6 \times 10^{-6}$) that was replicated in an independent cohort (OR$= 2.04$; $p= 8.3 \times 10^{-3}$) in high LD with SNP *rs915854*. Both variants are in noncoding regions; *rs2839629* is located in the 3'UTR of *PKNOX1*, and *rs915854* is in the intergenic region between *PKNOX1* and *CBS*. Expression quantitative trait loci showed that these variants alter *PKNOX1* and *CBS* expression presumably via cis-regulatory

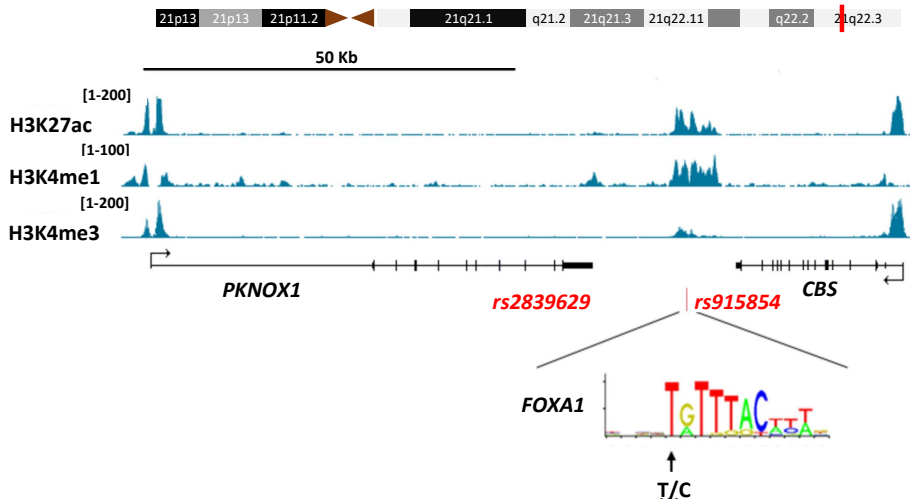

Figure 3. Histone marks *PKNOX1* locus. UCSC Genome Browser views of histone marks H3K27ac and H3K4me1 enrichment and H3K4me3 depletion within the region covering PKNOX1 and CBS in Hela cells. Arrow indicates the variant sequence and location in position-weight matrix for FOXA1.

elements in the case of *rs915854* as it falls within a regulatory region (Figure 3). Finally, we found a significant association between *rs2839629A* and *rs1024611G* that could have an impact on *MCP-1* expression levels. Given that these genes encode proteins, directly or indirectly, involved in neuropathic[16] and inflammatory[23] pain, the functional significance of these predictive SNPs is established. This discovery opens the way to investigate novel pathways linked to PKNOX1 and CBS activities for a better understanding of mechanisms underlying this neurotoxicity. This work generated a new hypothesis hypothesis regarding neurotoxicity mechanisms and provides new targets for neuroprotective strategies; however, additional international collaborative efforts including non-European countries are warranted to confirm or refute these findings and examine the impact of differential expression of both *PKNOX1* and *CBS* effects on bortezomib exposure in cell model. Our results are preliminary and cannot be proposed yet for a systematic use in the routine clinical practice. Nevertheless, our findings are one of the first steps that may allow for the identification of patients at increased risk of severe BiPN, and these patients may benefit from the use of alternative drugs, such as carfilzomib, and/or a more focused clinical management of this toxicity.

REFERENCES

1. Cavaletti G & Marmiroli P. Chemotherapy-induced peripheral neurotoxicity. *Nat Rev Neurol* . 2010; **6**(12):657–66.
2. Moreau P, Pylypenko H, Grosicki S, *et al.* Subcutaneous versus intravenous administration of bortezomib in patients with relapsed multiple myeloma: a randomised, phase 3, non-inferiority study. *Lancet Oncol* . 2011; **12**(5):431–40.
3. Delforge M, Blade J, Dimopoulos MA, *et al.* Treatment-related peripheral neuropathy in multiple myeloma: the challenge continues. *Lancet Oncol* . 2010; **11**(11):1086–95.
4. Mohty B, El-Cheikh J, Yakoub-Agha I, Moreau P, Harousseau JL, & Mohty M. Peripheral neuropathy and new treatments for multiple myeloma: background and practical recommendations. *Haematologica* . 2010; **95**(2):311–9.
5. Richardson PG, Delforge M, Beksac M, *et al.* Management of treatment-emergent peripheral neuropathy in multiple myeloma. *Leukemia* . 2012; **26**(4):595–608.
6. Moreau P, San Miguel J, Ludwig H, *et al.* Multiple myeloma: ESMO Clinical Practice Guidelines for diagnosis, treatment and follow-up. *Ann Oncol* . 2013; **24 Suppl 6**:vi133–7.
7. Johnson DC, Corthals SL, Walker BA, *et al.* Genetic factors underlying the risk of thalidomide-related neuropathy in patients with multiple myeloma. *J Clin Oncol* . 2011; **29**(7):797–804.
8. Corthals SL, Kuiper R, Johnson DC, *et al.* Genetic factors underlying the risk of bortezomib induced peripheral neuropathy in multiple myeloma patients. *Haematologica* . 2011; **96**(11):1728–32.
9. Favis R, Sun Y, van de Velde H, *et al.* Genetic variation associated with bortezomib-induced peripheral neuropathy. *Pharmacogenet Genomics* . 2011; **21**(3):121–9.
10. Broyl A, Corthals SL, Jongen JL, *et al.* Mechanisms of peripheral neuropathy associated with bortezomib and vincristine in patients with newly diagnosed multiple myeloma: a prospective analysis of data from the HOVON-65/GMMG-HD4 trial. *Lancet Oncol* . 2010; **11**(11):1057–65.
11. Marchini J, Howie B, Myers S, McVean G, & Donnelly P. A new multipoint method for genome-wide association studies by imputation of genotypes. *Nat Genet* . 2007; **39**(7):906–13.
12. Rovin BH, Lu L, & Saxena R. A novel polymorphism in the MCP-1 gene regulatory region that influences MCP-1 expression. *Biochem Biophys Res Commun* . 1999; **259**(2):344–8.
13. Wright J E K, Page SH, Barber SA, & Clements JE. Prep1/Pbx2 complexes regulate CCL2 expression through the -2578 guanine polymorphism. *Genes Immun* . 2008; **9**(5):419–30.
14. Page SH, Wright J E K, Gama L, & Clements JE. Regulation of CCL2 expression by an upstream TALE homeodomain protein-binding site that synergizes with the site created by the A-2578G SNP. *PLoS One* . 2011; **6**(7):e22052.
15. Pham MH, Bonello GB, Castiblanco J, *et al.* The rs1024611 regulatory region polymorphism is associated with CCL2 allelic expression imbalance. *PLoS One* . 2012; **7**(11):e49498.
16. Zhang H, Boyette-Davis JA, Kosturakis AK, *et al.* Induction of monocyte chemoattractant protein-1 (MCP-1) and its receptor CCR2 in primary sensory neurons contributes to paclitaxel-induced peripheral neuropathy. *J Pain* . 2013; **14**(10):1031–44.
17. Zhang J & De Koninck Y. Spatial and temporal relationship between monocyte chemoattractant

protein-1 expression and spinal glial activation following peripheral nerve injury. *J Neurochem* . 2006; **97**(3):772–83.

18. Groh J, Heinl K, Kohl B, *et al.* Attenuation of MCP-1/CCL2 expression ameliorates neuropathy in a mouse model for Charcot-Marie-Tooth 1X. *Hum Mol Genet* . 2010; **19**(18):3530–43.

19. Yuan F, Yosef N, Lakshmana Reddy C, *et al.* CCR2 gene deletion and pharmacologic blockade ameliorate a severe murine experimental autoimmune neuritis model of Guillain-Barre syndrome. *PLoS One* . 2014; **9**(3):e90463.

20. Wang Y, Qu R, Hu S, Xiao Y, Jiang X, & Xu GY. Upregulation of cystathionine beta-synthetase expression contributes to visceral hyperalgesia induced by heterotypic intermittent stress in rats. *PLoS One* . 2012; **7**(12):e53165.

21. Schemann M & Grundy D. Role of hydrogen sulfide in visceral nociception. *Gut* . 2009; **58**(6):744–7.

22. Zhang HH, Hu J, Zhou YL, *et al.* Promoted interaction of nuclear factor-kappaB with demethylated cystathionine-beta-synthetase gene contributes to gastric hypersensitivity in diabetic rats. *J Neurosci* . 2013; **33**(21):9028–38.

23. Miao X, Meng X, Wu G, *et al.* Upregulation of cystathionine-beta-synthetase expression contributes to inflammatory pain in rat temporomandibular joint. *Mol Pain* . 2014; **10**:9.

24. Arnold M, Raffler J, Pfeufer A, Suhre K, & Kastenmuller G. SNiPA: an interactive, genetic variant-centered annotation browser. *Bioinformatics* . 2015; **31**(8):1334–6.

25. GTEx Consortium. Human genomics. The Genotype-Tissue Expression (GTEx) pilot analysis: multitissue gene regulation in humans. *Science* . 2015; **348**(6235):648–60.

26. Grundberg E, Small KS, Hedman AK, *et al.* Mapping cis- and trans-regulatory effects across multiple tissues in twins. *Nat Genet* . 2012; **44**(10):1084–9.

27. Van Ness B, Ramos C, Haznadar M, *et al.* Genomic variation in myeloma: design, content, and initial application of the Bank On A Cure SNP Panel to detect associations with progression-free survival. *BMC Med* . 2008; **6**:26.

28. Low SK, Takahashi A, Mushiroda T, & Kubo M. Genome-wide association study: a useful tool to identify common genetic variants associated with drug toxicity and efficacy in cancer pharmacogenomics. *Clin Cancer Res* . 2014; **20**(10):2541–52.

29. Wang WY, Barratt BJ, Clayton DG, & Todd JA. Genome-wide association studies: theoretical and practical concerns. *Nat Rev Genet* . 2005; **6**(2):109–18.

CHAPTER 10

Summaries

English summary

The studies in this thesis cover two main topics: development and comparison of prognostic markers in Multiple Myeloma (MM) (chapters 2-6), and characterization of the genetic basis of peripheral neuropathy, an important toxicity of MM treatment (chapters 7 and 8).

Chapter 2 (Kuiper *et al.* 2012): By gene expression profiling of 290 MM patients included in the HOVON-65/GMMG-HD4 clinical trial, a 92 gene classifier (EMC92) was developed, enabling the classification of patients into high- or standard risk. This classifier was validated in four external patient cohorts (newly diagnosed and relapsed) in which its performance was shown to be independent of other prognostic factors.

Chapter 3 (Kuiper *et al.* 2015): By exploiting the value of twenty known prognostic factors, which were systematically combined pair-wisely, we selected those combinations that improved prognostication. Among the most promising was the EMC92-ISS combination, enabling the classification of patients into four risk groups. The combinations that were found in the discovery phase were then validated in a similar group of patients that were left out of the discovery phase prior to the analysis.

Chapter 4 (submitted): Although approximately 65% of newly diagnosed MM patients are older than 65 years and thus likely non-transplant eligible, the EMC92-gene classifier has been validated using mainly newly diagnosed transplant eligible or relapsed patients. Only in a subset of the MRC-IX, newly diagnosed non-transplant eligible patients were included. Therefore, we applied the EMC92-gene classifier to 178 patients included in the HOVON-87 trial with a median age of 73 years. Also in this setting the classifier has a strong performance, independent of other prognostic factors.

Chapter 5 (submitted): The most important aspect of a prognostic predictor is its prognostic value. Precision is also important, i.e. upon repeatedly classifying a patient under similar conditions, the resulting outcome should remain the same. We have described a method to quantify the concordance between repeated measurements and a test for equal concordances.

Chapter 6 (Broyl *et al.* 2013): Recently, cereblon (CRBN) expression was

found to be essential for the activity of the immune modulatory drugs, thalidomide and lenalidomide. Using 96 thalidomide treated patients of the HOVON-65/GMMG-HD4 trial, we showed that higher levels CRBN expression were significantly associated with longer progression-free survival. In contrast, no association between CRBN expression and survival was observed in the arm with bortezomib maintenance.

Chapter 7 (Corthals *et al.* 2011): Peripheral neuropathy (PNP) is the dose limiting toxicity for bortezomib. Patients with higher grades of PNP require dose-reduction or even discontinuation of the treatment. Identification of an increased risk before start of the treatment could help treatment decisions. Therefore we tested the association between germline single nucleotide polymorphisms (SNPs) and the occurrence of PNP during bortezomib treatment in the IFM-2015-01 clinical trial. The SNPs were detected using an early SNP chip (with hypothesis driven design) containing 3400 features of which 56 were found to be univariately associated in the discovery set. However, neither in the discovery set, nor in the HOVON-65/GMMG-HD4 validation set, any of these reached significance after multiple testing correction. Based on the highest-ranking SNPs found using the uncorrected p-value in the discovery set, pathway analysis did demonstrate clear enrichment of neurological disease SNPs, possibly indicative for a combination of many small effects.

Chapter 8 (Magrangeas *et al.* 2016): The bortezomib treated HOVON65/-GMMG-HD4 patients have been re-genotyped using a more recent type of SNP array (with unbiased design) containing more than 900.000 SNPs. Similar analyses were performed with a slight alteration in the phenotype definition: PNP grades 0 and 1 versus grades >1. A SNP mapping to the 3' UTR of PKNOX1 was among the highest associations in the IFM discovery cohort that could be validated in the HOVON-65/GMMG-HD4 validation data in which it reached significance after multiple testing correction.

Nederlandse samenvatting

De studies in dit proefschrift beschrijven twee hoofdlijnen, namelijk: de ontwikkeling en vergelijking van prognostische markers in multiple myeloma (MM; hoofdstukken 2 tot en met 6), en onderzoek naar de genetische basis van perifere neuropathie, wat een ernstige en veel geziene bijwerking is tijdens de behandeling van MM (hoofdstukken 7 en 8).

Hoofdstuk 2 (Kuiper *et al.* 2012): Een prognostische classifier op basis van 92 genen is ontwikkeld in gen expressie profielen van 290 MM patiënten die waren geïncludeerd in de HOVON-65/GMMG-HD4 klinische studie. De classifier is gevalideerd in vier externe cohorten (zowel nieuw gediagnostiseerde als recidief patiënten) waarin de onafhankelijke prognostische waarde ten opzichte van bestaande prognostische markers aangetoond kon worden.

Hoofdstuk 3 (Kuiper *et al.* 2015): Door twintig bekende prognostische markers systematisch paarsgewijs met elkaar te combineren is getracht die combinaties te selecteren die een verbeterde voorspelling gaven van de prognose. De beste prestaties werden onder meer bereikt door de EMC92/ISS combinatie die patiënten categoriseerde in een van vier risico groepen. Deze classifier is gevalideerd in een onafhankelijke subset van de data.

Hoofdstuk 4 (submitted): Ondanks dat 65% van de nieuw gediagnostiseerde patiënten ouder zijn dan 65 jaar en dus waarschijnlijk ongeschikt zijn om beenmerg transplantie te ondergaan, is de EMC92 classifier voornamelijk gevalideerd op jongere nieuw gediagnosticeerde patiënten die wel een transplantatie ondergingen. Daarom is de EMC92 toegepast op 178 patiënten die zijn geïncludeerd in de HOVON87 studie. Deze patiënten hebben een mediane leeftijd van 73 jaar. Ook in deze setting bleef de prognostische waarde van de EMC92 behouden.

Hoofdstuk 5 (submitted): Naast het onderscheidend vermogen is ook precisie een belangrijk aspect van een classifier. Dat wil zeggen, het herhaaldelijk classificeren van een patiënt zou tot consistente uitkomsten moeten leiden. Wij hebben een algemene methode beschreven om de mate van overeenkomst tussen herhaaldelijke metingen te kwantificeren en de mate van overeenkomst tussen methodes te vergelijken.

Hoofdstuk 6 (Broyl *et al.* 2013): Onlangs bleek dat het tot expressie komen

van cereblon (CRBN) essentieel is voor de effectiviteit van zogenaamde 'immune modulatory' drugs zoals thalidomide en lenalidomide. Daarom hebben we gekeken naar de overleving op thalidomide of bortezomib onderhoudsbehandeling in HOVON65 patiënten ten opzichte van de gemeten CRBN expressie bij diagnose. Een toegenomen CRBN expressie was significant geassocieerd met langere progressie vrije overleving bij thalidomide onderhoudsbehandeling. Bij bortezomib was dit verband afwezig.

Hoofdstuk 7 (Corthals *et al.* 2011): Perifere neuropathie (PNP) is de dosisbeperkende toxiciteit voor bortezomib. Patiënten met ernstige neuropathie moeten behandeld worden met lagere dosis of de behandeling zal zelfs beëindigd moeten worden. Het herkennen van een verhoogd risico op PNP voor de start van de behandeling van belang zou gewenst zijn. Daarom hebben we gezocht naar verbanden tussen het optreden van PNP en het hebben van specifieke genotypes genaamd 'single nucleotide polymorphisms' (SNPs) bij patiënten in de IFM-2015-01 klinische studie. Met behulp van een van de eerste SNP chips konden we 3400 (hypothese gedreven) SNPs per patiënt bepalen. Hiervan werden er 56 univariaat gelinkt aan PNP in de IFM data. Geen van deze was echter significant na correctie voor multiple testing. De hoogst gerangschikte SNPs waren verrijkt met SNPs die in eerdere studies in verband werden gebracht met neurologische aandoeningen. Dit duidt mogelijk op het aanwezig zijn van vele SNPs die zwak geassocieerd zijn met PNP en dus enkel gevonden kunnen worden in studies met meer patiënten.

Hoofdstuk 8 (Magrangeas *et al.* 2016): Patiënten zijn opnieuw gegenotypeerd op een nieuwere SNP chip met meer dan 900.000 SNPs. Soortgelijke analyses zijn gedaan met een kleine aanpassing in de definitie van het fenotype: PNP grades 0 en 1 zijn vergelijken met grades >1. Een univariaat significant verband tussen hogere graads PNP en een variant in het PKNOX1 gen werd gevonden in de IFM data. Deze bevinding kon worden gevalideerd in de HOVON65 validatie data waarin de SNP significant was na correctie voor multiple testing.

List of publications

1. Kuiper R, Broyl A, de Knegt Y, *et al.* A gene expression signature for high-risk multiple myeloma. *Leukemia*. 2012;**26**(11):2406-2413.
2. Kuiper R, van Duin M, van Vliet MH, *et al.* Prediction of high- and low-risk multiple myeloma based on gene expression and the International Staging System. *Blood*. 2015;**126**(17):1996-2004
3. Broyl A, Kuiper R, van Duin M, *et al.* High cereblon expression is associated with better survival in patients with newly diagnosed multiple myeloma treated with Thalidomide maintenance. *Blood*. 2013;**121**(4):624-627.
4. Corthals SL, Kuiper R, Johnson DC, *et al.* Genetic factors underlying the risk of Bortezomib induced peripheral neuropathy in multiple myeloma patients. *Haematologica*. 2011;**96**(11):1728-1732.
5. Magrangeas F, Kuiper R, Avet-Loiseau H, *et al.* A Genome-Wide Association Study Identifies a Novel Locus for Bortezomib-Induced Peripheral Neuropathy in European Patients with Multiple Myeloma. *Clin Cancer Res.* 2016;**22**(17):4350-4355.
6. Broyl A, Corthals SL, Jongen JL, *et al.* Mechanisms of peripheral neuropathy associated with Bortezomib and vincristine in patients with newly diagnosed multiple myeloma: a prospective analysis of data from the HOVON-65/GMMG-HD4 trial. *Lancet Oncol.* 2010;**11**(11):1057-1065.
7. Corthals SL, Sun SM, Kuiper R, *et al.* MicroRNA signatures characterize multiple myeloma patients. *Leukemia*. 2011;**25**(11):1784-1789.
8. Pedotti P, t Hoen PA, Vreugdenhil E, *et al.* Can subtle changes in gene expression be consistently detected with different microarray platforms? *BMC Genomics*. 2008;9:124.
9. Wu P, Walker BA, Broyl A, *et al.* A gene expression based predictor for high risk myeloma treated with intensive therapy and autologous stem cell rescue. *Leuk Lymphoma*. 2014:1-8.
10. Mitchell JS, Li N, Weinhold N, *et al.* Genome-wide association study identifies multiple susceptibility loci for multiple myeloma. *Nat Commun*.

2016;7:12050.

11. Broijl A, Kuiper R, van Duin M, *et al.* Hoog- en laagrisico multipel myeloom kunnen worden voorspeld met de combinatie van EMC92 en ISS. *Ned Tijdschr Hematol*. 2017.
12. van Beers EH, van Vliet MH, Kuiper R, *et al.* Prognostic Validation of SKY92 and Its Combination With ISS in an Independent Cohort of Patients With Multiple Myeloma. *Clin Lymphoma Myeloma Leuk.*. 2017; **17**(9):555-562.
13. Went M, Sud A, Försti A, *et al.* Identification of multiple risk loci and potential regulatory mechanisms influencing susceptibility to multiple myeloma. Accepted by *Nat Commun* Jun 2018.
14. Went, M., Sud, A., Law, P.J. *et al.* Assessing the effect of obesity-related traits on multiple myeloma using a Mendelian randomisation approach. *Blood cancer j*. 2017;**7**(6):e573.
15. Kuiper R, Zweegman S, van Duin M, *et al.* Gene expression classifier SKY92 identifies high-risk multiple myeloma in elderly patients of the HOVON-87/NMSG-18 study. Submitted 2018.
16. Kuiper R, Huisman SMH, Hoogenboezem R, *et al.* Nopaco: A Non-Parametric test for concordance in unbalanced data.Submitted 2018.
17. Kuiper R, van Duin M, van Vliet MH, *et al.* Two group risk classification in multiple myeloma: validation of EMC92 gene expression signature as high risk marker and the EMC92-ISS combination as low risk marker. Submitted 2018.

Abbreviations

Term	Definition
95%CI	95% Confidence interval
AE	Adverse event
ANOVA	Analysis of variance
ASCT	Autologous stem cell transplantation
B2m	Beta-2-microglobulin
BiPN	Bortezomib induced Peripheral Neuropathy
BiTE	Bispecific T-cell Engagers
BOR	Drug: Bortezomib
CAR	Chimeric Antigen Receptor
CD1, CD2	Cluster: Cyclin D1 or D2 gene translocation
cDNA	Complementary DNA
CE	Conformité Européene
CEU	Central European
CHB	Han Chinese in Beijing
CHR	Chromosome
CRAB	Diagnostic criteria for MM: hyperCalcemia, Renal failure, Anemia, or lytic Bone lesions
CTA	Cluster: Cancer Testis Antigens
CTCAE	Common Toxicity Criteria for Adverse Events
CTDa	Treatment: attenuated Cyclophosphamide, Thalidomide, Dexamethasone
CVAD	Treatment: Cyclophosphamide, Vincristine, Doxorubicin, Dexamethasone
DNA	Deoxyribonucleic acid
EFS	Event free survival
EMC92	Erasmus Medical Center 92-gene classifier
FDR	False Discovery Rate

Term	Definition
FISH	Fluorescence in Situ Hybridization
FRMA	Frozen Robust Multi-Array normalization
FWER	Family-Wise Error Rate
GCRMA	Guanine Cytosine adjusted Robust Multi-Array normalization
GEO	Gene Expression Omnibus
GEP	Gene Expression Profiling
GMMG	German-Speaking Myeloma Multicenter Group
GPI50	Gene Proliferation Index 50-gene classifier
GWAS	Genome Wide Association Study
HDM	High dose Melphalan
HM19	Heidelberg-Montpelier 19-gene classifier
HO-<xx>	HOVON study with trial number <xx>
HOVON	Haemato Oncology Foundation for Adults in the Netherlands
HR	Hazard ratio or High-risk
HWE	Hardy–Weinberg equilibrium
HY	Cluster: Hyperdiploid
ICC	Intra Class Correlation coefficient
IFM15	Intergroupe Francophone du Myélome 15-gene classifier
IgH, IgH	Immunoglobulin-H or G
IMiD	Immunomodulatory Drug
IMWG	International Myeloma Working Group
Interm	Intermediate
ISS	International Staging System
IVD	In Vitro Diagnostic
LB	Cluster: Bone disease
LD	Linkage disequilibrium
LDH	Lactate dehydrogenase
MPR-R	Treatment: Melphalan, Prednisone, Lenalidomide plus Lenalidomide maintenance

Term	Definition
M-protein	Monoclonal protein
MAF	Minor allele frequency or MAF gene
MAS5	Microarray suite 5.0 gene expression normalization method
MDE	Myeloma Defining Events
MF	Cluster: MAF gene translocation cluster
MGUS	Monoclonal Gammopathy of Undetermined Significance
MM	Multiple Myeloma
MP	Treatment: Melphalan Prednisone
MPT-T	Treatment: Melphalan, Prednisone, Thalidomide plus Thalidomide maintenance
MRCIX6	Medical Research Council IX 6-gene classifier
mRNA	messenger RNA
MS	Cluster: MMSET gene translocation cluster
mSMART	Mayo Stratification for Myeloma And Risk-adapted Therapy
n.r.	Median not reached
NA	Not Applicable or Not Available
NCBI	National Center for Biotechnology
Neg	Negative
NMSG	Nordic Myeloma Study Group
Nopaco	Non-parametric concordance coefficient
OR	Odds Ratio
OS	Overall Survival
PAD	Treatment: Bortezomib, Adriamycin, Dexamethasone
PANP	Presence-Absence Calls from Negative Strand Matching Probesets
PCA	Principal Component Analysis
PCL	Plasma Cell Leukemia
PCLI	Plasma Cell Labeling Index
PFS	Progression Free Survival

Term	Definition
PI	Proteasome Inhibitor
PNP	Peripheral Neuropathy
Pos	Positive
PR	Cluster: Proliferation cluster
Prop.	Proportion
QC	Quality Control
R-ISS	Revised International Staging System
Rd	Treatment: Lenalidomide, low dose Dexamethasone
RMA	Robust Multi-array Averaging gene expression normalization
RNA	Ribonucleic acid
RS	Rank Score
RT-PCR	Real-Time Polymerase Chain Reaction
SD	Standard Deviation
SKY92	Skyline 92-gene classifier
SMM	Smoldering Multiple Myeloma
SNP	Single Nucleotide Polymorphism
SR	Standard-risk
SWOG	Southwest Oncology Group
TC-classification	Translocation and Cyclin-D classification system
Thal	Thalidomide
TiPN	Thalidomide induced Peripheral Neuropathy
TT2, TT3	Total therapy 2, Total therapy 3
Tx	Treatment
UAMS17 -70 -80	University of Arkansas for Medical Sciences 17, 70 or 80 gene classifiers
UTR	Untranslated Region
VAD	Treatment: Vincristine, Adriamycin, Dexamethasone
VCD	Treatment: Bortezomib, Cyclophosphamide and Dexamethasone
VD	Treatment: Vincristine, Dexamethasone

Term	Definition
VMD	Treatment: Bortezomib, Melphalan, Dexamethasone
VMP	Treatment : Bortezomib, Melphalan, Prednisone
VTD	Treatment: Bortezomib, Thalidomide, Dexamethasone
WHO	World Health Organization
YRI	Yoruba from Ibadan